ENVIRONMENTAL ENGINEERING
ASSOCIATION OF THAILAND

THAI ENVIRONMENTAL ENGINEERING JOURNAL

Vol. 39 No. 2 May – August 2025
ISSN (PRINT) : 1686 - 2961
ISSN (ONLINE) : 2673 - 0359

Thai Environmental Engineering Journal

Owner
Environmental Engineering Association of Thailand

Enquiries 122/4 Soi Rawadee, Rama IV Rd., Phayathai, Phayathai, Bangkok 10400

ENVIRONMENTAL ENGINEERING
ASSOCIATION OF THAILAND

Thai Environmental Engineering Journal

Vol. 39 No. 2 May – August 2025

ISSN (PRINT) : 1686 - 2961
ISSN (ONLINE) : 2673 - 0359

Thai Environmental Engineering Journal Vol. 39 No. 2 (2025) : 1-8
www.eeat.or.th

The Effect of Carbon Capture and Storage (CCS) on Quartz Rock and Groundwater: The case study of Thailand

Chanita Sirisaksathaporn[1], Supreeda Homklin[1], Sukhuma Chitapornpan[1], Chatkaew Chailuecha[1], Pimluck Kijjanapanich[2], Sulak Sumitsawan[2], Prattakorn Sittisom[2], Pharkphum Rakruam[2], Napat Jakrawatana[2], Patiroop Pholchan[2], Sarunnoud Phuphisith[2], Ekbordin Winijkul[3] and Wanawan Pragot[1*]

[1]School of Energy and Environment, University of Phayao, Phayao 56000, Thailand
[2]Department of Environmental Engineering, Faculty of Engineering, Chiang Mai University, Chiang Mai 50200, Thailand
[3]Environmental Engineering and Management, Asian Institute of Technology, Pathum Thani 12120, Thailand
[*]E-mail : wanawan.pr@up.ac.th

Article History; *Received: 31 March 2025, Accepted: 2 August 2025, Published: 28 August 2025*

Abstract

Carbon Capture and Storage (CCS) represents a critical technology for mitigating greenhouse gas emissions by capturing carbon dioxide from emission sources and its permanent sequestration in deep geological formations. This investigation examines the geochemical interactions between CO_2-saturated groundwater and quartz formations in the context of CCS implementation in Thailand's Korat basin. Quartz rock specimens were collected from the Korat basin and exposed to synthetic groundwater formulated to match the chemical composition of local groundwater samples. The synthetic solution was saturated with CO_2 to achieve acidic conditions (pH ~5), simulating the environment created during CO_2 injection. Rock-water interactions were monitored over 28 days under atmospheric conditions to assess both aqueous and solid phase transformations. Results revealed substantial geochemical evolution in both phases throughout the experimental period. Aqueous phase analysis indicated progressive increases in pH, total dissolved solids, and conductivity, consistent with dissolution and mineral trapping mechanisms. Moreover, the increasing of alkalinity, water hardness, and heavy metal concentrations (Fe, Mn, Cu, Zn, Pb, As) demonstrated active mineral dissolution and metal mobilization from the quartz matrix. Solid phase characterization confirmed mineral precipitation processes, evidenced by a 0.18% increase in rock mass, development of calcite crystal formations, and enhanced suspended solid content. While conducted over a limited timeframe, this research underscores the complex geochemical processes associated with CCS operations and emphasizes the necessity for comprehensive impact assessment and monitoring protocols in carbon storage project development.

Keywords : Carbon Capture and Storage (CCS); Quartz rock; Groundwater contamination; Mineral trapping

Introduction

The acceleration of industrial development and technological progress has significantly enhanced global living standards while simultaneously contributing to unprecedented levels of atmospheric carbon dioxide (CO_2) emissions, intensifying concerns about climate change and global warming. To address this critical environmental challenge, numerous nations worldwide, including Thailand, have committed to implementing comprehensive greenhouse gas reduction strategies, with Carbon Capture and Storage (CCS) emerging as a pivotal technology in this effort [1].

CCS represents a multi-stage process designed to mitigate CO_2 emissions from major industrial and energy sectors by capturing carbon dioxide at its source and permanently storing it in suitable geological formations. Despite its promising potential for climate change mitigation, CCS implementation raises significant concerns regarding the long-term integrity of storage sites, particularly the risk of CO_2 leakage through fractured rock formations or contamination of groundwater resources. These challenges necessitate comprehensive research and continuous monitoring protocols to ensure the safe and sustainable deployment of CCS technology over extended timeframes [2].

The fundamental mechanisms of CO_2 sequestration in geological formations involve complex interactions between gas, liquid, and solid phases, resulting in four distinct trapping mechanisms that operate over different temporal scales [3], (Figure 1). Structural and stratigraphic trapping serves as the primary containment method, utilizing impermeable cap rock layers to prevent vertical migration of supercritical CO_2 from porous reservoir rocks. Residual trapping occurs through capillary forces that immobilize CO_2 within pore spaces after water displacement. Dissolution trapping involves the formation of carbonic acid through CO_2 dissolution in formation water, creating bicarbonate and carbonate ions that increase fluid density and enhance storage security, particularly under high-salinity and low-temperature conditions. Mineral trapping [4]. represents the most thermodynamically stable sequestration mechanism, involving chemical reactions between dissolved CO_2 and divalent cations such as calcium (Ca^{2+}) and magnesium (Mg^{2+}) to form stable carbonate minerals including calcite ($CaCO_3$) and magnesium carbonate ($MgCO_3$) [5]. The ability of quartz-rich formations to support the process of CO_2 storage in the form of mineral trapping is crucial for the effectiveness of geological CO_2 sequestration, playing an important role in mitigating climate change [6]. Research has shown that the geochemical interactions in these formations can lead to the formation of stable carbonates, further strengthening their role in CO_2 storage [7]. In the study of the long-term stability of CO_2 storage in quartz rock within synthetic groundwater, along with the potential risk of CO_2 leakage from the storage site, continuous research and monitoring over a period of 2 to 10 years were suggested to ensure the safety and long-term effectiveness of CO_2 sequestration for future sustainability.

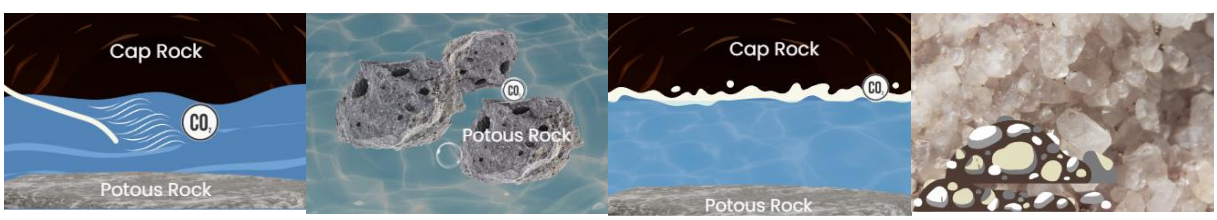

a. Structural and stratigraphic trapping b. Residual trapping c. Dissolution trapping d. Mineral trapping

Figure 1 Carbon dioxide capture processes of carbonation interactions

Thailand's Khorat Plateau region contains extensive quartz-rich geological formations that present unique opportunities for CO_2 sequestration research. Quartz formations, primarily composed of silicon dioxide, frequently contain associated minerals such as feldspar that provide essential calcium and magnesium content necessary for mineral trapping processes [3]. The porous microstructure of these quartz rocks potentially enhances their CO_2 storage capacity through increased surface area for geochemical reactions and improved permeability for fluid flow. The formation of dissolution-resistant carbonate minerals through CO_2-water-rock interactions represents a critical pathway for long-term carbon sequestration, with research demonstrating the potential for stable carbonate formation in quartz-rich environments [6, 7].

However, the geochemical processes associated with CO_2 injection create significant environmental considerations that require careful evaluation [8, 9]. The dissolution of CO_2 in groundwater produces carbonic acid [10], lowering pH and promoting enhanced mineral dissolution and ion mobilization. Previous studies have documented the release of various cations including Ca^{2+}, Mg^{2+}, and potentially toxic heavy metals such as Pb^{2+}, As^{2+}, and Zn^{2+} from host rock formations following CO_2 exposure [11]. These geochemical alterations can substantially impact groundwater quality through changes in taste, odor, color, and overall potability [12], while also affecting key water chemistry parameters including Total Dissolved Solids (TDS), bicarbonate (HCO^{3-}), and sulfite (SO_3^{2-}) concentrations. Although Oxidation Reduction Potential (ORP) typically remains stable during these processes [13], the cumulative effects on groundwater systems highlight the critical importance of comprehensive impact assessment and monitoring strategies.

Given the absence of previous research examining quartz rock formations for CO_2 sequestration applications in Thailand, this study addresses a significant knowledge gap in understanding the geochemical behavior of Thailand's geological formations under CCS conditions. The research aims to evaluate the CO_2 storage potential of quartz rocks from the Khorat Plateau while simultaneously assessing the associated impacts on groundwater chemistry and heavy metal mobilization. Through systematic investigation of physical and chemical changes in both rock and water phases following CO_2 exposure, this study seeks to provide essential data for evaluating the feasibility and environmental implications of implementing CCS technology using Thailand's indigenous geological resources. The findings will contribute to the broader understanding of CO_2-water-rock interactions in tropical geological settings and support evidence-based decision-making for future CCS deployment in Southeast Asia.

Materials and Methods

Synthetic groundwater

Synthetic water was prepared using the references data of the groundwater sampling from the well number of 5705D015 in Korat basin, Mueang Nakhon Ratchasima, Nakhon Ratchasima, Thailand. The synthetic water contained 19 mg/L of magnesium ion (Mg^{2+}) and 39 mg/L of calcium ion (Ca^{2+}). The reference data of the heavy metal concentration on this groundwater are less than the Thailand groundwater quality standard and provided in the Table 1.

Synthetic groundwater was prepared to replicate the chemical composition of local groundwater samples. To simulate the acidic conditions resulting from CO_2 injection, the solution was saturated with carbon dioxide, achieving a pH of approximately 5. Quartz rock samples were then immersed in the CO_2 saturated synthetic groundwater. The experiments were conducted under atmospheric conditions, and changes in the quartz were monitored over a 28-day period. The temperature, total dissolved solid (TDS), pH, and conductivity were measure daily using the Multi-parameter PCS Tester 35#ECPCSTEST35. The suspended solid (SS), alkalinity (Alk), hardness, and heavy metals were analyzed before (day 0) and after the period (day 28).

Table 1 Table of heavy metal concentrations in the Khorat Basin and groundwater quality standards [14–16]

Parameters	Sampling	Thailand standards (2009)	WHO standards (2004)	EPA standards (2018)
Ca^{2+}	39	-	-	-
Mg^{2+}	19	-	-	-
Fe (mg/L)	0.1	< 0.5	-	< 0.3
Mn (mg/L)	nd	< 0.3	< 0.4	< 0.05
Cu (mg/L)	nd	< 1	< 2.0	< 1.3
Zn (mg/L)	1.6	< 5	-	< 5
Pb (mg/L)	0.001	< 0.05	< 0.01	< 0.015
Cr (mg/L)	< 0.0024	-	-	-
As (mg/L)	< 0.0028	<0.05	<0.01	<0.01

Quartz rock

Quartz rock samples were collected from the Korat Basin, located in Mueang Nakhon Ratchasima, Nakhon Ratchasima Province, Thailand. A porous quartz sample was selected and cut into rough cubic pieces measuring approximately 30 × 33 × 48 mm to facilitate observation of changes during the experiment. The chemical and physical properties of the quartz were analyzed both before and after the 28-day immersion in CO_2-saturated synthetic groundwater. Two key parameters were measured: (1) the total mass of the rock, and (2) its mineral composition, determined using X-ray diffraction (XRD).

Results and Discussion

The results of the effect of carbon capture and storage (CCS) on quartz rock and groundwater in this study can be categorized into the effect to 1) pore fluid phase occurring in the synthetic groundwater with saturated CO_2 dissolution and 2) solid phase occurring in quartz rock. Testing parameters, methods and the results for liquid phase and solid phase were present in Table 2.

Pore fluid phase

After 28 days of soaking quartz rock samples in synthetic groundwater saturated with dissolved carbon dioxide gas, the distinguish changes in liquid were observed. Figure 2 showed the changes in water physical and chemical properties in the liquid phase during the samplings period. The temperature was almost steady at 26.7±0.61°C confirmed that observed changes are due to chemical processes, not thermal effects.

After injecting CO_2 gas into the synthetic groundwater (Day 0), CO_2 was transferred in the water and formed the liquid form dissolved CO_2. This hydrolysis process of CO_2 formed carbonic acid (H_2CO_3) which caused the pH drop to about 5, as shown in the following equations:

$$CO_2(g) \leftrightharpoons CO_2\,(aq) \qquad \textbf{Equation 1}$$

$$CO_2\,(aq) + H_2O(l) \leftrightharpoons H_2CO_3^-(aq) \qquad \textbf{Equation 2}$$

The decrease in pH is also associated with a decrease in oxidation-reduction potential (ORP), reflecting the increased reducing environment caused by CO_2 dissolution. Low pH and ORP enhance mineral weathering and metal leaching from rocks.

Then, there was a rapid increase in the pH, conductivity, and TDS in the first five days due to the reaction between the carbonate and hardness (Ca^{2+} and Mg^{2+}) and bicarbonate (HCO_3^-) of the synthetic groundwater. This process caused mineral trapping that the dissolution was transformed into other minerals by chemical precipitation process, as represented by the following equations:

$$Ca^{2+}, Mg^{2+} + CO_3^{2-}\,(aq) \rightarrow CaCO_3\,(s), MgCO_3\,(s) \qquad \textbf{Equation 3}$$

Table 2 Result of testing parameters and methods for synthetic groundwater with saturated CO_2 dissolution and quartz rock

Testing	Day 0	Day 28	Test method
Pore fluid phase			
pH	5.25	8.49	Multi-parameter PCS Tester 35#ECPCSTEST35
Conductivity (µS/cm)	90.5	176.7	
TDS (mg/L)	64.1	125.0	
Alk (mg/L)	6.60	28.00	Titration method
Hardness (mg/L)	66.80	80.00	
TOC	-1.543	-13.080	Combustion catalytic oxidation method
Fe (mg/L)	nd	<0.05	Atomic Absorption Spectrometry
Mn (mg/L)	nd	<0.04	
Cu (mg/L)	nd	<0.03	
Zn (mg/L)	<0.04	0.10	
Pb (mg/L)	nd	<0.05	
Cr (mg/L)	nd	nd	
As (mg/L)	<0.002	<0.002	
Solid phase			
SS (mg/L)	0.5	6.0	Gravimetric method
Mass (g)	70.6854	70.8098	Gravimetric method
Quartz (%)	98.2	97.3	XRD, BrukerD8 Advance diffractometer, ICDD method
Calcite (%)	1.8	2.7	

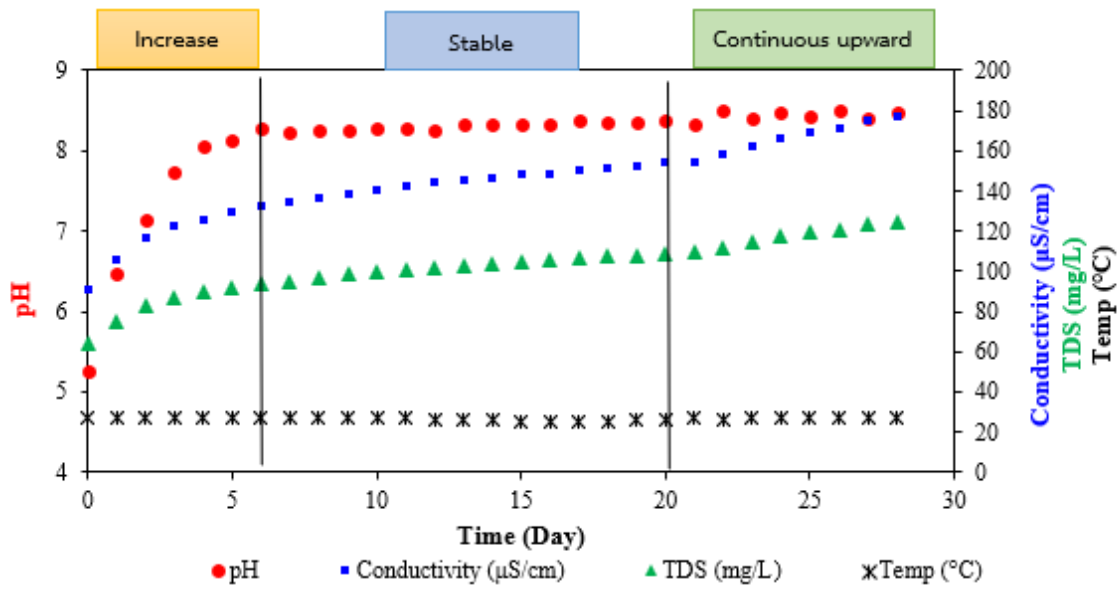

Figure 2 Temperature**,** pH, TDS, and conductivity of water sample over 28 days period

After that the pH was relatively stable after day at around 8-8.5 for the rest of the period, indicating a buffering reaction or the dissolution of alkaline minerals. Meanwhile, increases in conductivity, TDS, SS, alkalinity, hardness, and heavy metals (Fe, Mn, Cu, Zn, Pb, As) were observed due to the acidic properties of CO_2 dissolved in water. This led to the leaching of minerals and heavy metals from the quartz rock samples. However, the elevated values remained below the groundwater quality standards as shown in Table 1 [14]. The reactions mentioned above are expressed as follows.

$$H^+ + \text{Quartz rock} \rightarrow Ca^{2+}, Mg^{2+} + \text{heavy metal} \quad \textbf{Equation 4}$$

The overall, pH increased from acidic (~5.5) to alkaline (~8.5) due to neutralization of CO_2 acidified water by quartz or other minerals and conductivity and TDS trends reflect ongoing ion release into the solution. However, the experiment duration of 28 days is too short for the stabilization phase of the reaction between quartz rock and CO_2 dissolution. To observe clearer and stable results, a testing period of 2-10 years is required to allow the reactions occurring in the CO_2 dissolution process and mineral precipitation to fully take place, enabling effective carbon sequestration through mineral trapping [17].

Solid phase

The significant physical changes were observed indicating mineral trapping process. The dry mass increased by 0.18%, and the calcite structure within crystal morphology showed enhancement in the XRD (0.9%). This change indicated physical alterations resulting from the reaction between the rock and the water, leading to the formation and mineral precipitation of calcite. These changes suggested that CO_2 injection influenced both the pore fluid and the solid phase of the rock. During mineralization, divalent metal ions (M^{2+}) bond with carbonate ions, resulting in precipitation and the formation of stable calcite ($CaCO_3$) minerals [18] inside quartz rock structure.

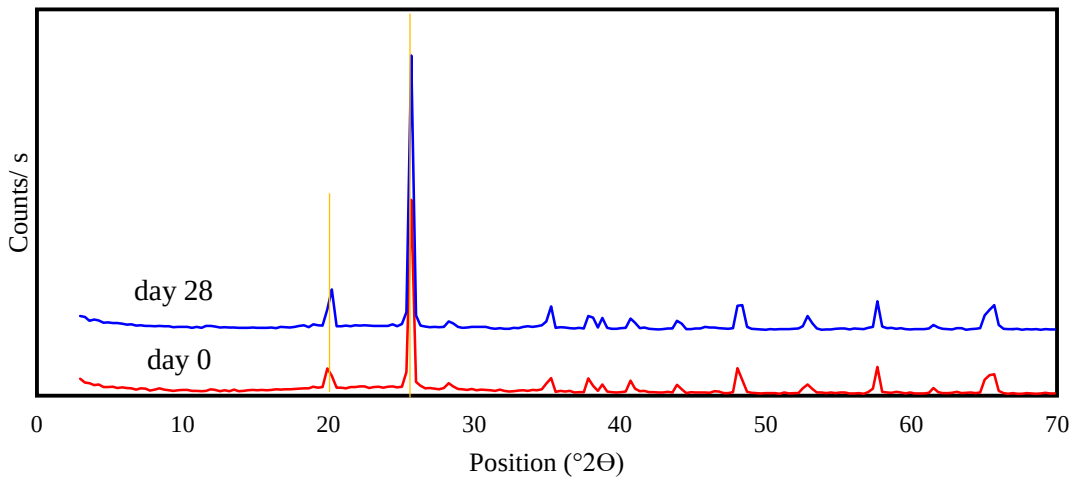

Figure 3 X-ray diffraction (XRD) of quartz rock at day 0 and day 28

Moreover, Figure 4 represented the occurrent of the small white precipitate in the sediments and beneath or around the edges of the rock and the increase of SS from 0.5 mg/l to 6 mg/l confirmed the mineral trapping process of divalent metal ions (M^{2+}) bond with carbonate ions as presented in Equation 3. The minerals in quartz rock are abundant, and when a reaction occurs, it leads to the leaching of these minerals. This process results in the formation of heavy metals in a dissolved form in the water, which then precipitate and form solid compounds [17].

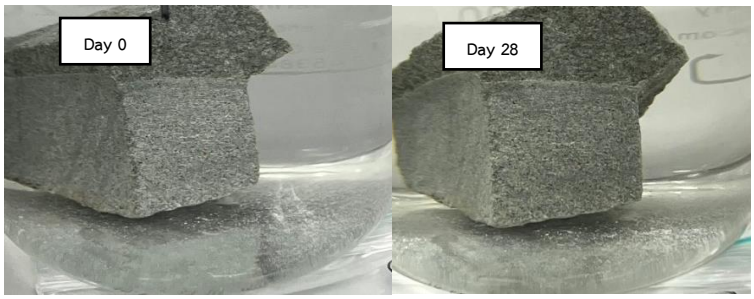

Figure 4 An experiment of soaking quartz rock in synthetic groundwater for a period of day 0 and day 28

Conclusions

This investigation of CO_2-water-rock interactions using quartz formations from Thailand's Korat basin provides valuable insights into the geochemical processes associated with carbon capture and storage implementation in tropical geological settings. The experimental findings demonstrate that quartz rock formations exhibit significant potential for CO_2 sequestration through multiple trapping mechanisms, while simultaneously revealing important environmental considerations that must be addressed in CCS project development.

Future research should focus on extending the experimental timeframe to better understand long-term geochemical evolution, investigating mitigation strategies for heavy metal mobilization, and conducting field-scale studies to validate laboratory findings under realistic geological conditions. This study represents a critical first step in evaluating CCS potential in Thailand and provides a foundation for evidence-based decision-making regarding the implementation of carbon sequestration technologies as part of the nation's climate change mitigation strategy. The findings emphasize that while geological CO_2 storage shows promise, successful implementation requires careful consideration of both storage efficiency and environmental protection to ensure sustainable and responsible deployment of CCS technology.

Acknowledgements

This work has partially received funding support from the National Scientific Research Fund via the Program Management Unit for Human Resources & Institutional Development, Research and Innovation (grant no. B40G660032), Chiang Mai University.

References

[1] Burnside NM, Naylor M. Review and implications of relative permeability of CO_2/brine systems and residual trapping of CO_2. 2014. International Journal of Greenhouse Gas Control. 23: 1-11. https://doi.org/10.1016/j.ijggc.2014.01.013.

[2] Gholami R, Raza A, Iglauer S. Leakage risk assessment of a CO_2 storage site: A review. 2021. Earth Sci Rev. 223: 103849. https://doi.org/https://doi.org/10.1016/j.earscirev.2021.103849.

[3] Zhao X, Liao X, Wang W, Chen C, Rui Z, Wang H. The CO_2 storage capacity evaluation: Methodology and determination of key factors. 2014. Journal of the Energy Institute. 87: 297-305. https://doi.org/https://doi.org/10.1016/j.joei.2014.03.032.

[4] Kim K, Kim D, Na Y, Song Y, Wang J. A review of carbon mineralization mechanism during geological CO_2 storage. 2023. Heliyon 9. https://doi.org/10.1016/j.heliyon.2023.e23135.

[5] Li Z, Lv Y, Liu B, Fu X. Reactive Transport Modeling of CO_2-Brine–Rock Interaction on Long-Term CO_2 Sequestration in Shihezi Formation. 2023. Energies (Basel) 16. https://doi.org/10.3390/en16020670.

[6] Fentaw JW, Emadi H, Hussain A, Fernandez DM, Thiyagarajan SR. Geochemistry in Geological CO_2

Sequestration: A Comprehensive Review. 2024. Energies (Basel) 17. https://doi.org/10.3390/en17195000.

[7] Jedli H, Hedfi H, Jbara A, Bouzgarrou S, Slimi K. Mineralogical and Geochemical Characteristics of Caprock Formations Used for Storage and Sequestration of Carbon Dioxide. 2015. Journal of Minerals and Materials Characterization and Engineering 03: 409-19. https://doi.org/10.4236/jmmce.2015.35043.

[8] Zhao Y, Wu S, Chen Y, Yu C, Yu Z, Hua G, et al. CO_2-Water-Rock Interaction and Pore Structure Evolution of the Tight Sandstones of the Quantou Formation, Songliao Basin. 2022. Energies (Basel) 15. https://doi.org/10.3390/en15249268.

[9] Ahmat K, Cheng J, Yu Y, Zhao R, Li J. CO_2-Water-Rock Interactions in Carbonate Formations at the Tazhong Uplift, Tarim Basin, China. 2022. Minerals 12. https://doi.org/10.3390/min12050635.

[10] Chang R, Kim S, Lee S, Choi S, Kim M, Park Y. Calcium carbonate precipitation for CO_2 storage and utilization: A review of the carbonate crystallization and polymorphism. 2017. Front Energy Res 5. https://doi.org/10.3389/fenrg.2017.00017.

[11] Zhao X, Deng H, Wang W, Han F, Li C, Zhang H, et al. Impact of naturally leaking carbon dioxide on soil properties and ecosystems in the Qinghai-Tibet plateau. 2017. Sci Rep 7. https://doi.org/10.1038/s41598-017-02500-x.

[12] Wei Y, Maroto-Valer M, Steven MD. Environmental consequences of potential leaks of CO_2 in soil. 2011. Energy Procedia, vol. 4, Elsevier Ltd, p. 3224-30. https://doi.org/10.1016/j.egypro.2011.02.239.

[13] Fagorite V, Chijioke F, Opara A, Onyekuru S, Oguzie E. Environmental and safety issues associated with geological carbon storage: a review. 2022. EuroMediterr J Environ Integr 7. https://doi.org/10.1007/s41207-022-00328-0.

[14] Department of Ground water Resources. Water Quality Report Of Thailand n.d.

[15] 2018 Edition of the Drinking Water Standards and Health Advisories Tables. Groundwater quality standards 2018.

[16] Thailand standards. 2009. Quality standards of Thailand. n.d.

[17] Fentaw JW, Emadi H, Hussain A, Fernandez DM, Thiyagarajan SR. Geochemistry in Geological CO_2 Sequestration: A Comprehensive Review. 2024. Energies (Basel) 17. https://doi.org/10.3390/en17195000.

[18] Ma J, Zhu X, Liu D, Wang S, Xue L, Li Q, et al. Effects of simulation leakage of CCS on physical-chemical properties of soil. 2014. Energy Procedia, vol. 63, Elsevier Ltd, p. 3215-9. https://doi.org/10.1016/j.egypro.2014.11.347.

Thai Environmental Engineering Journal Vol. 39 No. 2 (2025) : 9-17
www.eeat.or.th

Knowledge, Behavior, and Household Hazardous Waste Composition: Implications for Environmental Health in Nakhon Nayok Province, Thailand

Jitjira Chaiyarit[1], Kanittha Saengpae[2], Koranitch Jomkathok[2], Piyawan Roshom[2], Thananya Seehatab[2] and Prat Intarasaksit[2*]

[1]Department of Statistics, Faculty of Science, Khon Kaen University, Khon Kaen 40002, Thailand,
[2]Department of Public Health, Faculty of Physical Education, Sport and Health, Srinakharinwirot University, Bangkok 10110, Thailand
[*]E-mail : prat@g.swu.ac.th

Article History; *Received: 12 July 2025, Accepted: 18 August 2025, Published: 28 August 2025*

Abstract

Improper management of household hazardous waste (HHW) poses serious risks to environmental and public health, particularly in low-resource communities. This study examined the relationship between residents' knowledge and behavior regarding HHW management and assessed the composition of HHW generated at the household level in a community in Nakhon Nayok Province, Thailand. A cross-sectional study was conducted with 41 households using structured interviews and a seven-day HHW collection protocol. Descriptive statistics, Pearson correlation analysis, and physical waste composition assessment were applied. Findings revealed that 87.8% of respondents demonstrated high levels of knowledge, and 68.3% reported good HHW management practices. A statistically significant positive correlation was observed between knowledge and behavior ($r = 0.382$, $p = 0.014$), indicating that increased awareness modestly influenced safer practices. The HHW stream was primarily composed of pesticide containers (31.5%) and fluorescent bulbs (26.02%), reflecting potential environmental hazards in domestic waste streams. These results underscore the need for community-based interventions that combine public education with improved waste segregation systems. Targeted efforts to enhance awareness, infrastructure, and policy enforcement are essential to minimizing the environmental impact of HHW and protecting community health.

Keywords : Household hazardous waste; Waste management behavior; Environmental health; Waste composition analysis

Introduction

Municipal solid waste (MSW) presents a growing challenge for both urban and rural communities worldwide due to its escalating volume and increasingly complex composition [1]. Factors such as rapid urbanization, population growth, and evolving consumption patterns have significantly increased waste generation rates, placing immense strain on existing waste management infrastructure, particularly in developing countries [2]. Inefficiencies in collection, inadequate disposal systems, and limited public awareness continue to exacerbate both environmental degradation and public health threats [3, 4].

Among the various waste fractions, household hazardous waste (HHW) remains a less visible but highly consequential component of MSW. Although it constitutes a relatively small proportion of the total waste stream, HHW poses a disproportionately high risk to environmental and human health due to its toxic, corrosive, flammable, and reactive properties [5]. Common HHW sources include cleaning agents, disinfectants, pesticides, lubricants, batteries, and fluorescent lamps—many of which are

found in ordinary households and often disposed of improperly [5-7]. The residual contents of these products are hazardous and, when mixed with general waste, can contaminate landfills, leach into groundwater, or cause injuries to waste handlers [8].

HHW is particularly concerning in developing nations where segregation at source is rare and centralized treatment infrastructure is limited. In Thailand, HHW is routinely mixed with general household waste and collected without special handling by local authorities [9]. This practice increases the likelihood of environmental contamination and human exposure, especially among vulnerable populations such as children. Reported health risks include respiratory irritation, chemical burns, and accidental poisonings due to unsafe storage and disposal of hazardous household substances [10]. Inadequate public knowledge and behavioral practices further compound the risks, highlighting the need for targeted education and improved local waste governance [11].

While international studies have addressed HHW generation and its environmental impacts [12, 13], limited empirical research exists in the Thai context—particularly on the interplay between public knowledge, behavioral practices, and the physical composition of HHW at the household level. Understanding this relationship is essential for designing community-specific interventions, improving waste segregation systems, and informing local policy. Most existing studies have relied solely on self-reported knowledge or behavior data without validating those responses through actual waste audits. This approach limits the ability to assess whether awareness truly translates into safer HHW practices. Moreover, empirical data on HHW composition in semi-rural Thai households remain scarce. By integrating survey-based assessments with physical HHW collection and categorization, this study addresses a critical gap in evidence needed to support community-level interventions and policy design.

Therefore, this study aims to address this gap by (a) examining the relationship between knowledge and behavior in managing household hazardous waste, and (b) characterizing and quantifying HHW generated at the source in communities of Nakhon Nayok Province, Thailand.

Materials and Methods

Study Site and Population

This study was conducted in Tha Sai Subdistrict, Mueang District, Nakhon Nayok Province, Thailand. The target population comprised residents from seven villages within the subdistrict. A simple random sampling technique was used to select the study site. All seven villages were listed, and Village No. 5 (Ban Tha Sala) was randomly selected as the sampling location.

Sample Size Calculation

The sample size was calculated using the formula for estimating the population mean with known population size [14]. The population consisted of 155 households in Ban Tha Sala. The calculation was based on a 95% confidence level (CI) (Z = 1.96), a standard deviation (σ) of 1.5 derived from a previous study on knowledge of household hazardous waste management in That Subdistrict, Warin Chamrap District, Ubon Ratchathani Province [15], and a margin of error (d) of 0.4.

The sample size (n) was calculated as follows:

$$n = \frac{NZ_{\alpha/2}^2 \times \sigma^2}{d^2(N-1) + Z_{\alpha/2}^2\sigma^2}$$

Where:

n = required sample size
N = total population = 155 households
$Z_{\alpha/2}$ = standard normal critical value for 95%CI = 1.96
σ = standard deviation = 1.5 (from previous study [15])
d = acceptable margin of error = 0.4

Instrument Design

Data was collected using a structured questionnaire developed specifically for this study, comprising three main sections.

Section 1: General Information

This section included four closed-ended items capturing demographic information: gender, age, household size, and monthly household income.

Section 2: Knowledge of Household Hazardous Waste (HHW)

This section consisted of 15 closed-ended questions assessing participants' knowledge of HHW. Each correct response received one point; incorrect responses were scored zero. Total scores ranged from 0 to 15. Knowledge levels were classified into three categories using equal intervals: 0–5: Low, 6–10: Moderate; 11–15: High.

Section 3: Behavior in HHW Management

Fifteen items assessed HHW management behavior using a five-point Likert scale: "Always," "Often," "Sometimes," "Rarely," and "Never." The items included nine positive and six negative statements. Responses were scored such that higher values reflected more desirable behaviors, resulting in total scores ranging from 15 to 75. Behavior levels were classified as: 15–34: Low (needs improvement), 35–55: Moderate, 56–75: High (good behavior). The full questionnaire used to assess knowledge and behavior, the corresponding scoring rules, and the household hazardous waste (HHW) sorting taxonomy applied in this study are provided in the Supplementary Material (Appendices A–C).

Reliability Testing

The questionnaire was pilot tested with 30 individuals from a population similar to the study sample. Internal consistency for the knowledge section was measured using the Kuder-Richardson Formula 20 (KR-20), yielding a coefficient of 0.66, indicating moderate reliability. For the behavior section, Cronbach's alpha was 0.84.

HHW Composition Data Collection

To assess household HHW composition, a structured seven-day waste collection protocol was employed. Data collection was conducted over a continuous seven-day period in May 2025, following ethics approval. The selected timeframe avoided public holidays to better reflect typical household waste generation patterns. Each participating household received a dedicated container for separating HHW from general waste. Prior to the collection period, participants were trained using educational materials—such as posters and leaflets—that clearly explained the definition, types, and examples of HHW. Households were instructed to place items such as expired medications, used batteries, pesticide containers, and fluorescent bulbs into the provided containers. At the end of the seven-day collection period, the HHW from each household was retrieved, sorted, and categorized by type. Each category was weighed using a calibrated digital scale, and both the total weight and percentage composition of each HHW type were recorded and analyzed accordingly.

Statistical analysis

Data were analyzed using both descriptive and inferential statistics. For categorical (count) data, descriptive statistics included frequency and percentage. For continuous data, mean, standard deviation, median, minimum, and maximum values were calculated to describe central tendency and dispersion. To test the study hypothesis, Pearson's correlation coefficient was employed to examine the relationship between knowledge of household hazardous waste (HHW) and behavior in HHW management. The null hypothesis (H_0) posits that there is no correlation between knowledge and behavior in HHW management, while the alternative hypothesis (H_1) states that a correlation exists. The strength of the correlation was interpreted as follows: a correlation coefficient between 0.00 and 0.30 was considered negligible, 0.31 to 0.50 indicated a low correlation, 0.51 to 0.70 represented a moderate correlation, 0.71 to 0.90 was interpreted as a high correlation, and 0.91 to 1.00 indicated a very high correlation. All analyses were performed using IBM SPSS Statistics version 28.

Research ethics

The study was reviewed and approved by the Human Research Ethics Committee of Srinakharinwirot University, Thailand (reference no. SWUEC-681028)

Results and Discussion

This section presents the demographic and socioeconomic characteristics of the 41 households participating. The majority of respondents were female (n = 30, 73.2%), while male respondents accounted for 26.8% (n = 11). The mean age was 63.2 years (SD = 14.02), with a range of 33 to 91 years and a median age of 62 years. Regarding household size, most participants lived in households comprising three members. The average household size was 3.37 persons (SD = 1.99), with household sizes ranging from one to nine members. Concerning

household income, 87.8% of respondents (n = 36) provided income information. The mean monthly household income was 9,897.56 Thai Baht (SD = 14,076.31), while the median income was 5,000 Baht. Reported income ranged from a minimum of 600 Baht to a maximum of 80,000 Baht per month.

These findings indicate a predominance of older, female respondents with modest household sizes and relatively low-income levels, which may influence their capacity to manage household hazardous waste effectively.

The analysis revealed that most respondents (n = 36, 87.8%) demonstrated a high level of knowledge concerning household hazardous waste (HHW). A smaller proportion (n = 5, 12.2%) exhibited a moderate level of knowledge. Notably, none of the participants were classified as having low knowledge or falling into the "needs improvement" category. These findings suggest that the study population possesses a relatively strong awareness of HHW issues, which may be attributed to previous exposure to local public health campaigns, educational materials, or environmental initiatives. However, the absence of respondents in the low-knowledge category warrants further investigation to determine whether this reflects actual awareness or potential response bias.

The results indicated that most respondents (n = 28, 68.3%) exhibited good behavior in managing household hazardous waste (HHW), while the remaining 13 participants (31.7%) demonstrated moderate behavior. No respondents fell into the category requiring improvement. This behavioral profile reflects a generally high level of engagement with proper HHW management practices among participants.

Table 1 Socioeconomic of respondents

Characteristics	Number (Percentage)
Sex	
Male	11 (26.8)
Female	30 (73.2)
Age (yeas)	
Mean ± SD	63.2 ± 14.02
Median (Min – Max)	62 (33 – 91)
Household size	
Mean ± SD	3.37 ± 1.99
Median (Min – Max)	3 (1 – 9)
Monthly Household Income (THB)	
Mean ± SD	9,897.56 ± 14,076.31
Median (Min – Max)	5,000 (600 – 80,000)

Table 2 Knowledge Level of Respondents on Household Hazardous Waste (n = 41)

Knowledge Level	Frequency (n)	Percentage (%)
High knowledge	36	87.8
Moderate knowledge	5	12.2
Needs improvement	0	0.0
Total	41	100.0

Table 3 Behavior Level of Respondents in Managing Household Hazardous Waste (n = 41)

Behavior Level	Frequency (n)	Percentage (%)
Good behavior	28	68.3
Moderate behavior	13	31.7
Needs improvement	0	0.0
Total	41	100.0

The relationship between respondents' knowledge of household hazardous waste (HHW) and their behavior in HHW management was analyzed using Pearson's correlation coefficient. The analysis revealed a statistically significant positive correlation ($r = 0.382$, $p = 0.014$), indicating a low but meaningful association between the two variables. Given that the p-value was less than the threshold of 0.05, the null hypothesis (H_0)—which posits no relationship between knowledge and behavior—was rejected. These findings suggest that individuals with higher levels of HHW-related knowledge were more likely to engage in appropriate and safer waste management practices. Although the correlation strength was modest, the result aligns with previous research highlighting the influence of knowledge on environmentally responsible behavior. This underscores the potential value of targeted educational interventions to promote better household practices in managing hazardous waste.

Knowledge and Behavior in Managing Household Hazardous Waste

The findings revealed that most respondents demonstrated a high level of knowledge regarding household hazardous waste (HHW), with a mean score of 12.07 out of 15. This indicates a strong general understanding of HHW, including its definition, associated health and environmental hazards, and appropriate disposal practices [16, 17]. High accuracy in items related to chemical packaging, fluorescent bulbs, and awareness of community risks suggests that recent public health campaigns or environmental education efforts may have played a role in raising awareness [18, 19]. In terms of behavior, 68.3% of households demonstrated good HHW management practices. These included proper segregation of waste, use of sealed containers, and disposal via designated hazardous waste collection systems. Such behavior may reflect the influence of Thailand's national policies and local infrastructure supporting community-level HHW management [5].

However, some unsafe practices persist. These include the reuse of hazardous containers—such as paint cans—and improper disposal of expired medications. This finding aligns with prior studies showing that high knowledge does not always translate into safe behavioral practices due to low-risk perception, convenience barriers, or habitual routines [20].

The Pearson correlation analysis identified a statistically significant but low positive relationship between knowledge and behavior ($r = 0.382$, $p = 0.014$). This suggests that while knowledge is a contributing factor to improved HHW practices, it may not be sufficient alone. Behavioral outcomes are likely influenced by a combination of factors including infrastructure access, convenience, perceived risk, and social norms [21, 22]. These findings reinforce the need for interventions that combine educational outreach with improvements in local waste handling systems and behavioral nudges. While this study provides important insights into HHW management at the household level, it is important to acknowledge that the findings are based on a relatively small sample size ($n = 41$) drawn from a single semi-rural village. This limitation may restrict the generalizability of the results to broader populations. Nevertheless, the observed HHW composition patterns and the knowledge–behavior relationship are broadly consistent with previous community-based studies in similar contexts. Future research involving larger and more diverse populations across different geographic regions is warranted to validate and expand on these findings.

Table 4 Correlation Between Knowledge and Behavior in Household Hazardous Waste Management (n = 41)

Variables	Pearson Correlation (r)	*p*-value
Knowledge of HHW	1	
Behavior in HHW Management	0.382	0.014

Although 87.8% of participants demonstrated high knowledge regarding HHW, this did not fully eliminate unsafe disposal practices. Several underlying factors may explain this gap. First, perceived risk plays a significant role; individuals may underestimate the hazards of certain actions (e.g., reusing pesticide containers or discarding expired medicine into household trash) [20, 21]. Second, convenience and habit influence decision-making—many respondents lack access to specialized disposal infrastructure or have long-standing routines that are difficult to change [22]. Third, social norms and cultural practices can reinforce unsafe methods, particularly in semi-rural contexts [18, 19]. Finally, limited local enforcement and inadequate collection systems may reduce motivation to act on knowledge [5, 6]. These findings underscore the need for interventions that combine awareness with practical systems and community engagement.

Composition of Household Hazardous Waste

A total of 7.3 kilograms of household hazardous waste (HHW) was collected during the 7-day study period from 41 participating households, which collectively comprised 138 individuals. This corresponds to an average generation rate of approximately 0.178 kilograms per household and 0.053 kilograms per capita. These figures provide additional context for the percentage-based composition data shown in Figure 1. The HHW composition analysis showed that pesticide containers were the most common waste type, accounting for 31.5% of the total volume collected. This was followed by fluorescent bulbs (26.02%), paint containers and household cleaning products (each 9.58%), electronic waste (8.21%), engine oil containers (5.47%), and thinner bottles (5.47%). Less common items included laundry cleaning products (2.73%) and electrical wires (1.36%). These findings reveal that chemical- and lighting-related materials dominate the HHW stream, reflecting household practices typical of semi-rural or agricultural communities, where pesticide use is common and fluorescent lighting remains prevalent [23, 24]. The presence of items such as electronic components, engine oil containers, and solvent bottles suggests increased access to commercial and industrial-grade household products, which may not be disposed of safely without adequate public guidance.

Even less frequently occurring HHW items, such as laundry cleaners and electrical wires, represent potential health and environmental hazards if improperly managed. These materials can leach toxic substances into the environment or pose fire and injury risks if not segregated and processed appropriately [25-27].

The diversity of HHW types identified in this study highlights the urgent need for community-level interventions that promote safer handling, facilitate waste separation at source, and expand accessible collection infrastructure—particularly in semi-rural settings where mixed waste collection remains the norm.

As shown in Figure 1, pesticide containers accounted for the largest share of household hazardous waste (31.5%), followed by fluorescent bulbs (26.02%). Paint containers, household cleaning products, and electronic waste each comprised around 9-10% of the total. Less prevalent items included engine oil containers, thinner bottles, laundry cleaning products, and electrical wires.

These findings highlight the predominance of chemical-based and lighting-related waste in semi-rural households, likely reflecting common domestic and agricultural practices. The data underscore the need for improved community-level HHW collection infrastructure and targeted public education to address the safe disposal of hazardous materials.

The predominance of pesticide containers (31.5%) and fluorescent bulbs (26.02%) among the HHW stream poses significant environmental and health concerns. Pesticide containers often retain hazardous residues, and improper disposal (e.g., burning, reuse, or disposal of general waste) can lead to soil and water contamination or accidental poisoning. Fluorescent bulbs contain mercury vapor, which is highly toxic if released through breakage during storage or collection. These findings suggest an urgent need for safe storage guidelines at the household level and accessible drop-off systems for such high-risk items. Local governments should consider policy interventions to promote safe handling, including public education, enforcement of proper disposal standards, and investment in HHW-specific infrastructure. Risk-based prioritization of HHW categories—such as chemical and mercury-containing items—could help optimize limited resources and reduce community-level exposure risks.

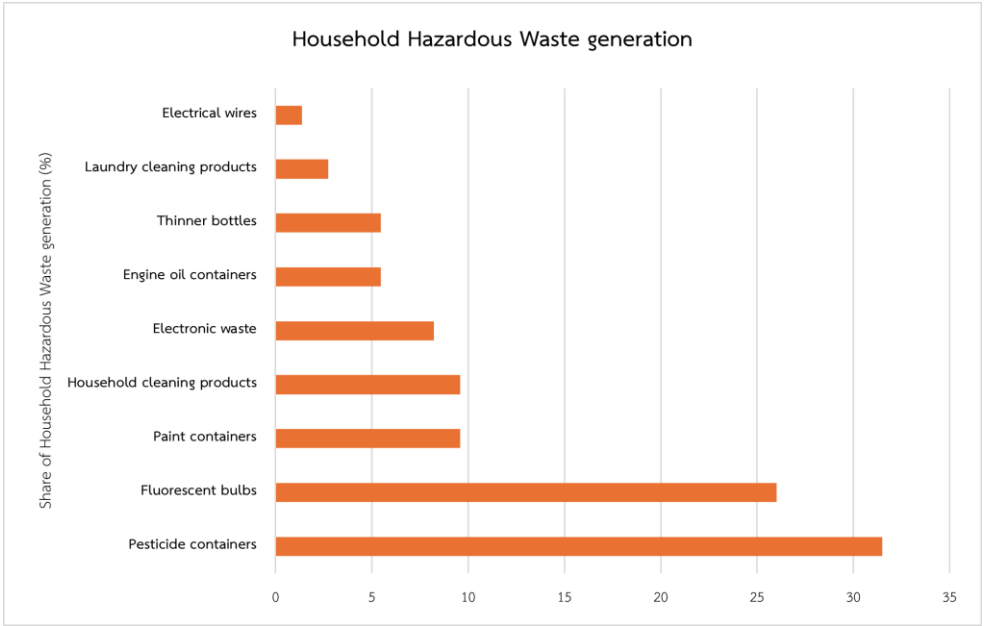

Figure 1 Percentage Composition of Household Hazardous Waste by Type (n = 41 households)

The use of pre-distribution educational materials (e.g., posters, brochures) in this study proved effective in improving source separation and HHW tracking. This aligns with prior studies demonstrating that providing households with knowledge *before* the act of disposal can significantly influence behavioral outcomes [28, 29]. Integrating public awareness campaigns with practical tools—such as clearly labeled containers and visual guides—can strengthen safe HHW practices in resource-limited settings.

Despite its contributions, this study has several limitations. First, the sample size was relatively small (41 households) and drawn from a single village, limiting generalizability. Second, self-reported knowledge and behavior data may be subject to social desirability bias. Although training and anonymity were used, some bias may persist. Third, the HHW audit was conducted over a single week in May, and seasonal variation could not be assessed. Finally, while regression analysis was considered, insufficient power (post hoc power = 0.481) limited its feasibility. Future research should involve larger, more diverse samples, cover multiple time points, and apply multivariate methods to better understand the knowledge–behavior gap and inform targeted interventions.

Conclusions

This study found that households in Ban Tha Sala, a semi-rural community in Nakhon Nayok Province, generally exhibited high levels of knowledge and good behavior regarding the management of household hazardous waste (HHW). However, the modest positive correlation between knowledge and behavior suggests that awareness alone does not guarantee safe disposal practices. The predominance of pesticide packaging and fluorescent bulbs in the HHW stream points to context-specific risks linked to agricultural and domestic lighting practices.

While these results are rooted in the conditions of Ban Tha Sala, they also mirror challenges faced by other semi-rural areas across Thailand, where HHW is often mixed with general waste due to infrastructural limitations and the absence of targeted local waste policies. Addressing these issues requires more than education alone. Community interventions should combine awareness campaigns that address behavioral norms and perceived risks with practical solutions, such as designated HHW drop-off points and integration of HHW management into school curricula and local health promotion activities.

At the policy level, local administrative organizations (LAOs) can utilize the study findings to inform planning and budgeting for HHW-specific services. For example, evidence from this study supports the establishment of household-level HHW collection points, community-based educational initiatives, and integration of HHW management into existing health promotion campaigns. In addition, collaboration between LAOs and national agencies could help standardize HHW protocols and secure sustainable funding mechanisms. These steps would help bridge the current implementation gap between knowledge and behavior while building long-term community resilience in waste governance. Further studies with expanded sampling frames are recommended to enhance the external validity of findings and support the development of scalable HHW management strategies at regional and national levels.

Supplementary Material

Supplementary data associated with this article, including the full questionnaire (Appendix A), scoring rules (Appendix B), and the HHW sorting taxonomy (Appendix C), are available in the online version of the paper.

References

[1] Pujara, Y., Pathak, P., Sharma, A. and Govani, J. 2019. Review on Indian Municipal Solid Waste Management practices for reduction of environmental impacts to achieve sustainable development goals. Journal of Environmental Management. 248: 109238.

[2] Intarasaksit, P. and Chaiyarit, J. 2021. Factors influencing appropriate management of household waste in developing country. Asia-Pacific Journal of Science and Technology. 26(01): APST-26-01-6.

[3] Khan, S., Anjum, R., Raza, S.T., Ahmed Bazai, N., and Ihtisham, M. 2022. Technologies for municipal solid waste management: Current status, challenges, and future perspectives. Chemosphere. 288 (Pt 1): 132403.

[4] Vyas, S., Prajapati, P., Shah, A.V., Varjani S. 2022. Municipal solid waste management: Dynamics, risk assessment, ecological influence, advancements, constraints and perspectives. Sci Total Environ. 814: 152802.

[5] Chaiyarit, J. and Intarasaksit, P. 2021. Household hazardous waste characterization and quantification at source in Thailand. Journal of the Air & Waste Management Association. 71(8): 989-94.

[6] Intarasaksit, P. and Pitaksanurat, S. 2019. Factors influencing appropriate management of household hazardous waste in Nakhon Nayok, Thailand: A multilevel analysis. J Air Waste Manag Assoc. 69(3): 313-9.

[7] Slack, R. and Letcher, T.M. 2011. Chapter 13 - Chemicals in Waste: Household Hazardous Waste. In: Letcher, T.M., Vallero, D.A., editors. Waste. Boston: Academic Press. 181-95.

[8] El-Saadony, M.T., Saad, A.M., El-Wafai, N.A., Abou-Aly, H.E., Salem, H.M., Soliman, S.M. and *et. al.* 2023. Hazardous wastes and management strategies of landfill leachates: A comprehensive review. Environmental Technology & Innovation. 31: 103150.

[9] Atthirawong, W. and Luangpaiboon, P. 2022. Hazardous waste management system for Thailand's local administrative organization via route and location selection. J Air Waste Manag Assoc. 72(10): 1121-36.

[10] Adelodun, B., Ajibade, F.O., Ibrahim, R.G., Ighalo, J.O., Bakare, H.O., Kumar, P. and *et. al.* 2021. Insights into hazardous solid waste generation during COVID-19 pandemic and sustainable management approaches for developing countries. J Mater Cycles Waste Manag. 23(6): 2077-86.

[11] Gutberlet, J. and Uddin, S.M.N. 2017. Household waste and health risks affecting waste pickers and the environment in low- and middle-income countries. Int J Occup Environ Health. 23(4): 299-310.

[12] Kumar, A., Thakur, A.K., Gaurav, G.K., Klemeš, J.J., Sandhwar, V.K., Pant, K.K. and *et. al*. 2023. A critical review on sustainable hazardous waste management strategies: a step towards a circular economy. Environmental Science and Pollution Research. 30(48): 105030-55.

[13] Lin, K., Zhao, Y. and Kuo, J.H. 2023. Data-driven models applying in household

hazardous waste: Amount prediction and classification in Shanghai. Ecotoxicol Environ Saf. 263: 115249.

[14] Daniel, W.W. 2005. Biostatistics : a foundation for analysis in the health sciences, 8th Edition. Hoboken, NJ: Wiley.

[15] Junsiri, S., Chaikhan, S., Anthaworapong, N., Thongdamrongtham, S. and Supasuk, D. 2022. Association between Knowledge, Attitudes, and Behavior of Household Hazardous Waste Management in That Sub-district, Warinchamrab Ubon Ratchathani. Journal of Health Science of Thailand. 31(3): 404-15.

[16] Decharat, S., Buacharoen, T., Khongrit, V. and Ridchuayrod, S. 2020. Residents' Awareness, Attitudes and Perceptions of Household Hazardous Waste Management in Pa-payom, Phatthalung: Knowledge, Attitude and Perception of the People in Household Hazardous Waste Management. Journal of Southern Technology. 13(1): 178-90.

[17] Safari, Y., Karimyan, K., Gupta, V.K., Ziapour, A., Moradi, M., Yoosefpour, N. and *et. al*. 2018. A study of staff's awareness and attitudes towards the importance of household hazardous wastes (HHW) management (A Case Study of Kermanshah University of Medical Sciences, Kermanshah, Iran). Data in Brief. 19: 1490-7.

[18] Janmaimool, P. 2017. Investigating pro-environmental behaviors of well-educated people in Thailand. International Journal of Sociology and Social Policy. 37(13/14): 788-807.

[19] Yukalang, N., Clarke, B. and Ross, K. 2017. Barriers to Effective Municipal Solid Waste Management in a Rapidly Urbanizing Area in Thailand. Int J Environ Res Public Health. 14(9): 1013.

[20] Janmaimool, P., Chontanawat, J. and Chudech, S. 2024. The effects of perceptions of environmental health risk and environmental risk on sustainable infectious waste management behaviours among citizens in Bangkok, Thailand. Cleaner and Responsible Consumption. 12: 100175.

[21] Chikowore, N. 2021. Factors influencing household waste management practices in Zimbabwe. Journal of Material Cycles and Waste Management. 23(1): 386-93.

[22] Knickmeyer, D. 2020. Social factors influencing household waste separation: A literature review on good practices to improve the recycling performance of urban areas. Journal of Cleaner Production. 245: 118605.

[23] Bondori, A., Bagheri, A., Allahyari, M.S. and Damalas, C.A. 2018. Pesticide waste disposal among farmers of Moghan region of Iran: current trends and determinants of behavior. Environ Monit Assess. 191(1): 30.

[24] Zhang, Y., Zhang, M., Weng, Z., Gao, X. and Liao, W. 2023. The Influence of Social Norms and Environmental Regulations on Rural Households' Pesticide Packaging Waste Disposal Behavior. Sustainability. 15(22): 15938.

[25] Dumas, O. and Le Moual, N. 2020. Damaging effects of household cleaning products on the lungs. Expert Rev Respir Med. 14(1): 1-4.

[26] Pacheco Da Silva, E., Dumas, O., and Le Moual, N. 2025. Effects of household cleaning products on the lungs: an update. Expert Rev Respir Med. 19(4): 313-24.

[27] Salonen, H., Salthammer, T., Castagnoli, E., Täubel, M. and Morawska, L. 2024. Cleaning products: Their chemistry, effects on indoor air quality, and implications for human health. Environ Int. 190: 108836.

[28] Robat, D.S., Sany, S.B.T., Siuki, H.A., Peyman, N. and Ferns, G. 2022. Impact of an Educational Training on Behavioral Intention for Healthcare Waste Management: Application of Health Action Model. Community Health Equity Research & Policy. 42(3): 299-307.

[29] Torres-Pereda, P., Parra-Tapia, E., Rodríguez, M.A., Félix-Arellano, E. and Riojas-Rodríguez, H. 2020. Impact of an intervention for reducing waste through educational strategy: A Mexican case study, what works, and why? Waste Manag. 114: 183-95.

Thai Environmental Engineering Journal Vol. 39 No. 2 (2025) : 19-30
www.eeat.or.th

The Variability in Soil Community and Its Enzymatic Function to Plant Promotion after Biochar Addition

Mujalin Pholchan[1*], Jearanai Thassana[2] and Khajitmanee Muangprom[3]

[1,2,3]Environmental Technology, Faculty of Science,
Maejo University, Chiangmai 50290, Thailand
[*]E-mail : mujalin@mju.ac.th

Article History; *Received: 1 July 2025, Accepted: 19 August 2025, Published: 28 August 2025*

Abstract

The widespread use of chemical inputs in contemporary agriculture has raised concerns regarding long-term soil health and sustainability. Biochar (BC), a carbon-rich byproduct of biomass pyrolysis, presents a viable alternative, offering improvements in soil structure, nutrient retention, and microbial activity. This study investigates the effects of modified biochar on soil microbial diversity and associated metabolic pathways that contribute to soil fertility and plant productivity. Five soil samples (D1 control without BC, D2 paddy field 1, D3 paddy field 2, D4 eggplant field, and D5 long yard bean field) were collected from agricultural sites for microbial community profiling. Metagenomic DNA was extracted and analyzed using QIIME2. A total of 371 microbial species were identified across samples. D1 exhibited dominance of Proteobacteria, Acidobacteriota, and Halobacterota. In contrast, D2–D5 showed increased abundance of Firmicutes and Actinobacteriota, with the emergence of phyla such as WPS-2 and the enrichment of functional genera including the ammonia-oxidizing bacterium MND1. Bacilli were detected in all samples, with the highest relative abundance observed in D5 (8.34%). Notably, Bacillus sp.—a component of the applied BC—was more abundant in D4 (0.12%) and D5 (0.58%) than in D1 (0.02%), indicating BC's potential to retain and promote beneficial microbial taxa. Microbial richness was highest in D2 (4887 OTUs), exceeding that of the control (D1, 4517 OTUs), confirming the diversity-enhancing effect of BC. D4 exhibited the most distinct microbial community (3403 OTUs). Functional annotation revealed increased abundance of proteins such as COG1595 and key enzymes including EC:2.7.7.7 and EC:1.6.5.3, which are associated with nucleotide synthesis and redox metabolism. The metabolic pathway PWY-3781 was most prominent post-BC application, with pathways PWY-7111, PWY-6277, and PWY-6122 also enriched in D3 compared to D1.These findings demonstrate that biochar promotes microbial diversity, enhances beneficial microbial populations, and activates key metabolic pathways, thereby contributing to improved soil quality and supporting sustainable agricultural practices.

Keywords : biochar; microbial diversity; metabolic pathways; plant growth; soil fertility

Introduction

Contemporary agriculture relies on chemicals to achieve high-quality yields. However, the long-term and repeated use of chemicals in the same area not only decreases soil quality but also disrupts and damages the soil microbial system. Therefore, the shift towards using biological materials instead of chemicals is an alternative that should be given attention. Biochar is an agricultural waste from the pyrolysis process. It is an environmentally friendly biological material at a low cost that has been widely applied in environmental studies due to its various properties e.g. high carbon content, large surface area, high cation exchange capacity, and stable structure [1]. Due to its adsorption capacity, biochar is an effective biological material for eliminating contaminants [2], including heavy metal pollutants [3] and organic contaminants such as dyes [4]. Moreover, biochar is also used to improve soil quality and promote plant growth. Biochar has been used to examine soil properties and the growth of plants. It helps increase the pH of the soil and promotes higher final biomass, root biomass, plant height, and number of leaves [5].

In addition to its physical and chemical benefits, biochar also influences the soil microbiome. Previous studies have reported that biochar application can increase microbial diversity [6], including a substantial rise in beneficial genera such as Bacillus and Pseudomonas by up to 100% [7], both of which are known to promote plant growth and nutrient cycling. Some studies have also shown that biochar can increase soil enzyme activity, such as urease activity by 23.1%, alkaline phosphatase activity by 25.4%, and dehydrogenase activity by 19.8% [8]. Biochar has also been shown to enhance soil enzyme activities, with increases of 23.1% in urease, 25.4% in alkaline phosphatase, and 19.8% in dehydrogenase activity [8]. Despite these promising findings, most research has concentrated on short-term effects, leaving long-term impacts on microbial diversity, abundance, and functional dynamics less understood. Moreover, while biochar has been linked to enhanced microbial activity, its influence on specific microbial metabolic pathways, particularly those related to carbon and nitrogen cycling, requires further investigation. Given these knowledge gaps, this study presents a preliminary evaluation of the effects of modified biochar addition on soil microbial diversity and key metabolic pathways associated with plant growth and soil quality. While limited in duration and scope, the findings provide important baseline evidence that can guide future long-term investigations and support the development of sustainable agricultural practices and soil management strategies.

Methodology

Experimental design and biochar application

For the application of biochar in crop cultivation, the experiment was arranged in a randomized complete block design (RCBD) with plot sizes of 0.8×8.1 m. for eggplant 0.9×10.5 m for long yard bean and 10.5×9.5 m for rice. Two treatments of each crop were included: a control and a biochar-amended treatment. All treatments received fertilizer according to the recommended rates for each crop, with a 15-15-15 formula applied twice for all plants. Rice straw biochar was produced by pyrolysis at 500 °C for 1 hour, then sieved through a mesh smaller than 355 µm and subsequently encapsulated with microbial cells following a previously established method. The microbial culture consisted of a mixed culture of *Bacillus sp*. The modified biochar was applied to the experimental plots at the appropriate rate of 1% w/w prior to crop planting.

Soil sampling

Soil samples (D1: control without BC, D2: paddy field 1, D3: paddy field 2, D4: eggplant field, and D5: long yard bean field) were collected from approximately 15 locations following a zigzag random sampling pattern after planting at a depth of 0-15 cm. All samples originated from the same soil series, which had been used to grow rice and different types of vegetables, to ensure consistency in soil type. The samples were air-dried, ground, and sieved through an 80-mesh screen prior to chemical analysis. The analyzed parameters included soil pH, organic matter content, and cation exchange capacity (CEC) determined by the distillation method. Total nitrogen was measured using the Kjeldahl method (Multi EA 4000), available phosphorus was determined by the Bray II extraction method, and exchangeable potassium (K) was analyzed using atomic absorption

spectroscopy (AAS). All analyses were conducted at the Central Laboratory, Faculty of Agriculture, Chiang Mai University. Separate soil samples were collected for microbial diversity analysis. These were preserved in 50 mL centrifuge tubes with absolute ethanol at a 1:1 volume ratio and stored at −20 °C prior to DNA extraction.

DNA extraction and metagenomic analysis

Total DNA was extracted from the soil sample using the nucleospin® soil (Bio-rad laboratories, USA) following the manufacturer's instructions. The DNA samples were then sent for metagenomic sequencing analysis which was performed on Illumina HiSeq platform by Novogene Biological Information Technology (Tianjin, China). 16 S rRNA genes of distinct 16SV3–V4 regions were amplified used specific primers with the barcode. All PCR reactions were carried out with Phusion® High-Fidelity PCR Master Mix (New England Biolabs) and sequencing libraries were generated using NEBNext Ultra DNA Library Pre ® Kit for Illumina. The library quality was assessed on the Qubit@ 2.0 Fluorometer (Thermo Scientific) and Agilent Bioanalyzer 2100 system. Sequences analysis were performed by Uparse software (Uparse v7.0.1001) (Edgar, 2013). Sequences with ≥97% similarity were assigned to the same OTUs. Representative sequence for each OTU was screened for further annotation. Alpha and Beta diversity analysis were calculated with QIIME2. and displayed with R software (Version 2.15.3). Venn and Flower diagram, Ternary plot as well as were relative abundances also generated [9].

Results and Discussions

Effect of Biochar on phylum-level shifts in soil microbial community structure

The microbial diversity analysis using the Metagenomic method in all soil samples revealed the presence of both Bacteria and Archaea. From Figure 1, which indicates the evolutionary relationships of microorganisms in each phylum and the abundance of microbial groups in the soil samples (D1 – D5) through a phylogenetic tree, various dominant microbial communities were identified (65 phyla, 154 classes, 331 orders, 434 families, 732 genera, and 371 species) such as *Bacillus* and *Alicyclobacillus* (Phylum Firmicutes), *Sphingomonas* (Phylum Proteobacteria), and *Nitrospira* (Phylum Nitrospirota).

Shifts in microbial diversity after BC addition

The relative abundance of soil samples in Figure 2 have 10 dominant microbial phyla. In control (D1) before BC were applied, Proteobacteria, Acidobacteriota, and Halobacterota were the most abundant microbial phyla. Proteobacteria are functions related to carbon, nitrogen, and sulfur cycling. Acidobacteriota survive in acidic environments and influencing nitrogen, phosphorus, and plant growth dynamics [10]. And Halobacterota, which is Archaea that survive in high-salinity environments and can promote plant growth [11]. According to the results, the soil from D1 is in extreme condition, which should improve for better microbial growth. The dominant genus after BC addition (D3) is Ammonia-oxidizing bacterium (MND1) (3.29%). Ammonia-oxidizing bacteria (AOB) plays a role in promoting root cytokinin synthesis that contributes to enhancing plant growth. Additionally, AOB is the primary bacteria in soil nitrification, leading to an increase of release nitrate (NO_3^-) in the soil [12]. The increased abundance of MND1 after BC addition indicates that biochar helps to enhance the population of beneficial soil microorganisms. This coincides with the extended and well-developed root systems observed in the samples where biochar was applied, indicating improved agricultural performance (data not shown).

In the areas where modified biochar (BC) were applied (D2-D5), relative abundance results showed an increase in microbial populations, along with new microbial phyla. For instance, *Candidatus* phylum Eremiobacterota (WPS-2), which is commonly found in bare soil environments [13], was detected after the addition of BC. It was found that the Firmicutes population increased in D2, D4 and D5, representing the phylum of BC-associated microorganisms in this study. Actinobacteriota populations significantly increased in D4 and D5. Similarly, a study on clay soil reported an increase in Actinobacteriota after applying biochar at 20 t/m³ [14].

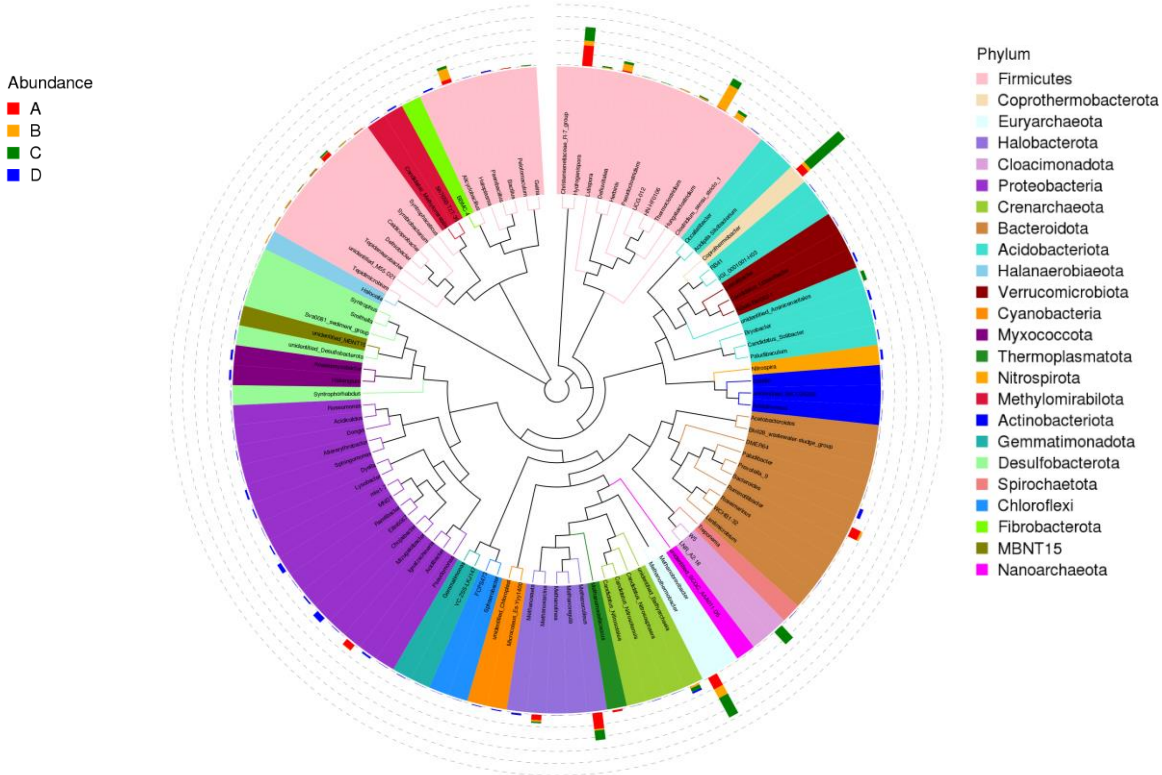

Figure 1 Phylogenetic tree and the abundance of the soil samples (D1 – D5)

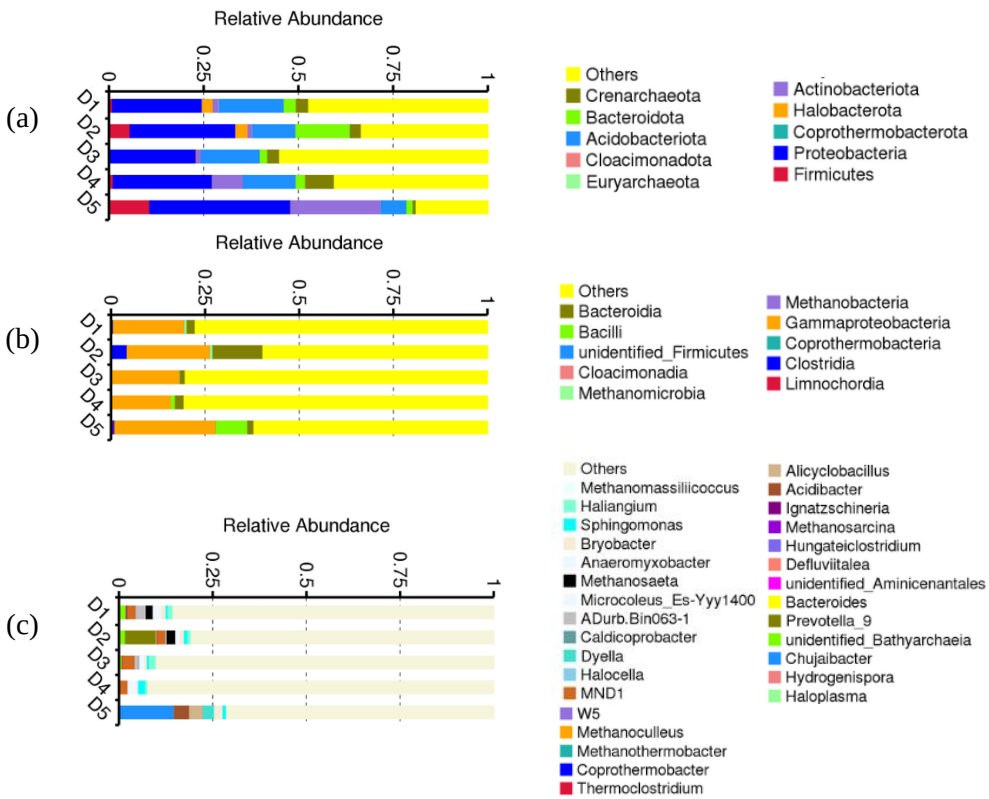

Figure 2 Relative abundances of major taxonomic groups from soil samples
(a) phylum level (b) class level (c) genus level

In Figure 3 shown that Bacilli (Phylum Firmicutes) is mostly found in D5 (8.34%), D4 (1.06%), D2 (0.18%), D1 (0.18%), and D3 (0.04%) respectively. This can improve the soil microenvironment by modulating the microbial community and soil quality through water and nutrient retention within the soil, as well as reducing soil salinity. Resulting in the enhancement of plant growth and an increase in yield [15]. According to the results, BC used in this study are a mixed culture (*Bacillus* sp.) that found in mostly test areas, it can imply that biochar can retain and maintain the soil-improving microorganisms in varying environmental conditions. Meanwhile, the microbial populations of D3 is decrease due to unsuitable soil conditions for microbial growth.

These results align with research on biochar and bioorganic fertilizer (BOF) containing *Bacillus* sp., which similarly enhanced microbial diversity in saline-alkaline soil, comparable to the BC used in this study. The study found Actinobacteriota present in soils both with and without biochar and BOF. Moreover, Firmicutes population also increased after biochar or BOF application [16], consistent with the above experimental results. The research demonstrated that biochar and BOF alter microbial diversity and community structure, with the application of both biochar with BOF resulting in more effective improvements than either biochar or BOF alone [16]. Indicating that the BC addition in this study supports the efficient application of biochar.

Effects of biochar on soil microbial diversity and abundance

The highest microbial diversity was observed in D2 (n = 4,887), whereas the lowest was in D5 (n = 1,436). In comparison, D2 also had higher microbial diversity than D1 (n = 4,517), as shown in Figure 4. Differences in fertilizer use and field management between sites may have contributed to variations in microbial communities, which should be considered when interpreting the results. Table 1 presents the baseline soil physicochemical properties (pH, organic matter, CEC, texture, moisture content) for all sampling sites. The lowest fertility indicators (OM, nutrients, CEC) found from D1 (control), representing poor baseline soil without amendments. However, moderate OM and nutrient levels in the paddy fields (D2 and D3) appeared after biochar addition, while D3 had the highest TN, indicating that rice–soil systems can retain nitrogen more effectively. In addition, very high levels of P, K, and NO_3^- were found in D4 and D5, reflecting either intensive fertilization or the effect of biochar addition on enhancing soil K and P availability. Although the variation in microbial communities may be partially explained by differences in baseline soil physicochemical properties, previous research has shown that biochar can significantly enhance soil microbial diversity [6]. Therefore, it can be concluded that biochar contributes to increasing microbial diversity. Although this study was based on a one-time application of biochar and its short-term effects may not have a significant impact on soil bacterial communities, it did enhance certain soil conditions. These improvements included an increase in soil pH, enhanced soil moisture retention, higher concentrations of potassium and phosphorus, and an increase in cation exchange capacity (CEC). In terms of long-term effects, Zhang et al. (2022) found that biochar significantly improved soil fertility and increased the relative abundance of Proteobacteria, while the abundance of Acidobacteria decreased.

However, there is specificity of microorganisms that depends on the environmental conditions. According to the quantity of microorganisms, as shown in Figure 5, the highest and lowest specifics and differences of microorganisms are D4 (3403 OTUs) and D5 (1280 OTUs) respectively. According to the experimental results, 3 microbial species were found in all soil samples: *Bacillus* sp., *Clostridium* sp. (*Clostridium sensu stricto 1*), and *Arenimonas* sp. In addition, unidentified_Chloroplast was also found in all soil samples, which due to residual genetic material from Cyanobacteriia.

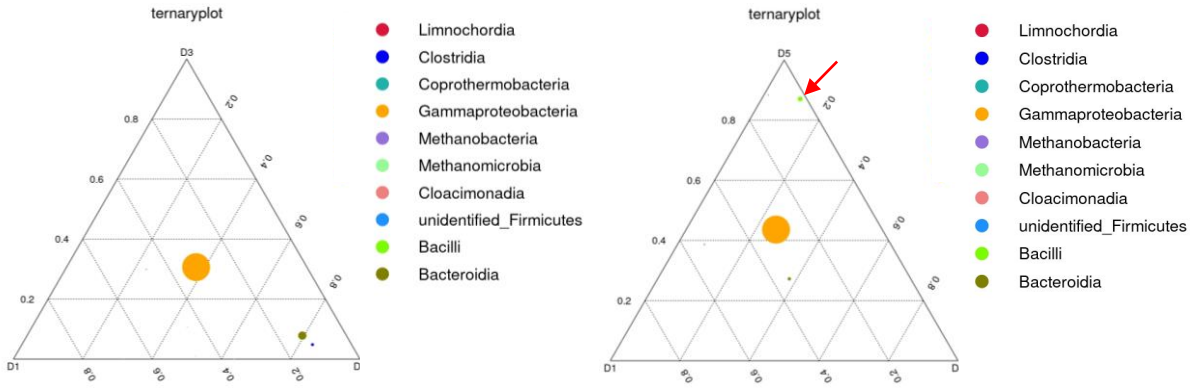

Figure 3 Ternary plot of soil samples (a) D1, D2, D3 (b) D1, D4, D5

Table 1 Soil properties for D1 (control without BC), D2 (paddy field 1), D3 (paddy field 2), D4 (eggplant field), and D5 (long yard bean field)

Soil samples	Organic matter (%)	Total Nitrogen (%)	Available Phosphorus (mg/kg)	Exchangeable Potassium (mg/kg)	Nitrate (NO_3) (mg/kg)	CEC (meq/100g)
Control without BC (D1)	0.67	0.08	14.99	0.75	28.45	2.92
Paddy field 1 (D2)	0.81	0.03	51.17	112.25	21.46	5.34
Paddy field 2 (D3)	1.64	0.15	46.78	91.00	35.79	3.63
Eggplant field (D4)	1.85	0.02	147.92	517.00	82.04	5.34
Long yard bean field (D5)	1.20	0.08	81.96	365.50	179.68	6.66

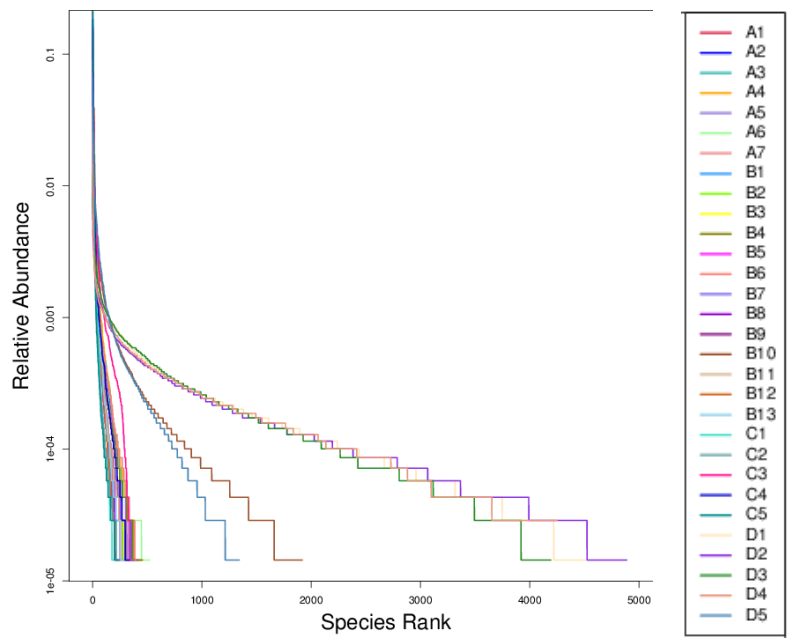

Figure 4 Species Rank showing Relative abundance of soil samples (D1 – D5)

Upon the addition of BC, a significant increase in *Bacillus* sp. was observed in D4 (0.0012054) and D5 (0.0057687) compared to D1 (0.0001722). As D1, D2, and D3 samples are collected from paddy fields, there is a higher correlation in soil microbiomes than D4 and D5 as shown in Figure 5. Conversely, following the addition of BC, changes in microbial diversity were observed, there is no presence identical microorganisms in D2–D3–D4–D5 (0), despite these soil samples are of the same type but cultivated with different plants. This clearly indicates that BC addition contributes to enhancing microbial diversity.

Biochar-Induced Enhancement of Soil Enzyme Activity and Metabolic Pathways

The analysis of enzymes or metabolic pathways can predict soil health and fertility. The functions of various enzymes can refer to a significant role in energy transfer, organic matter breakdown, and nutrient cycling from soil microorganisms. The enhancement of enzyme activity would affect the metabolic pathways of bacteria, leading to several reaction end-products based on their different functional contributions. The results of enzyme analysis from 5 soil samples revealed that D1 contained 10 distinct enzymes and Clusters of Orthologous Groups (COGs). The most abundant enzyme and COG found in D1 were EC:1.6.5.3 and COG0438, respectively. As shown in Table 2, the enzymes that increased after BC addition were EC:2.7.7.7, EC:3.6.4.12, EC:1.6.5.3, EC:2.1.1.72, and EC:1.2.7.11.

EC:2.7.7.7 is directly responsible for DNA synthesis and involved in transferring phosphorus-containing groups, specifically nucleotidyl transferases. EC:3.6.4.12 are also called molecular motors. This enzyme involved in unwinding DNA during DNA replication, DNA repair and recombination, chromosome segregation, and transcription initiation. Recently discovered that DNA helicases may involve in plant DNA recombination, as their abundance becomes prominent during the meiotic prophase of plants [17]. Additionally, DNA helicases is associated with the hydrolysis of phosphoric ester bonds in polynucleotides. EC:1.6.5.3 is an energy-conserving enzyme complex (Complexes I, 1, 2, 3), which is the first phosphorylation site of mitochondria and the respiratory complexes. This enzyme belongs to the hydrolase and amidase groups that are responsible for catalyzing the hydrolysis of the amide bond between the carbonyl group and the nitrogen atom. EC:1.6.5.3 was the most abundant enzyme in samples D1–D4, except for D5. EC:2.1.1.72 is responsible for producing a species-characteristic methylation pattern on adenine residues in a specific short base sequence in the host cell DNA, and is associated with S-adenosylmethionine–protein-arginine N-methyltransferases. And EC:1.2.7.11 is an essential enzyme in microbial one-carbon metabolism, belonging to the 2-oxoacid oxidoreductase group. This enzyme oxidatively decarboxylates different 2-oxoacids to form their CoA derivatives.

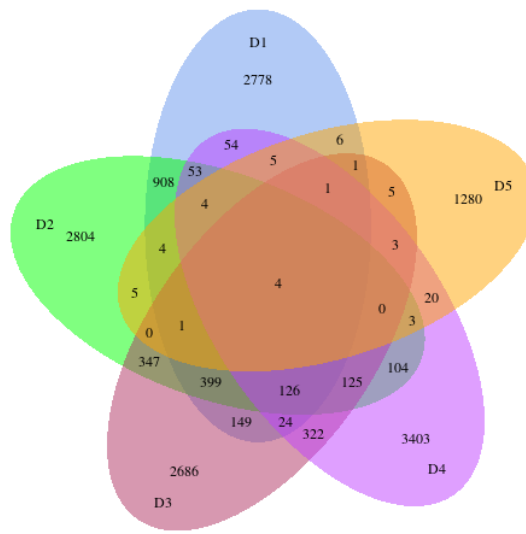

Figure 5 Venn diagram of soil samples

Table 2 Comparison of prominent enzymes from soil samples

Enzyme Commission (EC) number	Accepted Name	Soil samples				
		D1	D2	D3	D4	D5
EC:2.7.7.7*	DNA-directed DNA polymerase	0.013315	0.013435	0.013768	0.012851	0.012729
EC:3.6.4.12*	DNA helicase	0.011838	0.012217	0.012156	0.011122	0.011131
EC:1.6.5.3*	NADH:ubiquinone reductase	0.014261	0.013716	0.014998	0.014136	0.012556
EC:1.2.7.3	2-oxoglutarate synthase	0.003573	0.003992	0.003460	0.002429	0.001763
EC:2.7.13.3	histidine kinase	0.009984	0.009620	0.010220	0.009129	0.010377
EC:2.7.7.6	DNA-directed RNA polymerase	0.005981	0.005886	0.005858	0.006145	0.005445
EC:3.5.1.28	N-acetylmuramoyl-L-alanine amidase	0.001646	0.001979	0.001638	0.001739	0.002381
EC:5.2.1.8	peptidylprolyl isomerase	0.008104	0.008900	0.007880	0.007046	0.006900
EC:2.1.1.72*	site-specific DNA-methyltransferase (adenine-specific)	0.003819	0.003882	0.004042	0.003782	0.002511
EC:1.2.7.11*	2-oxoacid oxidoreductase (ferredoxin, OFOR)	0.002606	0.002802	0.002557	0.001996	0.001566

Note: (*) The increased enzyme after BC addition.

The results indicate that the increase in EC:2.7.7.7 reflects an enhancement in DNA synthesis, suggesting that BC contributes to the growth of microbial populations in the soil. Additionally, the higher levels of EC:1.6.5.3 compared to other enzymes demonstrate that the main activity in all soil samples is electron exchange that occurs in the electron transport chain of oxidative phosphorylation.

Interestingly, the analysis of COGs (Table 3) shown that COGs highly increased after BC addition were COG0745, COG1595, and COG1132. COG0745 belongs to the OmpR family and is involved in transcription as a DNA-binding response regulator with REC and winged-helix (wHTH) domains. The abundance of COG0745 increased Obviously in D3 – D5. COG1595 belongs to the sigma24 family and is involved in transcription as a DNA-directed RNA polymerase specialized sigma subunit. The abundance of COG1595 increased in all soil samples after the addition of BC. And COG1132 is a transport protein associated with the ABC-type multidrug and LPS transport system, specifically the ATPase and permease component MsbA. Its abundance increased Obviously in D3 – D5. From the experimental results, the analysis of COGs revealed the metabolic activity and corresponding essential proteins of the bacterial community, with COG1595 identified as a key protein in the soil with BC addition.

The prediction analysis of metabolic pathways is the analysis within soil samples using PICRUSt2. The most 10 abundant metabolic pathways are shown in Figure 6. According to the metabolic pathway analysis of the samples after BC addition (D3), there was a noticeable increase in the proportion of metabolic pathways compared to the control without BC (D1). The most abundant metabolic pathway found in all samples was PWY-3781, or Aerobic Respiration I (cytochrome c). PWY-3781 is an aerobic respiration pathway that parallels the transport of electrons from the oxidation of NADH, leading to ATP synthesis. This metabolic pathway is performed in plants, animals, and some bacteria via complexes I-IV. Complex I accepts NADH, while complex II accepts the TCA cycle intermediate succinate. The flow of electrons causes protons to be pumped from the matrix side to the intermembrane space, creating a proton gradient. These protons then flow back through the ATP-synthesizing complex in the mitochondrial or bacterial inner membrane, resulting in ATP synthesis. In microorganisms, NADH:ubiquinone oxidoreductases can also catalyze the reoxidation of cytosolic NADH to regenerate NAD^+ such as *Saccharomyces cerevisiae* [18-21]. This is consistent with the above experimental results that showed the presence of EC:1.6.5.3 (Table 1).

Table 3 Comparison of prominent COGs from soil samples

COGs number	Classification	Accepted Name	Soil samples				
			D1	D2	D3	D4	D5
COG0438	TRANSFERASE	Lipopolysaccharide 1,6-galactosyltransferase	0.006011	0.005790	0.006285	0.005686	0.005220
COG1131	TRANSPORT PROTEIN	Ribosome-associated ATPase	0.003302	0.003157	0.003546	0.003429	0.003814
COG0745*	TRANSCRIPTION	DNA-binding response regulator	0.003535	0.003512	0.003603	0.003609	0.004415
COG0642	TRANSFERASE	Signal transduction histidine kinase	0.005481	0.005205	0.005756	0.005157	0.004529
COG1595*	TRANSCRIPTION	DNA-directed RNA polymerase specialized sigma subunit	0.003755	0.003787	0.004022	0.003930	0.004142
COG1132*	TRANSPORT PROTEIN	-	0.002134	0.002103	0.002310	0.002238	0.002301
COG1028	OXIDOREDUCTASE	NAD(P)-dependent dehydrogenase	0.004781	0.004389	0.005080	0.005100	0.005066
COG0451	ISOMERASE	Nucleoside-diphosphate-sugar epimerase	0.004911	0.004375	0.005100	0.004508	0.003938
COG0840	SIGNALING PROTEIN	Methyl-accepting chemotaxis protein (MCP)	0.001795	0.002027	0.001589	0.001252	0.001522
COG1136	MEMBRANE PROTEIN	-	0.002867	0.002682	0.002856	0.002441	0.002435

Note: (*) The increased COGs after BC addition

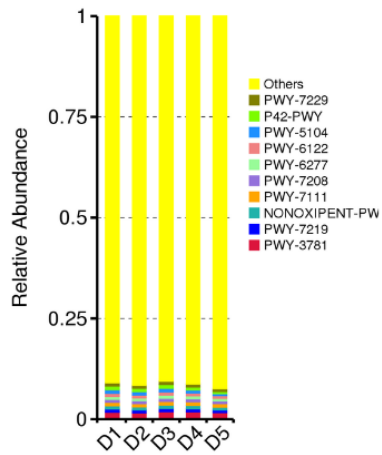

Figure 6 Prediction analysis of metabolic pathways in soil samples

Moreover, the metabolic pathways that increased after BC addition were PWY-7111, PWY-6277, and PWY-6122. PWY-7111 is the Pyruvate Fermentation to Isobutanol (engineered) pathway, where isobutanol is a higher alcohol and a by-product of yeast fermentation. This metabolic pathway is commonly engineered in microbial hosts such as *Saccharomyces cerevisiae*, *Escherichia coli*, and *Bacillus subtilis*. In this pathway, the last two reactions of the Ehrlich pathway are combined with the pathway for valine biosynthesis from pyruvate through the mutual intermediate 3-methyl-2-oxobutanoate to produce isobutanol [22, 23]. PWY-6277 is the superpathway of 5-aminoimidazole ribonucleotide (AIR) biosynthesis. This metabolic pathway's end product is 5-amino-1-(5-phospho-β-D-ribosyl)imidazole (AIR), which is a key intermediate in the biosynthesis of purine nucleotides and thiamine. AIR is synthesized from 5-phospho-α-D-ribose 1-diphosphate (PRPP) through 5 steps. PWY-6122 is the 5-aminoimidazole ribonucleotide biosynthesis II pathway, which parallels the PWY-6277 as it also produces AIR as the end product. However, this metabolic pathway is found in *E. coli*, as the third step is catalyzed by a different enzyme compared to PWY-6277. The metabolic

pathways that increased after BC addition are associated with the production of various compounds, such as isobutanol and AIR.

According to the results, both the abundance of soil microbiome and microbial diversity were observed, along with the effectiveness of BC on soil microorganisms. Additionally, enzymes and metabolic pathways were observed as well. By examining the changes in metabolic pathways, several observations can be used for further research, such as soil quality, microbial activity and diversity, as well as soil enzyme activity. The results indicate that BC contributed to increasing microbial diversity and populations in soil, leading to enhanced microbial activity and an increase in enzyme quantities, which are linked to important metabolic pathways that promote plant growth and soil quality. However, the scope of the research is limited in terms of the range of biochar addition and the investigation of long-term effects and beneficial microorganisms, so further studies are required within this context.

Conclusions

The microbial diversity analysis results of soil samples (D1-D5) revealed 65 phyla, 154 classes, 331 orders, 434 families, 732 genera, and 371 species. Before the addition of BC (D1), Proteobacteria, Acidobacteriota, and Halobacterota were the most abundant microbial phyla, indicating that the soil was in an extreme condition. Regarding the soil after the addition of BC (D2-D5), there was an increase in the populations of Firmicutes and Actinobacteriota, along with new microbial phyla, such as WPS-2, and dominant genera, such as ammonia-oxidizing bacterium (MND1) (3.29%), which is a primary bacterium in soil nitrification.

Additionally, Bacilli have been found as well (D5 (8.34%), D4 (1.06%), D2 (0.18%), D1 (0.18%), and D3 (0.04%)), which are microorganisms that can improve the soil microenvironment. *Bacillus* sp. was observed in D4 (0.12%) and D5 (0.58%) compared to D1 (0.02%). Since BC used in this study is a mixed culture of *Bacillus* sp., it can be implied that biochar can retain and maintain soil-improving microorganisms under varying environmental conditions and also indicates that biochar helps to enhance the population of beneficial soil microorganisms. The results showed that the highest microbial diversity is in D2 (n=4887), which is higher than in D1 (n=4517). Therefore, it can be concluded that BC contributes to increasing microbial diversity. And also found that D4 (3403 OTUs) has the highest specifics and differences in microbiome.

Moreover, COG1595 is a key protein in the soil after BC addition, and it was also found that enzymes, including EC:2.7.7.7 and EC:1.6.5.3, increased after BC addition. This increase suggests that BC contributes to the enhancement of DNA synthesis, leading to an increase in microbial populations in the soil. Furthermore, the main activity of the soil microbiome involves electron exchange, which occurs in the electron transport chain of oxidative phosphorylation.

The most prominent metabolic pathway is PWY-3781 (Aerobic Respiration I (cytochrome c)), which aligns with the presence of EC:1.6.5.3. After the addition of BC (D3), several metabolic pathways increased compared to the control without BC (D1). The metabolic pathways that increased include PWY-7111, PWY-6277, and PWY-6122. In conclusion, biochar can support soil-improving microorganisms and increase microbial populations that enhance microbial activity, resulting in greater microbial diversity and improved soil fertility, which in turn supports better plant health and growth.

Acknowledgement

This research was financially supported by the Fundamental Fund in the year 2024 no. MJU 1-67-08-002.

References

[1] Rizwan, M., Ali, S., Qayyum, M.F., Ibrahim, M., Zia-ur-Rehman, M., Abbas, T. and Ok, Y.S. 2016. Mechanisms of biochar-mediated alleviation of toxicity of trace elements in plants: a critical review. Environmental science and pollution research international. 23(3): 2230-48.

[2] Kaetzl, K., Lübken, M., Nettmann, E., Krimmler, S. and Wichern, M. 2020. Slow sand filtration of raw wastewater using biochar as an alternative filtration media. Scientific reports, 10(1): 1229.

[3] Yang, W., Wang, Z., Song, S., Han, J., Chen, H., Wang, X., Sun, R., and Cheng, J. 2019. Adsorption of copper (II) and lead(II) from seawater using hydrothermal biochar derived from Enteromorpha. Marine pollution bulletin, 149: 110586.

[4] Park, J.-H., Wang, J., Meng, Y., Delaune, R. and Seo, D.-C. 2019. Adsorption/desorption behavior of cationic and anionic dyes by biochars prepared at normal and high pyrolysis temperatures. Colloids and Surfaces A: Physicochemical and Engineering Aspects. 572: 274-282.

[5] Carter, S., Shackley, S., Soh.i, S., Tan, B., and Haefele, S. 2013. The Impact of Biochar Application on Soil Properties and Plant Growth of Pot Grown Lettuce (Lactuca sativa) and Cabbage (Brassica chinensis). Agronomy. 3: 404-418.

[6] Wenhuan X., Hanmei X., Manuel D.-B., Michael J. G., Xiaoming Z. and Honghua R. 2023. Global meta-analysis reveals positive effects of biochar on soil microbial diversity, Geoderma, 436: 116528.

[7] Gebisa, L. 2018. Effects of Biochar Application on Beneficial Soil Organism Review. Interantional Jounal of research in agriculture and forestry. 7: 6-12.

[8] Pokharel, P., Ma, Z. and Chang, S. 2020. Biochar increases soil microbial biomass with changes in extra- and intracellular enzyme activities: a global meta-analysis. Biochar, 2.

[9] Edgar, R.C. 2013. UPARSE: highly accurate OTU sequences from microbial amplicon reads. Nature Methods, 10(10): 996-998.

[10] Gonçalves, O., Fernandes, A., Tupy, S., Ferreira, T., Almeida, L., Creevey, C. and Santana, M. 2023. Insights into Plant Interactions and the Biogeochemical Role of the Globally Widespread Acidobacteriota Phylum. Soil Biology and Biochemistry. 92: 109369.

[11] Hernández-Canseco, J., Bautista-Cruz, A., Sánchez-Mendoza, S., Aquino-Bolaños, T. and Sánchez-Medina, P. 2022. Plant Growth-Promoting Halobacteria and Their Ability to Protect Crops from Abiotic Stress: An Eco-Friendly Alternative for Saline Soils. Agronomy, 12(4): 804.

[12] Wang, X.-L., Zhen-Qiang S., Hao Y., Lin Q., Wei L., Jiang S. and Peng S. 2023. Unveiling the dual role of heterotrophic ammonia-oxidizing bacteria: enhancing plant regrowth through modulating cytokinin delivery. Frontiers in Microbiology. 14 : 1268442.

[13] Sheremet, A., Jones, G. M., Jarett, J., Bowers, R. M., Bedard, I., Culham, C., Eloe-Fadrosh, E. A., Ivanova, N., Malmstrom, R. R., Grasby, S. E., Woyke, T. and Dunfield, P. F. 2020. Ecological and genomic analyses of candidate phylum WPS-2 bacteria in an unvegetated soil. Environmental microbiology, 22(8): 3143-3157.

[14] Zhang, J. and Shen, J.-L. 2022. Effects of biochar on soil microbial diversity and community structure in clay soil. Annals of Microbiology. 72(1): 35.

[15] Xia, H., Hongguang, L., Ping, G., Pengfei, L., Qiang, X., Qian, Z., Mingyue, S., Qiang, M., Fuhai, Ye. and Weizhen Y. 2025. Study of the mechanism by which Bacillus subtilis improves the soil bacterial community environment in severely saline-alkali cotton fields. Science of The Total Environment. 958: 178000.

[16] Gu, Y.-y., Liang, X.-y., Zhang, H.-y., Fu, R., Li, M. and Chen, C.-j. 2023. Effect of biochar and bioorganic fertilizer on the microbial diversity in the rhizosphere soil of Sesbania cannabina in saline-alkaline soil. Frontiers in Microbiology. 14: 1-14.

[17] Sarwat, M. and Tuteja, N. 2018. Chapter 7 - DNA Helicase-Mediated Abiotic Stress Tolerance in Plants, in Biochemical, Physiological and Molecular Avenues for Combating Abiotic Stress Tolerance in Plants, S.H. Wani, Editor., Academic Press. 103-115.

[18] Feng, Y., Li, W., Li, J., Wang, J., Ge, J., Xu, D., Liu, Y., Wu, K., Zeng, Q., Wu,

J.-W., Tian, C., Zhou, B. and Yang, M. 2012. Structural insight into the type-II mitochondrial NADH dehydrogenases. Nature. 491: 478-82.

[19] Marres, C.A., S. de Vries, and Grivell, L.A. 1991. Isolation and inactivation of the nuclear gene encoding the rotenone-insensitive internal NADH: ubiquinone oxidoreductase of mitochondria from Saccharomyces cerevisiae. European Journal of Biochemistry. 195(3): 857-62.

[20] Luttik, M. A., Overkamp, K. M., Kötter, P., de Vries, S., van Dijken, J. P. and Pronk, J. T. 1998. The Saccharomyces cerevisiae NDE1 and NDE2 genes encode separate mitochondrial NADH dehydrogenases catalyzing the oxidation of cytosolic NADH. The Journal of biological chemistry. 273(38): 24529-24534.

[21] Small, W.C. and McAlister-Henn, L. 1998. Identification of a cytosolically directed NADH dehydrogenase in mitochondria of Saccharomyces cerevisiae. Journal of Bacteriology. 180(16): 4051-5.

[22] Savrasova, E. A., Kivero, A. D., Shakulov, R. S., and Stoynova, N. V. 2011. Use of the valine biosynthetic pathway to convert glucose into isobutanol. Journal of industrial microbiology and biotechnology. 38(9): 1287-1294.

[23] Blombach, B. and Eikmanns, B.J. 2011. Current knowledge on isobutanol production with Escherichia coli, Bacillus subtilis and Corynebacterium glutamicum. Bioengineered bugs. 2(6): 346-350.

Thai Environmental Engineering Journal Vol. 39 No. 2 (2025) : 31-41
www.eeat.or.th

Mass Flow Analysis of Carbon Capture, Utilization, and Storage (CCUS) Potential in Thailand

Danupon Srinongsaeng[1], Napat Jakrawatana[2] and Wanawan Pragot[3]*

[1]School of Energy and Environment, University of Phayao, Phayao 56000, Thailand
[2]Department of Environmental Engineering, Faculty of Engineering,
Chiang Mai University, Chiang Mai 50200, Thailand
[3*]School of Energy and Environment, University of Phayao, Phayao 56000, Thailand
[*]E-mail : wanawan.pr@up.ac.th

Article History; *Received: 26 March 2025, Accepted: 21 August 2025, Published: 28 August 2025*

Abstract

This study analyzes the carbon dioxide flow in Thailand to assess the potential of Carbon Capture, Utilization, and Storage (CCUS) technologies. It utilizes data from academic literature and reports to conduct a qualitative analysis of CO_2 flow within Carbon Capture and Utilization (CCU) and Carbon Capture and Storage (CCS) processes. The mass flow analysis was performed using the e!Sankey Diagram software to simulate three scenarios: Scenario 1 involves utilizing captured CO_2 from industrial plants to produce various products such as beer, soft drinks, soda, urea fertilizer, and cement pellets. Scenario 2 focuses on storing all captured CO_2 from industrial plants in depleted natural gas or oil reservoirs within Thailand. Scenario 3 combines both CCU and CCS approaches to evaluate the overall CO_2 flow within the country's system. The main industries analyzed include power generation, cement production, and iron and steel manufacturing, which accounted for 107,498.98 ktCO_2 equivalent of greenhouse gas emissions in 2022. Post-combustion CO_2 capture using amine-based absorbents was identified as the most suitable method for these industries. The analysis highlighted the potential for CO_2 capture and utilization across various industrial sectors, as well as the feasibility of underground CO_2 storage in Thailand. The study found that CO_2 utilization and storage could reduce emissions by 25.07% under favorable conditions. In summary, CCUS technology can effectively reduce CO_2 emissions from power plants, cement, and steel industries while promoting a circular economy through the beneficial reuse of captured CO_2.

Keywords : Carbon Capture Utilization and Storage (CCUS); CO_2 Emission; Mass Flow Analysis; Climate Change Mitigation; Thailand

Introduction

Greenhouse gas (GHG) emissions significantly contribute to environmental degradation, climate change, sea-level rise, biodiversity loss, and adverse health effects, primarily resulting from human activities such as the combustion of fossil fuels, industrial processes, agriculture, and transportation [1]. Major sources of CO_2 emissions include electricity generation from coal and natural gas, manufacturing, and the use of fossil fuels in transportation, while methane (CH_4) and nitrous oxide (N_2O), predominantly from the agricultural sector and waste management, significantly exacerbate global warming, leading to the deterioration of ecosystems, economies, and overall quality of life without effective mitigation measures [2].

Carbon capture, utilization, and storage (CCUS) presents an effective strategy for reducing these GHG emissions through an integrated suite of technologies focused on capturing carbon dioxide (CO_2) from high-emission sources like power plants and industrial facilities to prevent atmospheric release and enable its conversion into valuable products. CCUS encompasses two main branches: carbon capture and utilization (CCU) and carbon capture and storage (CCS) [3].

Carbon Capture and Utilization (CCU) involves the reuse of captured CO_2 , with the capture process including several methods such as pre-combustion capture, which gasifies fossil fuels to produce hydrogen and CO_2 followed by CO_2 separation before combustion, primarily used in hydrogen or synthetic fuel production; post-combustion capture, which extracts CO_2 from flue gas after fossil fuel combustion using chemical solvents like amine-based absorption; oxy-fuel combustion, which burns fossil fuels in pure oxygen to produce flue gas mainly of CO_2 and water vapor for easier separation; and Direct Air Capture (DAC), which captures CO_2 directly from ambient air using solid sorbents or liquid solvents, offering potential for negative emissions despite being energy-intensive.

Wide range of technologies for CO_2 capture includes amines, organic compounds reacting with CO_2 to form carbamates like monoethanolamine (MEA) [4]; carbonate solutions that react with CO_2 to form bicarbonate; solid sorbents [5] like zeolites, activated carbon [6], and metal-organic frameworks (MOFs) [7] that adsorb CO_2 ; membranes made of polymers, ceramics, or composites that selectively permeate gases to separate CO_2 ; algae capture, which uses microalgae to fix CO_2 through photosynthesis; and cryogenics, employing very low temperatures to condense and separate CO_2. Captured CO_2 can be directly reused in Enhanced Oil Recovery (EOR) [8] by injecting it into oil or gas fields to enhance recovery and facilitate underground storage, and in the food and beverage industry [9] for carbonated drinks and as a refrigerant; indirect utilization [10] involves converting CO_2 into products like synthetic fuels and chemicals such as methanol, urea, and hydrocarbons through reactions with hydrogen from renewable sources. Carbon Capture and Storage (CCS) [3], on the other hand, involves the permanent storage of CO_2 in geological formations, ensuring it does not re-enter the atmosphere, thereby mitigating climate change impacts.

CCUS plays a vital role in mitigating climate change and achieving carbon neutrality by reducing emissions in hard-to-decarbonize sectors such as power generation, cement, and steel production. While globally recognized, CCUS research and implementation in Thailand remain limited, with notable gaps in emission data, economic feasibility studies, storage capacity assessments, and policy integration. Prior work by Zhang et al. (2022) [11] highlights Thailand's geological storage potential and concepts for CCS infrastructure but does not quantify CO_2 mass flows. This study builds upon previous research by employing Mass Flow Analysis to evaluate CO_2 capture, utilization, and storage pathways in Thailand. The central hypothesis of this study is whether Thailand possesses the capacity to utilize and store the CO_2 emissions generated annually. Despite significant advancements in CO_2 capture and storage technologies, there remains a critical gap in understanding the spatial and quantitative integration of these emissions within Thailand's infrastructure. This study addresses this gap by integrating quantitative emissions data with spatial planning, thereby enhancing the potential for effective CCUS deployment.

Materials and Methods

This research was conducted as a qualitative study through data collection from literature reviews and reports (Table 1). The study focused on analyzing CO_2 mass flow in the application of CCUS technology in Thailand, specifically in terms of CCU (Carbon Capture and Utilization) and CCS (Carbon Capture and Storage). The emission-generating industries considered in this study included all CO_2 emitters industries of Thailand that have capability for CCUS technology. The dataset is obtained from Thailand's 2024 Biennial Transparency Report (BTR), which contains CO_2 emission data for the year 2022, although the report was published in 2024. The criteria for selecting emission sources in combustion process industries were included four key criteria: (1) Emission Data Availability – ensuring that only sources with reliable and up-to-date data were considered to support accurate analysis and modeling; (2) Point Source Emission – focusing on concentrated emission points, such as industrial stacks, to enhance capture efficiency and cost-effectiveness; (3) Magnitude of Emissions – prioritizing large emitters to maximize overall GHG reduction and resource efficiency; and (4) Capture Potential – assessing the technical feasibility and practicality of

applying CO_2 capture technologies to ensure successful and sustainable implementation.

There are many types of capture media and mechanisms. This research scope included amine-based solutions, adsorption using solid sorbents, membrane separation, and cryogenic techniques. However, each mechanism had its limitations, such as high energy consumption (particularly for solvent regeneration), solvent degradation, high capital investment, and limited scalability depending on industrial applications and geographical location. Therefore, the criteria for selecting the capture media were set included capture efficiency, cost, operation lifetime, TRLs, and number of existing full-scale applications.

Following a comprehensive criteria-based selection, data on CO_2 emissions, captured CO_2, and its utilization and storage were analyzed using mass flow analysis with e! Sankey Diagram software (version 5.2.1) to evaluate the CO_2 mass flows of CCUS technologies in Thailand. Three simulation scenarios were developed to examine the CO_2 flow pathways, with each process presenting a distinct CO_2 mass balance profile.

Scenario 1: CCU routes by captured CO_2 from industrial plants would be repurposed in products such as beer, soft drinks, soda, urea fertilizer, cement clinker, and for enhanced oil recovery (EOR). The goal was to support a circular economy by utilizing CO_2 as an industrial input. Utilization estimates were based on industry data as shown in Table 2.

Scenario 2: This scenario models CCS pathways by assuming that all CO_2 captured from industrial plants is stored in depleted natural gas fields or oil reservoirs within Thailand. The objective is to evaluate the CO_2 storage potential of the industrial sector in underground sites, using 10 years of historical data on utilized oil and gas fields. Preliminary estimates of underground CO_2 storage capacity were derived from national oil drilling records and proven oil reserve data.

Scenario 3: Combining CCU and CCS routes by considering the total mass flow of CCUS of Thailand. This is the evaluation of both utilization and storage potential through the following simulation scenarios.

Table 1 The sources of data for this study

Data	Sources
CO_2 capture technology	Available literature data from 2004 to 2024 [3]
CO_2 emission	Thailand 2024 Biennial Transparency Report (BTR) [11]
CO_2 usage	The market demand for CO_2 directly utilization (CCU) for the beverage and the CO_2 indirectly utilization for urea, and cement industries are identified based on the production of Thailand products using the data from Thailand statistic data during January - December 2022 by Office of Industrial Economics (OIE) [12]
CO_2 enhance oil recovery	Thailand CO_2 enhance oil recovery (CCU-EOR) from the report of petroleum procurement from both land and sea petroleum sources during January - December 2022 by Department of Mineral Fuels [13]
CO_2 storage capacity	Thailand oil reservoirs (CCS) from the report of petroleum procurement from both land and sea petroleum sources during 2012 - 2022 by Department of Mineral Fuels [13]

Table 2 The assumption for CO_2 utilization based on the CO_2 concentration in the products

Products	CO_2 concentration	References
Beer	3.5% W/V	[14]
Soft drinks and soda	4.5% W/V	[15]
Urea	5.5% W/W	[16]
Cement clinker	7.5% W/W	[17]

Results and Discussion

The selection of greenhouse gas (GHG) emission sources in combustion process industries was based on four key criteria: (1) Emission Data Availability – ensuring that only sources with reliable and up-to-date data were considered to support accurate analysis and modeling; (2) Point Source Emission – focusing on concentrated emission points, such as industrial stacks, to enhance capture efficiency and cost-effectiveness; (3) Magnitude of Emissions – prioritizing large emitters to maximize overall GHG reduction and resource efficiency; and (4) Capture Potential – assessing the technical feasibility and practicality of applying CO_2 capture technologies to ensure successful and sustainable implementation.

Table 3 Selection of industrial plants to be studied

Industry	Criteria 1	Criteria 2	Criteria 3	Criteria 4	Total
	Emission Data Availability	Point source emission	Magnitude of Emissions	Capture Potential	
Energy Industries [18-20]	1	1	1	2	6
Cement Production [19, 21]	1	1	1	2	6
Lime Production [22, 23]	1	1	1	1	4
Glass Production [21, 23]	1	1	0	0	2
Chemical production [24, 25]	1	0			1
Iron and steel Production [24]	1	1	1	2	6
Pulp and Paper Industry [9, 26]	1	1	0	0	2
Food and Beverage Industry [9]	0				0

Note: Criteria details are provided below;

1) Emission data availability (1 = Availability of emission data, 0= No availability of emission data)

2) Point source emission (1 = Point source emission, 0 = Nonpoint source emission)

If any industries have the value of criteria 1 (emission data availability) and criteria 2 (point source emission) equal to 0, they were not further included for other criteria.

3) Magnitude (2 = emission ≤ 20%, 1 = 10% < emission < 20%, 0 = emission ≤10% of the total emission)

- 20% is used as the *upper threshold* because if an emission source accounts for more than one-fifth of total emissions, it is considered a major emitter, where actions targeting that single sector can have a significant impact at the national level.
- 10% is used as the *lower threshold* to distinguish small emission sources from those that are strategically important.

4) Capture Potential

- 2 = Good: High CO_2 concentration (>10–15%), continuous and centralized emissions, minimal process disruption, proven in similar industries.
- 1 = Fair: Moderate CO_2 concentration (5–10%), less consistent or multiple sources, more modifications needed, some cost/technical limits.
- 0 = Poor: Low CO_2 concentration (<5%), dispersed or intermittent emissions, inadequate infrastructure, high capture cost per CO_2 unit.

Table 3 presented a systematic approach for identifying priority industrial sectors for CCUS deployment in Thailand, emphasizing minimum requirements for emission data availability and point-source emissions to ensure accurate assessment and technical feasibility. The energy industry, cement production, and iron and steel production ranked highest, collectively emitting 107,498.98 $ktCO_2eq$ in 2022—over one-quarter of the nation's total emissions—positioning them as strategic targets for large-scale emission reductions. These sectors possess favorable conditions for CCUS implementation, including continuous high-volume flue gas streams, centralized emission points, and high capture potential, which facilitate the adaptation of existing infrastructure with fewer technical barriers compared to smaller or more dispersed industries. Although no sensitivity analysis was conducted, a preliminary uncertainty assessment was carried out. The findings revealed a high degree of uncertainty, primarily due to limitations in data quality, as information was not collected continuously but obtained only from producers or national-level sources. Nevertheless, the researchers deemed the available data sufficiently reliable for the purposes of this analysis.

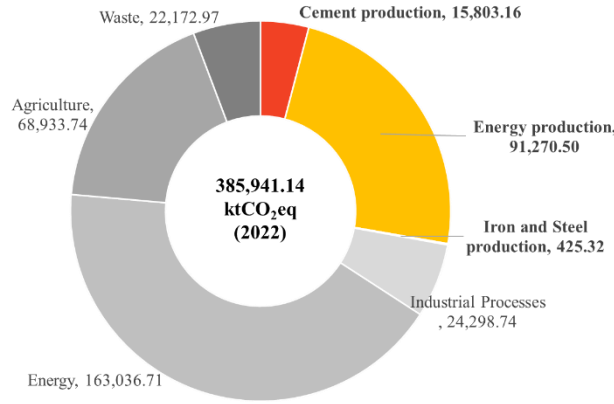

Figure 1 Total GHG emissions by sector 2022 (Adapted from [11])

Table 4 Selection of capture technology 2024 Biennial Transparency Report (BTR)

Criteria / Technology	**Post-combustion**	**Pre-combustion**	**Oxy-fuel combustion**	**Direct Air Capture (DAC)**
Compatibility with Existing Systems	Excellent – easy retrofit	Requires full system rebuild	Requires boiler modification	Installed separately from production
Cost	Medium to high	High – major system changes	High – needs pure CO_2 production	Very high – energy intensive
Suitable CO_2 Concentration Level	4–15% CO_2 (from flue gas)	High ~20–40% CO_2 (syngas)	High ~80% CO_2 (with O_2 combustion)	Very low (0.04% CO_2 in air)
Technology Readiness Level (TRL)	8–9	6–8	6–8	5–7
Space and Resource Requirements	Moderate space and water use	Requires more system management	High energy and O_2 demand	Extremely high energy usage
Industry Suitability	Power, cement, steel, Oil Refineries, Chemical Plants, Food & Beverage, Textile & Garment, Ceramics & Glass	Gasification-based industries	New power plant designs	Areas without point-source CO_2
Economic Feasibility	More feasible for retrofits	Not viable if building new	Too expensive currently	Not suitable for large-scale use
Reference	[27-29]	[28, 30]	[28, 31]	[32, 33]

Table 4 indicated that among the available capture technologies, post-combustion CO_2 capture is the most suitable option for retrofitting existing facilities in the selected industries. Since this method does not require modifications to the combustion process, it offers a practical and cost-effective solution with a medium to high-cost relative to other approaches. With a Technology Readiness Level (TRL) of 8-9, the technology is considered ready for integration into existing systems. Based on the available data sources.

The criteria presented in Table 5 indicated that amine-based solvents are the most suitable capture media due to their high selectivity, efficiency, and proven large-scale applicability in CO_2 capture. Compared with membrane and solid sorbent technologies, amine systems offer greater operational flexibility, higher capture rates (85-98%), and adaptability to a wide range of fuel types, including coal, natural gas, and biomass. These systems have been successfully implemented in industry for decades, and with a Technology Readiness Level (TRL) of 8-9, the technology is considered ready for deployment. The identical capture losses observed across all three scenarios can be attributed to the capture technology itself. However, the application of monoethanolamine (MEA) in Thailand is challenged by the country's hot and humid climate. Under such conditions, MEA alone may experience reduced absorption efficiency and increased solvent losses. Therefore, heat-tolerant blends, such as methyldiethanolamine (MDEA) combined with piperazine (PZ) or (AMP)-based solvents, are considered more suitable. The performance of these blends can be further enhanced through pre-cooling and impurity removal processes.

Then, all qualified data were analyzed using the e!Sankey Diagram software version 5.2.1, which applies Mass Flow Analysis and the Law of Conservation of Mass to track CO_2 flows from emission sources through capture processes to utilization (CCU) or storage (CCS). The software processes input data on CO_2 emissions, capture technology efficiencies, and utilization/storage capacities, performs mass balance calculations, and renders flows with widths proportional to actual quantities, enabling clear visualization of the overall system and potential bottlenecks. Three simulated scenarios were employed to observe the direction of CO_2 mass flow, each process exhibiting a distinct proportion of CO_2 mass balance, allowing multiple scenarios to be compared in a single view and facilitating communication of national-scale CCUS assessments.

In scenario 1, the total captured CO_2 in this scenario was 96,749.08 ktCO_2 eq. The gas was allocated across six applications, with the highest volume (24,091.47 kt CO_2eq) used in Enhanced Oil Recovery (EOR). Other sectors included beverage industries (beer, soft drinks, soda), urea fertilizer production, and cement clinker manufacturing. However, only 28.4% of the captured CO_2 could be utilized based on market demand and process limitations, leaving 69,269.44 ktCO_2 eq that required further handling, likely via geological storage.

Table 5 Capture Media Selection Criteria

Criteria	Amines	Carbonate Solutions	Solid Sorbents	Membranes	Algae-based Capture	Cryogenic
Capture Efficiency (%)	85-98	70-90	80-95	75-92	60-80	95-99
Cost (USD/tCO_2eq)	30-60	25-50	40-70	50-80	60-100	70-120
Operation lifetime (year)	2-5	3-7	5-10	5-10	1-3	10-20
Technology Readiness Level (TRL)	8-9	7-9	5-7	6-8	3-5	8-9
Number of full-scale applications (Plants)	>100	>50	<10	<20	<5	>30
Reference	[34-36]	[37, 38]	[5, 39, 40]	[5, 39, 40]	[41, 42]	[43, 44]

In scenario 2, all captured CO_2 (96,749.08 $ktCO_2$ eq) was assumed to be stored in geological formations such as depleted oil and gas reservoirs. Thailand's total estimated underground storage capacity was 345,226.43 $ktCO_2$, meaning that only 28.02% of this capacity would be used. This indicates that the country has ample geological potential to support future CCS operations.

In scenario 3, after evaluating the results from both utilization and storage pathways, it was confirmed through simulation and verification that all (100%) of the captured CO_2 could be either used or stored safely. This comprehensive approach ensures that no emissions escape into the atmosphere, supporting total emission management. The width of each flow corresponds to the volume of CO_2, making it clear that energy industries are the largest source, and storage in old oil and gas fields is the largest destination

Factors influencing the mass flow of CO_2 in CCUS systems, both currently and in the future, include the quantity and sources of CO_2 emissions which vary with production levels and energy use; the efficiency and technology of capture methods affected by environmental conditions and technical readiness; market demand and the capacity of underground storage sites; policies and regulations that either encourage or hinder investment incentives; the availability of infrastructure for CO_2 transportation; geographical and environmental factors impacting system design and safety; as well as social acceptance and economic impacts. These interrelated factors significantly determine the efficiency, scale, and long-term sustainability of CCUS implementation.

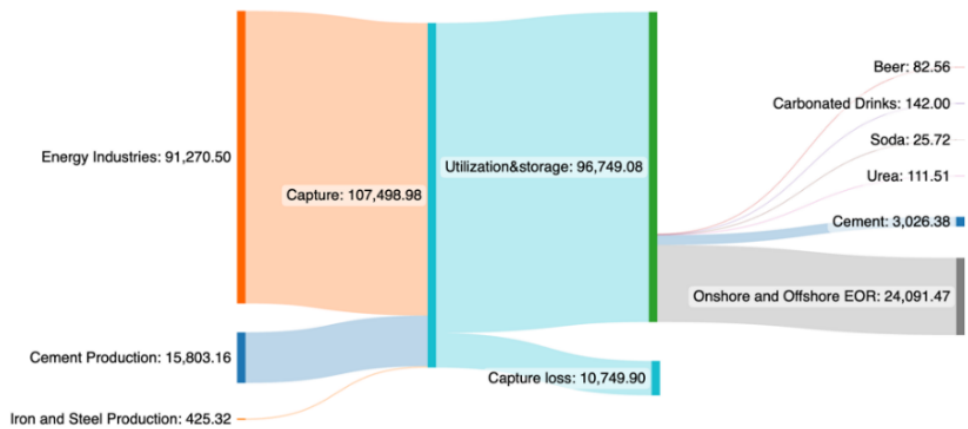

Figure 2 Mass balance of scenario 1

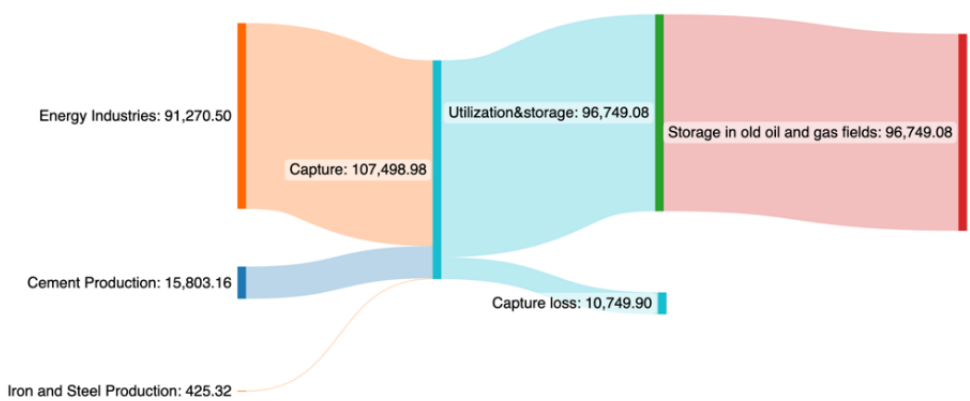

Figure 3 Mass balance of scenario 2

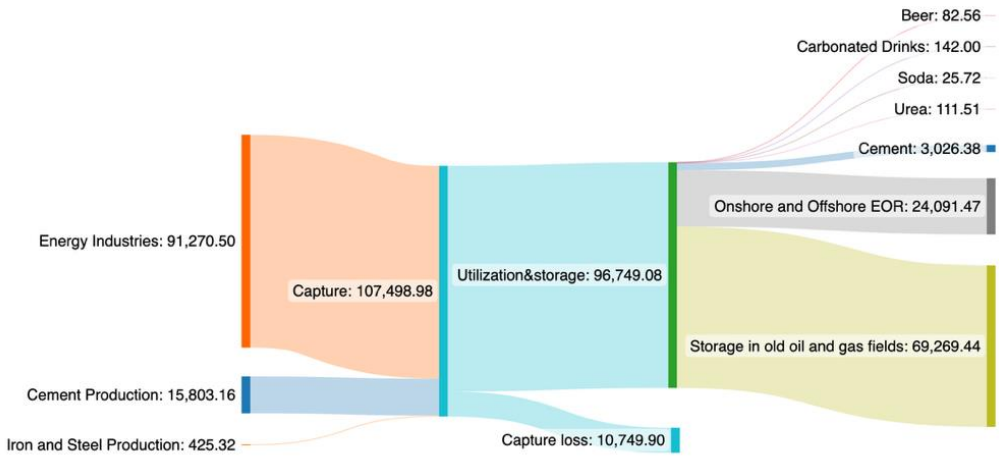

Figure 4 Mass balance of scenario 3

Conclusions

The study confirmed that CCUS technology is suitable for power plants, cement, and iron and steel industries, as it can effectively reduce CO_2 emissions directly at the source. Post-combustion capture technology using amines as absorbents was identified as particularly suitable for these selected industrial plants due to its high efficiency in capturing carbon dioxide (CO_2) directly from flue gas at the emission point and its compatibility with complex industrial environments. This technology has been proven commercially viable, and its widespread adoption demonstrates confidence in its practicality. In addition to reducing CO_2 emissions, the captured carbon can be reused across various sectors, contributing to the development of a circular economy. Examples of CO_2 utilization include its use in the production of beer and carbonated beverages, as a feedstock in fertilizer and clinker manufacturing, and for enhanced oil recovery (EOR). The study also found that the three largest CO_2 emission sources could collectively reduce total emissions by 25.07% if CCUS were implemented at full commercial scale.

While Thailand has considerable potential for CO_2 capture and storage, significant challenges remain, including investment uncertainties, technical constraints, high costs, and environmental considerations. This preliminary study produced encouraging results but also revealed several limitations. Future research should incorporate cost and economic analyses, assess emissions from the entire CCUS process, and explore policy measures such as pricing mechanisms, infrastructure development, and comprehensive CO_2 data management to better support effective utilization and storage.

References

[1] U.S. Environmental Protection Agency, Office of Transportation and Air Quality. 2022. The 2022 EPA Automotive Trends Report: Greenhouse Gas Emissions, Fuel Economy, and Technology since 1975, Executive Summary (EPA-420-S-22-001, December 2022). www.epa.gov/automotive-trends.

[2] Intergovernmental Panel on Climate Change (IPCC). 2023. Changing State of the Climate System. In Climate Change 2021 – The Physical Science Basis. Cambridge University Press, pp. 287–422. doi:10.1017/9781009157896.004.

[3] Metz, B., O. Davidson, H.C. de Coninck, M. Loos, and L.A. Meyer (eds.). 2005. IPCC Special Report on Carbon Dioxide Capture and Storage. Prepared by Working Group III of the Intergovernmental Panel on Climate Change. United Kingdom and New York. https://www.ipcc.ch/site/assets/uploads/2018/03/srccs_wholereport-1.pdf

[4] Nakrak, S., T. Yurata, B. Chalermsinsuwan, P. Tontiwachwuthikul, and T. Sema. 2021. Preliminary mass transfer performance of CO_2 absorption into AMP-PZ-MEA ternary amines. https://ssrn.com/abstract=3821405.

[5] Lee, S.Y. and S.J. Park. 2015. A review on solid adsorbents for carbon dioxide capture. Journal of Industrial and Engineering Chemistry. doi:10.1016/j.jiec.2014.09.001.

[6] Siriwardane, R.V., M.S. Shen, E.P. Fisher, and J.A. Poston. 2001. Adsorption of CO_2 on molecular sieves and activated carbon. Energy and Fuels. 15(2): 279-284. doi:10.1021/ef000241s.

[7] Millward, A.R. and O.M. Yaghi. Metal-organic frameworks with exceptionally high capacity for storage of carbon dioxide at room temperature.

[8] Thomas, S. 2008. Enhanced oil recovery – An overview. Oil and Gas Science and Technology. 9-19. doi:10.2516/ogst:2007060.

[9] Siregar, H.A., R. Melisa, I. Irawati, Z. Zulhelmi, and F. Kamilah. 2024. The capital structure determinants in food and beverage industry. Bilancia: Jurnal Ilmiah Akuntansi. 8(3): 231. doi:10.35145/bilancia.v8i3.4476.

[10] Ho, H.-J., A. Iizuka, E. Shibata, and T. Ojumu. 2022. Circular indirect carbonation of coal fly ash for carbon dioxide capture and utilization. Journal of Environmental Chemical Engineering. 10(5): 108269. doi:10.1016/j.jece.2022.108269.

[11] United Nations Framework Convention on Climate Change (UNFCCC). 2024. Thailand's First Biennial Transparency Report. https://unfccc.int/documents/645098.

[12] The Office of the Securities and Exchange Commission. 2022. Report Industrial Statistics 2022. Thailand. https://i.index.oie.go.th/industrialStatisticsReport.aspx.

[13] Department of Mineral Fuels, Ministry of Energy. 2022. Thailand's petroleum supply including onshore and offshore in January–December 2022. Thailand. https://dmf.go.th/public/supply/data/index/menu/966/id/13/.

[14] Speers, R.A., and A.J. MacIntosh. 2013. Carbon dioxide solubility in beer. Journal of the American Society of Brewing Chemists. 71(4): 242-247. doi:10.1094/ASBCJ-2013-1008-01.

[15] Abu-Reidah, I.M. 2019. Carbonated beverages. In Trends in Non-alcoholic Beverages. Elsevier, 1-36. doi:10.1016/B978-0-12-816938-4.00001-X.

[16] Bellia, F. 1968. Technological progress in the production of urea. In Chemical Fertilizers. Elsevier, 49-63. doi:10.1016/b978-0-08-003605-2.50011-2.

[17] Abdul, W., Rößler, C., Kletti, H., Mawalala, C., Pisch, A., Bannerman, M. N. and Hanein, T. 2025. On the variability of industrial Portland cement clinker: Microstructural characterisation and the fate of chemical elements. Cement and Concrete Research, 189. https://doi.org/10.1016/j.cemconres.2024.107773.

[18] Intergovernmental Panel on Climate Change (IPCC). 2015. Climate Change 2014: Synthesis Report – Longer Report.

[19] Netherlands Environmental Assessment Agency and Joint Research Centre. 2016. Trends in Global CO_2 Emissions 2016 Report.

[20] Leeson, D., N. Mac Dowell, N. Shah, C. Petit, and P.S. Fennell. 2017. A techno-economic analysis and systematic review of carbon capture and storage (CCS) applied to the iron and steel, cement, oil refining and pulp and paper industries, as well as other high purity sources. International Journal of Greenhouse Gas Control. 61: 71-84. doi:10.1016/j.ijggc.2017.03.020.

[21] Organisation for Economic Co-operation and Development (OECD). 2008. CO_2 Capture and Storage: A Key Carbon Abatement Option. doi:10.1787/9789264041417-en.

[22] Parkhi, A., D. Young, S. Cremaschi, and Z. Jiang. 2023. Carbon dioxide capture from the Kraft mill limekiln: Process and techno-economic analysis. Discover Chemical Engineering. 3(1). doi:10.1007/s43938-023-00024-7.

[23] Li, H., L. Dong, Y.T. Xie, and M. Fang. 2017. Low-carbon benefit of industrial symbiosis from a scope-3 perspective:

A case study in China. Applied Ecology and Environmental Research. 15(3): 135-153. doi:10.15666/aeer/1503_135153.

[24] McQueen, N., C.M. Woodall, P. Psarras, and J. Wilcox. 2019. CCS in the iron and steel industry. In Carbon Capture and Storage. The Royal Society of Chemistry, 353-391. doi:10.1039/9781788012744-00353.

[25] Bui, M., Adjiman, C. S., Bardow, A., Anthony, E. J., Boston, A., Brown, S., Fennell, P. S., Fuss, S., Galindo, A., Hackett, L. A., Hallett, J. P., Herzog, H. J., Jackson, G., Kemper, J., Krevor, S., Maitland, G. C., Matuszewski, M., Metcalfe, I. S., Petit, C., … Mac Dowell, N. 2018. Carbon capture and storage (CCS): The way forward. Energy and Environmental Science. Royal Society of Chemistry. 11(5): 1062-1176. https://doi.org/10.1039/c7ee02342a.

[26] Hasanbeigi, A., L. Price, and E. Lin. 2012. Emerging energy-efficiency and CO_2 emission-reduction technologies for cement and concrete production: A technical review. Renewable and Sustainable Energy Reviews. doi:10.1016/j.rser.2012.07.019.

[27] Abu-Zahra, M.R.M., L.H.J. Schneiders, J.P.M. Niederer, P.H.M. Feron, and G.F. Versteeg. 2007. CO_2 capture from power plants. Part I. A parametric study of the technical performance based on monoethanolamine. International Journal of Greenhouse Gas Control. 1(1): 37-46. doi:10.1016/S1750-5836(06)00007-7.

[28] Boot-Handford, M. E., Abanades, J. C., Anthony, E. J., Blunt, M. J., Brandani, S., Mac Dowell, N., Fernández, J. R., Ferrari, M. C., Gross, R., Hallett, J. P., Haszeldine, R. S., Heptonstall, P., Lyngfelt, A., Makuch, Z., Mangano, E., Porter, R. T. J., Pourkashanian, M., Rochelle, G. T., Shah, N., … Fennell, P. S. 2014. Carbon capture and storage update. Energy and Environmental Science. Royal Society of Chemistry. 7(1): 130-189. https://doi.org/10.1039/c3ee42350f.

[29] Rochelle, G.T. 2009. Amine scrubbing for CO_2 capture. Science. 325(5948): 1652-1654. doi:10.1126/science.1176731.

[30] Rubin, E.S., I.M.L. Azevedo, P. Jaramillo, and S. Yeh. 2015. A review of learning rates for electricity supply technologies. Energy Policy. doi:10.1016/j.enpol.2015.06.011.

[31] Wall, T.F. 2007. Combustion processes for carbon capture. Proceedings of the Combustion Institute. 31(1): 31-47. doi:10.1016/j.proci.2006.08.123.

[32] Fuss, S., Lamb, W. F., Callaghan, M. W., Hilaire, J., Creutzig, F., Amann, T., Beringer, T., De Oliveira Garcia, W., Hartmann, J., Khanna, T., Luderer, G., Nemet, G. F., Rogelj, J., Smith, P., Vicente, J. V., Wilcox, J., Del Mar Zamora Dominguez, M., & Minx, J. C. 2018. Negative emissions - Part 2: Costs, potentials and side effects. Environmental Research Letters. Institute of Physics Publishing. 13(6). doi:10.1088/1748-9326/aabf9f.

[33] Keith, D.W., G. Holmes, D. St. Angelo, and K. Heidel. 2018. A process for capturing CO_2 from the atmosphere. Joule. 2(8): 157-1594. doi:10.1016/j.joule.2018.05.006.

[34] Murai, S., M. Daigo, Y. Kato, Y. Maesawa, T. Muramatsu, and S. Saito. 2014. Development of hindered new amine absorbents for CO_2 capture. Energy Procedia. 1933-1939. doi:10.1016/j.egypro.2014.11.203.

[35] Rochelle, G.T. 2009. Amine scrubbing for CO_2 capture. Science. 325(5948): 1652-1654. Sep. 2009. doi:10.1126/science.1176731.

[36] Loachamin, D., J. Casierra, V. Calva, A. Palma-Cando, E.E. Ávila, and M. Ricaurte. 2024. Amine-based solvents and additives to improve the CO_2 capture processes: A review. Chem Engineering. 8(6). Dec. 01, 2024. doi:10.3390/chemengineering8060129.

[37] Borhani, T.N.G., A. Azarpour, V. Akbari, S.R. Wan Alwi, and Z.A. Manan. 2015. CO_2 capture with potassium carbonate solutions: A state-of-the-art review. International Journal of Greenhouse Gas Control. 41: 142-162. Oct. 2015. doi:10.1016/j.ijggc.2015.06.026.

[38] Kajolinna, T., K. Melin, O. Linjala, and J. Roine. 2024. Performance of novel carbonate-based CO_2 post-combustion capture process. International Journal of Greenhouse Gas Control. 136. Jul. 2024. doi:10.1016/j.ijggc.2024.104173.

[39] Krutka, H., S. Sjostrom, T. Starns, M. Dillon, and R. Silverman. 2013. Post-combustion CO_2 capture using solid sorbents: 1 MWe pilot evaluation. Energy Procedia. pp. 73-88. 2013. doi:10.1016/j.egypro.2013.05.087.

[40] Zentou, H., Hoque, B., Abdalla, M. A., Saber, A. F., Abdelaziz, O. Y., Aliyu, M., Alkhedhair, A. M., Alabduly, A. J. and Abdelnaby, M. M. 2025. Recent advances and challenges in solid sorbents for CO_2 capture. Carbon Capture Science and Technology. Elsevier Ltd. 15. https://doi.org/10.1016/j.ccst.2025.100386.

[41] Razzak, S.A., M.M. Hossain, R.A. Lucky, A.S. Bassi, and H. de Lasa. 2013. Integrated CO_2 capture, wastewater treatment and biofuel production by microalgae culturing—A review. Renewable and Sustainable Energy Reviews. 27: 622-653. doi:10.1016/j.rser.2013.05.063.

[42] Li, G., and J. Yao. 2024. A review of algae-based carbon capture, utilization, and storage (algae-based CCUS). Gases. 4(4): 468-503. doi:10.3390/gases4040024.

[43] Baxter, L.L., S. Burt, L. Baxter, and A. Baxter. 2009. Cryogenic CO_2 capture as a cost-effective CO_2 capture process. 2009. https://www.researchgate.net/publication/264875049.

[44] Hart, A. and N. Gnanendran. 2009. Cryogenic CO_2 capture in natural gas. Energy Procedia. 69-706. doi:10.1016/j.egypro.2009.01.092.

Thai Environmental Engineering Journal Vol. 39 No. 2 (2025) : 43-52
www.eeat.or.th

Carbon Footprint Assessment and GHG Mitigation Potential of Canned Tuna Spread Products in Thailand

Jirawat Jirajitmeechai[1,3], Cheema Soralump[1*], Vorapot Kanokkantapong[2] and Sirakarn Leungsakul[3]

[1]Department of Environmental Engineering, Faculty of Engineering, Kasetsart University, Bangkok 10900, Thailand
[2]Department of Environmental Science, Faculty of Science, Chulalongkorn University, Bangkok 10330, Thailand
[3]Department of Industrial Works, Bangkok 10400, Thailand
[*]E-mail : Cheema.c@ku.th

Article History; *Received: 13 July 2025, Accepted: 22 August 2025, Published: 28 August 2025*

Abstract

This study evaluated the carbon footprint (CFP) of tuna spread product produced by canned tuna factory in Thailand according to ISO 14067:2018 standards and Product Category Rules (PCRs) for processed and ready-to-eat food products. The assessment scope is cradle to gate, excluding secondary packaging of raw materials and products. The functional unit (FU) is defined as one can (net weight 85 grams) of tuna spread product. The carbon footprint of the tuna spread product is 408.08 gCO_2eq per FU. The proportion of greenhouse gas emissions comes from non-tuna ingredient, steam and hot water, tuna meat, and primary packaging, with values of 65.12, 11.40, 9.02, and 7.00 % respectively. GHGs reduction potentials are installing solar panels with power storage, increasing renewable energy consumption, changing to electric-powered ships and trucks, changing packaging to retort cup, implementing zero waste to landfill, and switching boiler fuel to biomass. Implementing all measures can reduce greenhouse gas emissions by up to 30.09% of the CFP of the classic style canned tuna spread product.

Keywords : Greenhouse gas emissions; Carbon footprint; Canned tuna spread; Tuna Industry; Thailand

Introduction

The processed tuna industry is a significant seafood processing industry in Thailand. Thailand is the world's number one exporter of canned tuna in 2023, primarily using imported tuna with a small fraction of tuna caught by Thai ship. The life cycle of canned processed tuna products, including the carbon footprint of the products, has been studied in several key countries for canned tuna exports, such as Spain, Ecuador, and Portugal including Thailand. Mungkung *et al.* (2012) [1] found that majority of greenhouse gas (GHGs) of canned tuna came from tuna meat with significant GHGs from primary packaging. Hospido *et al.*(2006) [2] found that plastic pouch has lower environmental impacts than tin can, however consumers' acceptance should be considered as well as economic value and end of waste management. Poovarodom *et al.* (2012) [3] further explored impact of different packaging of canned tuna in sunflower oil and found that retort cup has lower GHG than plastic pouch and metal can. Avadí *et al.* (2015) [4] suggested that a bigger packaging could lower CFP; and aluminium can has lower GHG than tin can. Cortés *et al.* (2021) [5] suggested that, to reduce CFP, the company should consider increasing number of

products within its scope to share GHG emissions to other products. De Vlieghere *et al.* (2023) [6] suggested that using local contents and local supply chain can reduce GHG emissions.

From our investigation, we found that the processing of tuna meat into ready-to-eat products and premium pet food can significantly enhance product yield and augment the value of by-products. Additionally, other fish parts were sent elsewhere for various uses: fish bones have been utilized for fish meal, and fish entrails have been employed for animal feed. One of ready-to-eat products from Pattaya Food Industries Co., Ltd., a sandwich tuna spread is selected for this study based on its sale growth potential in Thailand with 1.5 million cans in 2023. With increasing awareness on carbon emission, Thailand is actively pursuing carbon reduction policies with the goal of achieving carbon neutrality by 2050 and net-zero greenhouse gas emissions by 2065. However, there is little to no study on an environmental impact of this product. Therefore, this study focuses on the impact on climate change and estimates the carbon footprint of the classic style canned tuna spread product. This study also explores GHGs reduction potential for the tuna processing industry to assess the possibility to achieve national policy to reduce greenhouse gas emissions by 30-40% by 2030.

Methodology

This study used the carbon footprint assessment method according to ISO 14067: 2018 [7] and followed Product Category Rules for Prepared and Ready to Eat Products [8].

Goal and Scope Definition

The main goals of this study are (1) to calculate the carbon footprint of the canned tuna spread product, (2) to identify GHGs reduction potential for the tuna processing industry.

A case study of canned tuna spread product (Classic Tuna Spread, Nautilus Brand) is presented based on data of year 2023 from a canned tuna factory in Thailand. The assessment scope is defined as cradle to gate, covering the process of obtaining raw materials, transportation, production process, water production process, steam production process, wastewater treatment system, and waste management within the factory until the product is stored in the warehouse for shipment. Secondary packaging is not considered in this study. The system boundary is shown in Figure 1.

The functional unit is 1 can of tuna spread product (net weight 85 grams). The inventory of tuna spread production in 2023 is approximately 400,000 cans accounting for less than 0.1% of total production of the factory in that year. Mass allocation is used to distribute utilities and environmental burdens among different products.

Inventory Analysis

This study collected primary data from the company records, including data on domestic and international fish catching, raw materials and packaging, production process and waste management. Carbon emissions for fish catching are not available, therefore emission factors of fuel consumption in tuna fishing [10] were used instead. Sea transportation data was obtained from Captain Statement, Movement Document of the Department of Fisheries, and distances from Searates [11]. Loading factors for sea transportation are assumed to be 100% and distance of single trip is used since shipping vessels exchange goods at different ports along the way. Emissions from land transport were assessed based on vehicle types, distances, and loading factors. Land transportation data of each raw material was obtained from company records and Google Map. Loading factors for land transportation are calculated based on number of shipments and order volume of the same year. One-way empty loading, 0%, was assumed since company has no back hauling policy.

Data on raw materials and packaging were collected from the company's database. Primary data on the production process obtained from the company includes the use of tap water, electricity, steam production, and wastewater treatment system within the factory. Waste management data was considered based on disposal methods and location of disposal contractors. Inventory data is shown in Table 1.

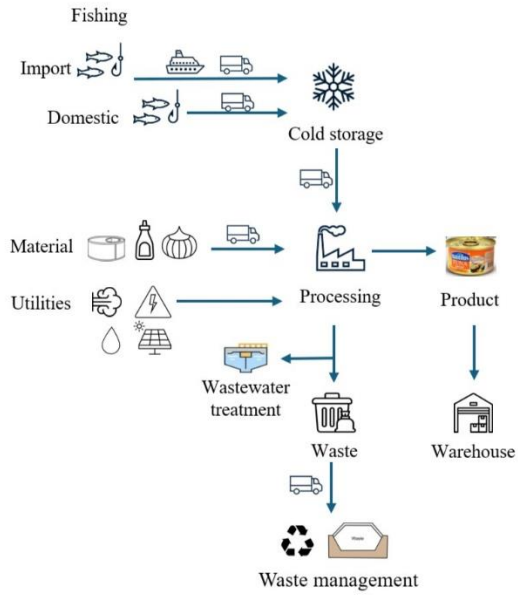

Figure 1 System boundary of the carbon footprint assessment of the tuna spread product

Table 1 Inventory data for the tuna spread processing

Input	Unit	Value per FU	Transport distance (km)
Ingredients			
Raw tuna (Import)	g	13.70	5,900 - 16,522[(a)]
			48-52[(b)]
Raw tuna (domestic)	g	3.30	5 - 1,005[(c)]
			9-12[(d)]
Mayonnaise (egg-based)	g	39.95	88
Water chestnut	g	22.10	120
Onion	g	5.95	12
Iron lid	g	3.00	13
Aluminum can	g	6.00	13
Utilities			
Electricity (mixed grid)	kWh	2.17×10^{-2}	
Electricity (solar power)	kWh	1.29×10^{-3}	
Water	liter	1.57	
Steam[(e)]	kg of steam	0.11	
wastewater	liter	1.21	

Note: (a) Transport distance from tuna landing port to Bangkok Port (ship),
(b) Transport distance from Bangkok Port to cold storage (road),
(c) Transport distance from domestic tuna landing port to cold storage (road),
(d) Transport distance from cold storage to factory (road),
(e) utilize Sub-bituminous coal and heavy oil grade A

Greenhouse gas emissions coefficients used in this study were considered according to the guidelines for selecting greenhouse gas emissions coefficients from Thailand Greenhouse Gas Management Organization (Public Organization) (TGO) in the following order: 1) TGO database, 2022 [12] 2) environmental database of basic materials and energy in Thailand 3) peer reviewed research paper and thesis conducted in Thailand 4) SimaPro software Version 8.3 and Background processes were taken directly from Ecoinvent Version 3.0 production process database. IPCC 2013 GWP 100a V1.03 calculation method was selected to align with the national database. Emission factors used in this study are shown in Table 2 and Table 3.

Table 2 Secondary data on input emission factors for materials and energy

Item	EF Source
Material	
Raw tuna catching	Parker *et al*. (2015) [10]
Diesel oil (for sea transportation)[(a)]	Ecoinvent Version 3.0
Diesel oil (for land transportation)[(b)]	TGO, 2022
Mayonnaise (egg-based)	Saget *et al*. (2021) [13]
Water chestnut	Jirajitmeechai *et al.* (2025) [14]
Onion	TGO, 2022
Iron lid (tin free steel)	TGO, 2022
Aluminium can (aluminum plate with deep drawing, steel press)[(c)]	TGO, 2022 and Ecoinvent Version 3.0
Aluminum Sulphate (PAC)	TGO, 2022
Utility	
Electricity (Mixed grid)	TGO, 2022
Electricity (Solar power)	Khan *et al*. (2024) [15]
Tap water	TGO, 2022
Fuel oil	TGO, 2022
Heavy oil	TGO, 2022
Lignite coal	TGO, 2022
Sub-bituminous coal	TGO, 2022
Stationary Combustion	TGO, 2022
Waste management	
Municipal solid waste landfill (Compaction)	Liamsanguan *et al*. (2008) [16]
Open dumping	TGO, 2022

Note: EF = GHG Emission factor
(a) Diesel oil used in fishing vessels occurs outside Thailand.
(b) Diesel oil used in fishing vessels occurs within Thailand.
(c) EF of aluminum can is calculated from aluminum plate with EF from TGO (2022) and EF of can forming with deep drawing process from Ecoinvent Version 3.0.

Table 3 Secondary data on input emission factors for transport

Type of transport	Source	Item
transoceanic ship with reefer	Ecoinvent Version 3.0	Raw tuna
10-wheel truck	TGO, 2022	Raw tuna
4-wheel vehicle	TGO, 2022	Onion, water chestnut, waste
6-wheel vehicle	TGO, 2022	Can, mayonnaise, waste

Results and Discussion

The results of GHG emissions of the Classic Tuna Spread product are presented in Figure 2, grouped into 6 categories. The majority of GHG emissions come from non-tuna ingredients, 65.12%, followed by from processing, 16.60%, tuna meat, 9.02%, packaging, 7.00%, transportation, 1.99%, and waste disposal, 0.27%. GHGs from non-tuna ingredients were investigated further; it found that 39.55 grams of mayonnaise contribute highest GHG emissions, 167.22 gCO_2eq, since it is the main ingredient of tuna spread. Carbon footprint of Mayonnaise mainly comes from vegetable oil, in which reference study used sunflower oil [13]. Considering emission factors of different vegetable oil, changing of vegetable oil type may significantly affect the carbon footprint of Mayonnaise [9].

The second highest GHG emission is from 22.10 grams of water chestnuts, the second highest content of all ingredients, contribute 96.47 gCO_2eq. GHG emissions from production processes mainly come from hot water and steam utilization, 46.51 gCO_2eq. It should be noted that sub-bituminous coal is used as fuel for the boiler; CO_2 emission from fossil fuel combustion could not be avoided. Electricity used in the process comes from two sources, one is from the electricity grid of Provincial Electricity Authority (PEA), and another is from 301.72 kW roof-top solar panel accounting for 5.39% of total electricity power consumption. Land transportation of raw materials and sea transportation of tuna fish account for 1.99% of total GHG emissions. The diesel fuel consumption for fishing vessels was determined using the fuel intensity associated with tuna catching in the Atlantic, Pacific, and Indian Oceans [10], with SimaPro software Version 8.3 GHG emissions factor applied to diesel for imported tuna and TGO's GHG emission factor for domestic tuna fishing. Total GHG emission for tuna landing at ports in Thailand is 36.80 gCO_2eq. Another major GHG emission comes from primary packaging, 28.56 gCO_2eq. Emission factor of aluminum can produce in Thailand is not available, therefore emission factor of aluminum can was calculated from emission factor of aluminum sheet and single stroke deep drawing process from SimaPro software. The lid of the aluminum can is made of tin free steel; an emission factor from TGO is used. Secondary packaging of raw materials was either sent back to producers or to recyclers for reuse or recycle, hence it is not covered in this study. Waste from tuna cutting such as bones, guts and blood were sent to produce fish meal and pet food, however, fatty sludge from wastewater treatment system, bottom ash and fly ash from boiler were sent to landfill.

To compare CFP of this study with other studies, the GHG emission per FU from different studies as shown in Table 4 are converted to GHG emission per one kilogram of edible content in the products as shown in Figure 3. It is found that raw tuna products, pouched loin tuna and bagged frozen loin tuna, have lower GHG emissions than most of cooked tuna products. Among cooked tuna products, GHG emissions vary depending on type of liquid filled in the products and containers. The ready to eat product in this study, canned tuna spread even without considering post-consumer waste, has higher GHG per kilogram edible product than all canned tunas. This was caused by small portion of tuna meat, 20%, mixed with non-tuna ingredients, 80%, that have higher GHG emissions such as mayonnaise (47%), water chestnut (26%), and onion (7%). Among different landed fish, there are 0.36 $kgCO_2eq$ per kg sardine landed [17] and 1.14 $kgCO_2eq$ per kg tuna landed [10]. Although landed sardine has lower GHG emission than landed tuna, canned sardine with olive oil has highest GHG emissions per kg sardine meat, in which aluminium canned contributes highest to total GHG emissions of the product [18].

Potential for Reducing Greenhouse Gas Emissions of Classic Tuna Spread product

The potential for reducing greenhouse gas emissions of canned tuna products, as shown in Figure 4, is assessed based on research findings and company data.

(1) The study of Moultak *et al.* (2017) [20] shows that switching type of transportation to electric-powered ships and trucks can reduce greenhouse gas emissions by 40%. Additionally, utilizing electricity generated from clean energy sources, such as solar power, can further reduce emissions by up to 89.80%. With this GHG reduction rate from utilizing electric-powered vessels in fishing activities, greenhouse gas emissions could be reduced up to 8.10% of total GHG emissions from canned tuna spread product. Transitioning all transportation to electric-powered vehicles that utilize renewable energy may result in an additional 1.78% of total GHG emissions reduction.

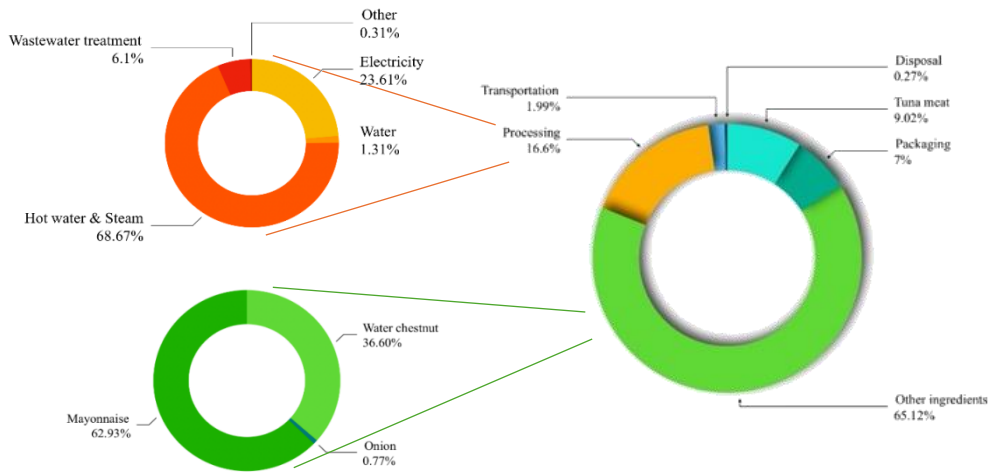

Figure 2 The proportion of greenhouse gas emissions of the Classic Tuna Spread product

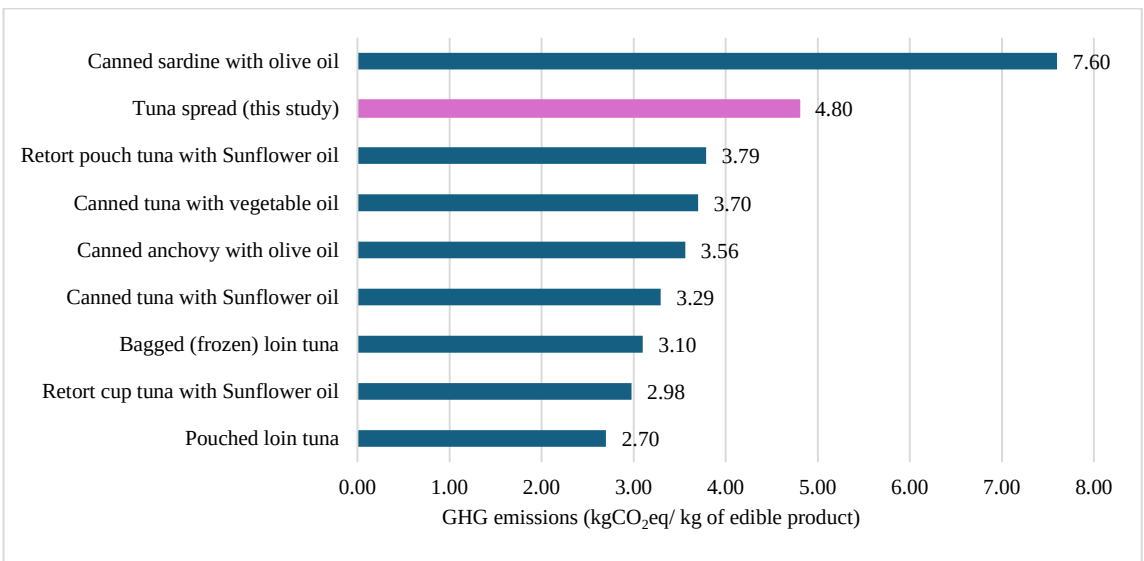

Figure 3 The greenhouse gas emissions of processed seafood products

Table 4 The greenhouse gas emissions of processed seafood products

Reference / Country	Targeted species	FU	System boundaries	GHG emissions ($kgCO_2eq/FU$)
This study / Thailand	tuna yellowfin (*Thunnus albacares*), skipjack (*Katsuwonus pelamis*) and albacore tuna (*Thunnus alalunga*)	1 can of product	Cradle to gate	0.408
Poovarodom *et al.* (2012) [3] / Thailand	tuna	Chrome-coated steel can, with an aluminum lid (net weight 85g)	Cradle to grave	0.280
		Retort pouch (net weight 85g)	Cradle to grave	0.322
		Retort cup (net weight 80g)	Cradle to grave	0.253
Almeida *et al.* (2015) [18] / Portugal	European pilchard (*Sardina pilchardus*)	1 kg of edible, canned sardine with olive oil	Cradle to gate	7.6
Avadi *et al.*, (2015) [4] / Ecuador	tuna yellowfin (*Thunnus albacares*), skipjack (*Katsuwonus pelamis*) and bigeye (*Thunnus obesus*)	1 kg of canned tuna in vegetable oil	Cradle to gate	3.7
		1 kg of pouched loins	Cradle to gate	2.7
		1 kg of bagged (frozen) loins	Cradle to gate	3.1
Laso *et al.* (2017) [19]/ Spain	Anchovy (*Engraulis encrasicolus*)	1 can of fish in extra virgin olive oil (aluminum can, 30g of anchovy and 20 g of extra virgin olive oil (EVOO))	Cradle to gate	0.178

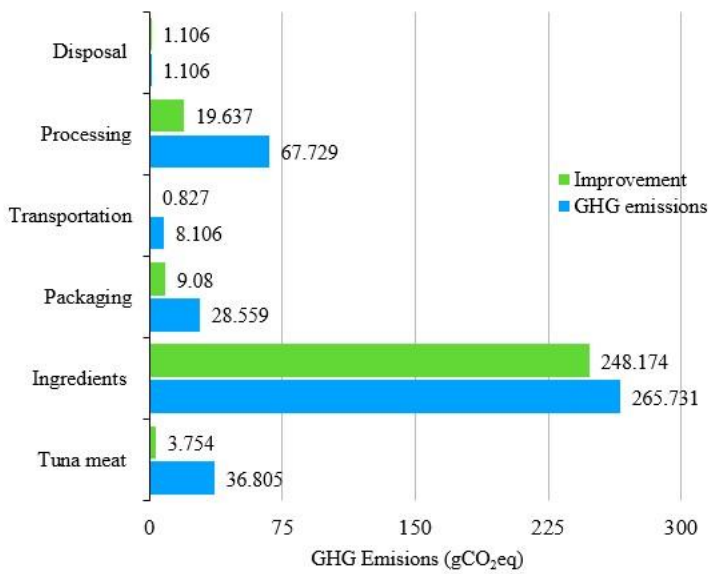

Figure 4 Potential for reducing greenhouse gas emissions of canned tuna spread products

(2) According to Thailand's PDP2018 Revision 1 plan, increasing the proportion of electricity generation from renewable energy sources will enable the use of electricity to reduce greenhouse gas emissions by 24.51% n B.E. 2580, in which can reduce GHG emissions from cold storage room by 0.205% of the total GHG emissions.

(3) The company decided to install rooftop solar panels in 2023 covering 33% of the total roof area, in which solar panels could produce electricity with a maximum power generation about 30% of total electricity consumption and be consumed by the plant during the daytime. In 2024, the company utilized electricity from photovoltaics about 8.64% of total electricity consumption of the whole year. If the company had decided to maximize rooftop solar panel installation equipped with energy storage sources, with additional consideration of the PDP2018 Revision 1 plan, the greenhouse gas emissions would be reduced by up to 61.92% in B.E. 2580, in which accounted for 1.91% of the total GHG emissions. The greenhouse gas emission coefficient from solar cells produced in China with a lifespan of 30 years and used in tropical humid areas with a value of 33.9 gCO_2eq/kWh was selected [13].

(4) Poovarodom *et al.* (2012) [3] compared CFP of tuna with different packaging and found that by changing packaging from metal can to plastic pouch and retort cup can reduce carbon footprint by 58.6% and 68.2%, respectively. By switching from aluminum cans to retort cups, CFP would be decreased by upto 4.77% of the total GHG emissions.

(5) Switching fuel from sub-bituminous coal to parawood pallet biomass can reduce greenhouse gas emissions by up to 76.73%, which contributes to 8.75% of the total GHG emissions.

(6) Jirajitmeechai *et al.* (2015) [14] demonstrated that changing disposal method from landfilling to utilizing water chestnut peel for making soil conditioner can significantly reduce carbon dioxide emissions by 18.2%, in which accounted for 4.30% of the total GHG emissions.

(7) Utilizing waste (fat sludge) as energy, along with using the methane gas produced from wastewater treatment plant, can reduce greenhouse gas emissions by up to 100%.

Table 5 Potential for Reducing Greenhouse Gas Emissions of Classic Tuna Spread product

Mitigation and Reduction Measures	Potential GHG reduction (%)*	Reduction contribution to CFP (%)	Reference
Change to electric-powered ships and trucks	40% (electricity from normal grid mix) / 89.80% (electricity from renewable energy)	8.10% (electric-powered fishing ships) 1.78% (electric-powered ships and trucks for raw material transportation)	Moultak *et al.* (2017) [20]
Increase renewable energy in grid mix	24.51% (B.E. 2580) (cold storage room)	0.21%	Thailand's PDP2018 Revision 1 plan
Increase electricity from photovoltaics	61.92% (B.E. 2580, with power storage) (production)	1.91%	Khan *et al.* (2024) [15], and Thailand's PDP2018 Revision 1
Change packaging	58.6% (plastic pouch) / 68.2% (retort cup)	4.77% (retort cup)	Poovarodom *et al.* (2012) [3]
Replace with biomass fuel	76.73% (parawood sawdust)	8.75%	Jirajitmeechai J., (2025) in publishing process (thesis) [21]
Zero waste to landfill	18.2% (chestnut peel) 100% (fat sludge)	4.30% 0.27%	Jirajitmeechai *et al.,* (2025) [14]
All measures		30.09 %	

Note: *compared with current practice, in 2023 (B.E. 2566)

Conclusions

The carbon footprint of the tuna spread product is 408.08 gCO_2eq per can with major contribution from ingredients and processing, respectively. With the current practice, all fish meat and bones have been utilized as products or raw materials for other industries. Additional greenhouse gas reduction measures that can be implemented immediately by manufacturers with small impact to customers are changing boiler fuel from coal to biomass, installing roof top solar panels, implementing better waste management, and maintaining zero waste to landfill policy. These immediate measures can reduce GHG by 15.23%. Further R&D is required before changing packaging from aluminum can to retort cup or plastic pouch, since this may require process adjustment as well as customer acceptance. As for changing internal combustion engine (ICE) vehicles to electric powered, the company may start to integrate electric powered vehicles into the fleet and request suppliers to take similar measured to reduce GHG emission. One significant GHG emissions is from power supply, it highly depends on national power development plan. If it can be expedited, further GHG reduction could be achieved. Implementing all measures together can reduce greenhouse gas emissions by up to 30.09 % of the total GHG emissions, resulting in a carbon footprint of 285.26 gCO_2eq per can.

References

[1] Mungkung, R., Gheewala, S. H., Kanyarushoki, C., Hospido, A., van der Werf, H., Poovarodom, N., Bonnet, S., Aubin, J., Moreira, M. T. and Feijoo, G. 2012. Product carbon footprinting in Thailand: A step towards sustainable consumption and production? Environmental Development. 3: 100-108.

[2] Hospido, A., Vazquez, M., Cuevas, A., Feijoo, G. and Moreira, M. 2006. Environmental assessment of canned tuna manufacture with a life-cycle perspective. Resources, Conservation and Recycling. 47(1): 56-72.

[3] Poovarodom, N., Ponnak, C. and Manatphrom, N. 2012. Comparative carbon footprint of packaging systems for tuna products. Packaging Technology and Science. 25(5): 249-257.

[4] Avadí, A., Bolaños, C., Sandoval, I. and Ycaza, C. 2015. Life cycle assessment of Ecuadorian processed tuna. The International Journal of Life Cycle Assessment. 20: 1415-1428.

[5] Cortés, A., Esteve-Llorens, X., González-García, S., Moreira, M. T. and Feijoo, G. 2021. Multi-product strategy to enhance the environmental profile of the canning industry towards circular economy. Science of The Total Environment. 791: 148249.

[6] De Vlieghere, A., Van Veghel, A. S. and Geeraerd, A. 2023. Life cycle assessment of importing canned tuna into Aruba through different supply chains, in varying can sizes and in oils, brine or tomato sauce. The International Journal of Life Cycle Assessment. 28(11): 1577-1589.

[7] ISO (International Organization for Standardization). (2018). ISO 14067: 2018 Greenhouse gases: Carbon footprint of products. Requirements and guidelines for quantification and communication.

[8] Thailand Greenhouse Gas Management Organization (TGO). 2024. Product Category Rules for Prepared and Ready to Eat Products. https://thaicarbonlabel.tgo.or.th/index.php?lang=TH&mod=Y0hKdlpIVmpkSE5mY25Wc1pYTT0.

[9] Schmidt, J. H. 2015. Life cycle assessment of five vegetable oils**.** Journal of Cleaner Production. 87: 130-138.

[10] Parker, R. W., Vázquez-Rowe, I. and Tyedmers, P. H. 2015. Fuel performance and carbon footprint of the global purse seine tuna fleet. Journal of Cleaner Production. 103: 517-524.

[11] SeaRates. 2025. Distance & Time. https://www.searates.com/distance-time/.

[12] Thailand Greenhouse Gas Management Organization (TGO). 2022. Emission Factor (CFP).

https://thaicarbonlabel.tgo.or.th/index.php?lang=EN&mod=Y0hKdlpIVmpkSE5mWlcxcGMzTnBiMjQ9.

[13] Saget, S., Costa, M., Styles, D. and Williams, M. 2021. Does circular reuse of chickpea cooking water to produce vegan mayonnaise reduce environmental impact compared with egg mayonnaise? Sustainability. 13(9): 4726.

[14] Jirajitmeechai, J., Soralump, C. and Kanokkantapong, V. Carbon Footprint of Peeled Chinese Water Chestnut. 24th National Environmental Conference at Bangsaen Heritage Hotel, Saen Suk, Chon Buri, Thailand on May 20-21, 2025.

[15] Khan, A. A., Reichel, C., Molina, P., Friedrich, L., Subasi, D. M., Neuhaus, H. and Nold, S. 2024. Global warming potential of photovoltaics with state-of-the art silicon solar cells: Influence of electricity mix, installation location and lifetime. Solar Energy Materials and Solar Cells. 269: 112724.

[16] Liamsanguan, C. and Gheewala, S. H. 2008. LCA: A decision support tool for environmental assessment of MSW management systems. Journal of environmental management. 87(1): 132-138.

[17] Almeida, C., Vaz, S., Cabral, H. and Ziegler, F. 2014. Environmental assessment of sardine (Sardina pilchardus) purse seine fishery in Portugal with LCA methodology including biological impact categories. The International Journal of Life Cycle Assessment. 19(2): 297-306.

[18] Almeida, C., Vaz, S. and Ziegler, F. 2015. Environmental life cycle assessment of a canned sardine product from Portugal. Journal of Industrial Ecology. 19(4): 607-617.

[19] Laso, J., Margallo, M., Fullana, P., Bala, A., Gazulla, C., Irabien, A. and Aldaco, R. 2017. Introducing life cycle thinking to define best available techniques for products: application to the anchovy canning industry. Journal of Cleaner Production. 155: 139-150.

[20] Moultak, M., Lutsey, N. and Hall, D. 2017. Transitioning to zero-emission heavy-duty freight vehicles. Washington, DC, USA: ICCT.

[21] Jirajitmeechai, J. 2025. Greenhouse gas emission management guidelines for the canned tuna industry [Unpublished master's thesis]. Kasetsart University.

Thai Environmental Engineering Journal Vol. 39 No. 2 (2025) : 53-61
www.eeat.or.th

A Study of Characteristics, Origins, and Fates of Ultrafine Particles Over Taichung City, Taiwan

Kijpat Thavorn[1], Win Trivitayanurak[1,2] and Ta-Chih Hsiao[3]

[1]Department of Environmental and Sustainable Engineering, Faculty of Engineering, Chulalongkorn University, Bangkok 10330, Thailand
[2]Aroon Sorathesn Center of Excellence in Environmental Engineering, Faculty of Engineering, Chulalongkorn University, Bangkok 10330, Thailand
[3]Graduate Institute of Environmental Engineering, National Taiwan University, Taipei 106, Taiwan
[*]E-mail : kjdome09@gmail.com

Article History; *Received: 15 July 2025, Accepted: 22 August 2025, Published: 28 August 2025*

Abstract

Ultrafine particles (UFPs, <0.1 μm) pose serious health risks and remain challenging to accurately monitor and model due to complex atmospheric processes. This study investigates UFP dynamics over Taichung City, Taiwan, utilizing April 2021 observational data from a Scanning Mobility Particle Sizer (SMPS) and simulations from the GEOS-Chem-TOMAS model. Observations included particle number size distributions (analyzed from 11.8 to 593.5 nm), sulfuric acid concentrations, and meteorological variables. The model employed 15 size bins and evaluated five nucleation schemes (Basecase, Binary, Binary ion, Ternary, Ternary ion) to assess new particle formation (NPF) sensitivity. Results indicate that Basecase, Ternary, and Ternary ion schemes simulated sporadic nucleation bursts; Binary schemes showed minimal activity. Despite visual coincidence with sulfuric acid peaks, simulated nucleation rates exhibited a weak linear correlation (Pearson $R \approx -0.04$), underscoring that NPF is a complex, non-linear process influenced by multiple atmospheric parameters beyond sulfuric acid, including ammonia, amines, and organic vapors, The model consistently and substantially underestimated observed particle number concentrations across all modes (NMBs ranging from -8.5% to -90.9%; correlation coefficients (absolute values) from 0.06 to 0.21) except for accumulation mode that the model display relatively good agreement of magnitude. The current model struggled to capture the overall magnitude and variability of particle number size distribution, underscoring the need for improving our understanding of the emission inventory as well as the boundary layer meteorology. With regard to new particle formation, crucially no clear classical "banana-shaped" NPF events were observed Importantly, no clear classical "banana-shaped" NPF events were observed in either the observational data or the model simulations throughout the study period. These findings underscore the critical need for improved nucleation and growth parameterizations, higher-resolution meteorological data, and refined local emission inventories to enhance the accuracy of urban aerosol modeling in subtropical environments.

Keywords : Ultrafine Particles; GEOS-Chem-TOMAS; Nucleation; Air Quality; Taichung; Atmospheric Modeling

Introduction

Ultrafine particles (UFPs), defined as particulate matter with diameters less than 0.1 μm, are of growing concern due to their adverse health effects [1, 2]. These particles can penetrate deep into the lungs, translocate into the bloodstream, and induce oxidative stress, potentially leading to cardiovascular, respiratory, and neurological diseases [3, 4]. Mounting evidence from toxicological and epidemiological studies supported by organizations like the World Health Organization (WHO) and the Health Effects Institute (HEI) suggests UFPs can trigger systemic inflammation and other adverse outcomes even at relatively low ambient concentrations. This is particularly concerning given the lack of official regulatory standards for UFP number concentrations in most countries, which contrasts with the mass-based metrics used for $PM_{2.5}$ and PM_{10}. Recent studies emphasize particle number concentration (PNC) as a more suitable metric for evaluating UFP exposure and informing public health policy [5].

New particle formation (NPF) is a significant source of UFPs in the atmosphere. This process involves the conversion of precursor gases into new particles, with key roles played by species such as sulfuric acid, ammonia, and organic compounds. These chemical reactions are highly sensitive to meteorological conditions, including solar radiation, temperature, and relative humidity, which influence the formation of condensable vapors and the removal of nascent particles [6, 7].

As with any air quality monitoring, spatial coverage is limited but air quality model can help supplement these gaps. Advanced chemical transport models, such as GEOS-Chem coupled with the TwO-Moment Aerosol Sectional (TOMAS) microphysics module, offer a robust framework for simulating aerosol number and mass size distributions [8]. Comparing model output against high-resolution observational data is essential for enhancing predictive accuracy and improving our understanding of UFP behavior.

This study investigates the characteristics, origins, and atmospheric evolution of UFPs over Taichung City, Taiwan, by integrating ground-based measurements with GEOS-Chem-TOMAS simulations. We aim to identify key processes driving new particle formation (NPF), evaluate various nucleation schemes, and assess the model's ability to replicate observed UFP dynamics. Findings are expected to enhance UFP representation in regional air quality models and provide insights for future regulatory and public health strategies.

Methodology

This study investigates ultrafine particle (UFP) behavior in Taichung, Taiwan, using both observational data and regional-scale modeling for the period April 2021. This specific month was selected due to the high completeness and quality of the observational data, particularly from the Scanning Mobility Particle Sizer (SMPS) measurements, which exhibited the fewest missing (NaN) values during this period, thus ensuring a robust dataset for detailed analysis of new particle formation events and reliable model-measurement comparison. Particle number size distribution (PNSD) measured by the Scanning Mobility Particle Sizer (SMPS), covering a size range of 11.8–593.5 nm, at the Tunghai University monitoring site in collaboration with National Taiwan University (NTU). Sulfuric acid and other meteorological variables, including solar radiation, relative humidity, and $PM_{2.5}$ concentrations, were monitored to support the analysis of atmospheric conditions influencing UFP formation. It should be noted that the SMPS instrument's lower detection limit of 11.8 nm inherently limits the observation of nascent NPF stages (particles typically form at sub-10 nm sizes). SMPS observations were averaged to hourly resolution before comparison with hourly model outputs.

For the modeling component, the GEOS-Chem chemical transport model [9] coupled with the TwO-Moment Aerosol Sectional (TOMAS) microphysics module was employed, following the configurations described by Trivitayanurak et al. (2008) [8]. The simulations were conducted using GEOS-FP assimilated meteorological data from NASA's Global Modeling and Assimilation Office, at a nested horizontal resolution of 0.25° × 0.3125°, encompassing the Taiwan region. The GEOS-Chem-TOMAS framework calculates aerosol number and mass concentrations across 15 discrete size bins ranging from 3 nm to 10 μm. To investigate the sensitivity of UFP formation to different nucleation pathways, five nucleation

schemes were evaluated: Basecase, Binary, Binary ion, Ternary, and Ternary ion.

The model's emissions inventory relies on a combination of global and regional datasets. For Asia, the MIX inventory is commonly used, which provides anthropogenic emissions on a regional scale. While this inventory offers a good overall picture, its spatial and temporal resolution may not fully capture local, highly variable sources like on-road traffic or small-scale industrial activities in a densely populated urban area like Taichung. This can lead to discrepancies between modeled and observed concentrations, especially for fresh, small particles.

The five nucleation schemes represent different theoretical pathways for new particle formation:

- Basecase: A standard kinetic nucleation scheme that represents the collision of precursor molecules to form a stable cluster.
- Binary Homogeneous Nucleation (BHN): Describes the formation of new particles solely from the condensation of sulfuric acid and water vapor. This is often less effective in the lower troposphere due to the high vapor pressure of water.
- Binary Ion-Mediated Nucleation (BIMN): Similar to BHN, but the process is catalyzed by atmospheric ions, which can significantly enhance nucleation rates by stabilizing the particle clusters.
- Ternary Homogeneous Nucleation (THN): An extension of BHN that includes a third component, typically ammonia, which acts as a stabilizing agent to lower the energy barrier for nucleation, making the process more efficient.
- Ternary Ion-Mediated Nucleation (TIMN): The most complex scheme, incorporating the effects of both ammonia and atmospheric ions to promote nucleation.

New particle formation (NPF) events were identified based on observed particle growth in the 11–20 nm range, with growth rates determined from changes in geometric mean diameter (Dpg), in line with Dal Maso et al. (2005) [10]. The classification of NPF events was conducted through visual inspection of PNSD surface plots and analysis of nucleation-mode particle evolution, consistent with methodologies outlined by Wang et al. (2023) [7].

Model diagnostics, including nucleation, condensation, and coagulation rates, were used to interpret observed events and assess the capability of each nucleation scheme in reproducing measured UFP trends. These insights are critical for understanding regional-scale UFP dynamics and improving model performance in simulating fine-scale aerosol processes.

Results and Discussions

The GEOS-Chem model simulation for April 2021, shown in Figure 1, illustrated the spatial distribution of total particle number concentrations (PNC) over Taiwan, revealing elevated levels in northeastern regions consistent with monsoonal winds and inland advection.

To understand observed particle dynamics and atmospheric conditions, Figure 2 presents the contour plots of hourly particle number size distribution (PNSD) for the study site at Taichung City, selected for the period of 20-25 April 2021 for both the observation and the simulated results. The PNSD is plotted in units of dN/dlogDp (#/cm³). My analysis found similar features of the contour plots for the rest of April 2021 thus they are not shown here. Due to the measurement limitation where the SMPS begins detection at 11.8 nm, the comparison of particles smaller than 11 nm is not possible. Despite this limitation, the observation data revealed there was no evidence of a classical "banana-shaped" new particle formation (NPF) events throughout the study period, as depicted in Figure 2 a) as an example.

A classical "banana-shaped" NPF event is a distinct pattern on a PNSD contour plot, characterized by a sharp, vertical increase in the number of particles in the nucleation mode, typically between 3–25 nm, followed by a clear, sustained diagonal upward shift as these newly formed particles grow into the Aitken mode (25–100 nm) over several hours. The plot resembles a "banana" as the particle size increases with time.

For the simulation, there is no NPF occurred during the study period as well, as shown in Figure 2b) as an example. The plot

depicts particle growth behavior but none with the feature of a major NPF event that is typically followed by growth that lasts over several hours.

Upon comparison of the PNSD in Figure 2, the measured data was consistently higher and also with more variability. The lower temporal variability in modeled PNSD is attributed to the nature of the model grid representing averaged concentrations over a grid area, which may not fully resolve the fluctuations occurring at a spot site. The modeled PNSD allows an investigation down to 3 nm and demonstrates a peak of the nucleation mode particles occurring every day at regular hours typical of the morning traffic rush hours. The observed PNSD, on the other hand, shows a higher variation with multiple peaks at morning traffic rush hours, midday, and another in the evening. The absence of midday and evening peaks in the model highlights gaps in emission inventories that may not readily reflect real-world fluctuations and limitations in the representation of evening boundary layer meteorology. Another important feature of the simulated PNSD is the persistent concentrations above 10 nm with a major peak at 20 nm and a fewer occurrence of another peak at 100 nm.

Analysis of meteorological parameters revealed that persistently high relative humidity (often exceeding 70-80% during daytime), solar radiation in the range of 500-800 W/m², and low SO_2 concentrations (typically below 1 ppb) likely inhibited NPF. Furthermore, the environment was characterized by elevated background aerosol concentrations and generally low levels of critical precursor gases. These elevated background particles contribute to a substantial condensation sink, efficiently scavenging low-volatility vapors and newly formed clusters, thereby suppressing nucleation. Combined with non-optimal meteorological conditions, these factors likely explain the observed absence of classical NPF events in Taichung.

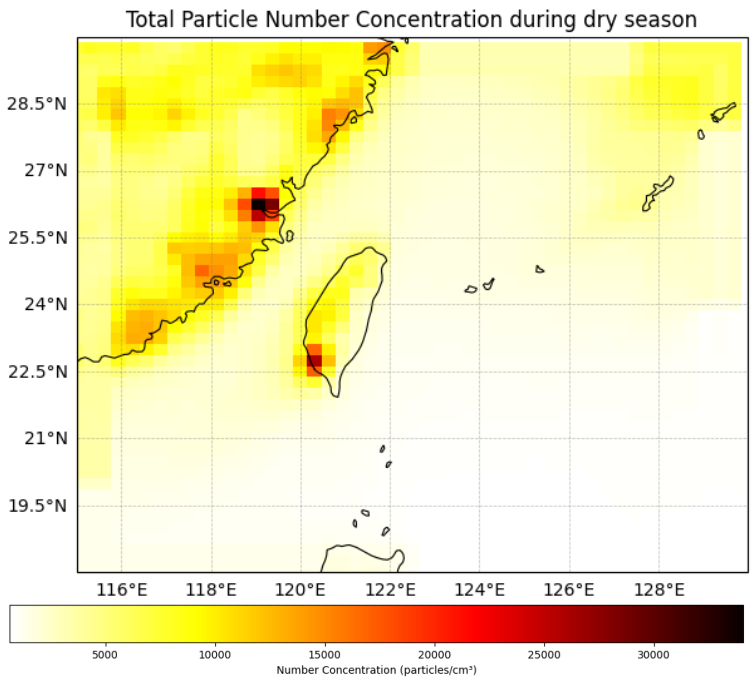

Figure 1 Spatial distribution of total particle number concentrations (PNC) over Taiwan, simulated by the GEOS-Chem model averaged for April 2021 period

a)

b)

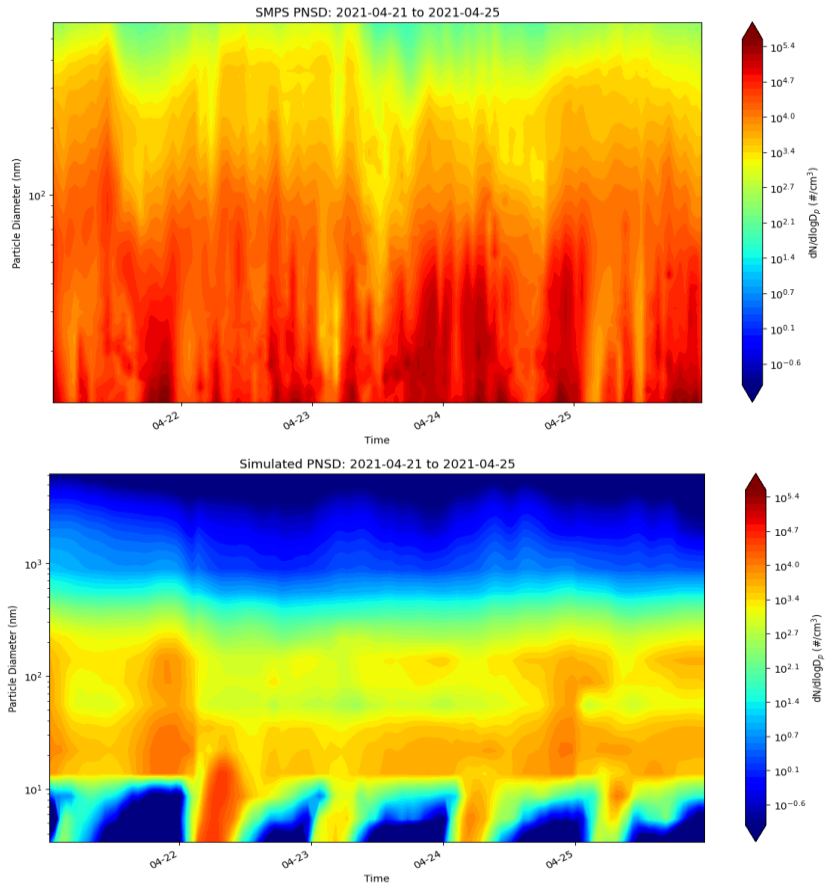

Figure 2 PNSD Contour Plot at Tunghai University, Taichung City, during 21-25 April 2021, including a) measurement by SMPS and b) simulated by GEOS-Chem-TOMAS model. The measured PNSD covers sizes of 11.8-593.5 nm while the simulated PNSD covers 3 nm to 10 microns

To better understand the particle dynamics, it is important to distinguish between the three primary particle modes:

- Nucleation Mode (<25 nm): Dominated by particles freshly formed from gas-to-particle conversion (new particle formation). These are highly sensitive to precursor gas concentrations and photochemical activity.
- Aitken Mode (25-100 nm): Formed primarily by the growth of nucleation mode particles through coagulation and condensation of semi-volatile vapors.
- Accumulation Mode (100-1,000 nm): Formed by the coagulation and condensation of smaller particles. These particles have a longer atmospheric lifetime and are less sensitive to rapid, local processes.

To quantitatively assess the model's performance, Figure 3 and Figure 4 compare simulated and observed particle number concentrations (PNCs) as time-series plot and scatter plots, respectively, for total PNC (≤50 nm) and individual modes (nucleation, Aitken, and accumulation). The model consistently and substantially underestimated observed particle concentrations across all modes except the accumulation mode. The accumulation mode provides better agreement because these larger particles are less dependent on rapid, local processes like primary emissions or nucleation, which are poorly resolved by the model. Their concentrations are more influenced by regional

transport and long-term accumulation, which the model is better equipped to simulate. The time-series plot in Figure 3 d) and the scatter plot in Figure 4 c) display significantly better agreement between modeled and observed PNC compared to other size modes. For total PNC (≤50 nm), the model showed a Normalized Mean Bias (NMB) of -90.88% and a Root Mean Square Error (RMSE) of 37,006.79 #/cm³. Mode-specific analysis revealed NMBs ranging from -8.49% for accumulation mode to -89.22% for Aitken mode, and -86.31% for nucleation mode. Correlation coefficients (R) were notably low across most modes, with R^2 values ranging from 0.0036 (Total PNC) to 0.04 (Nucleation Mode) and 0.03 (Aitken Mode). However, the accumulation mode exhibited a relatively strong correlation (R^2 = 0.78). This indicates that the model largely fails to reproduce the observed temporal variability and synchronous changes in particle concentrations, highlighting a significant challenge in capturing UFP dynamics at local scales.

The time-averaged PNSD for both simulated and observed data showed that while the model qualitatively captures the general shape, it systematically underestimates mean concentrations and exhibits higher variability than observed, particularly at the smallest (<13 nm) and largest (>600 nm) particle sizes. The notably wide standard deviation in the sub-13 nm range suggests that the model simulates sporadic and intense bursts of new particle formation or very rapid initial growth/loss, which, even if short-lived, lead to significant variability around the mean.

Diurnal variations were also examined in Figure 5; the model fails to capture the variations exhibited by observed data for all size modes. Only in the accumulation mode did the modeled data display comparable values but the morning peak at 7:00 and 10:00 were also missing underscoring the challenges in emission representation and possibly in the photochemical reactions simulated in the model relative to the real ambient environment [11].

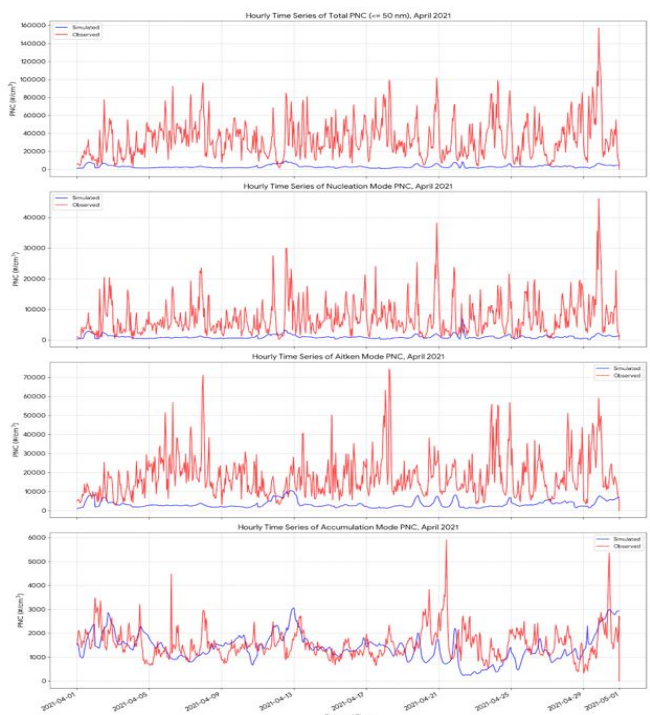

Figure 3 Hourly Time Series of Simulated (Blue) and Observed (Red) PNC for April 2021 Presented as a) Total PNC, b) Nucleation Mode, c) Aitken Mode, and d) Accumulation Mode PNC

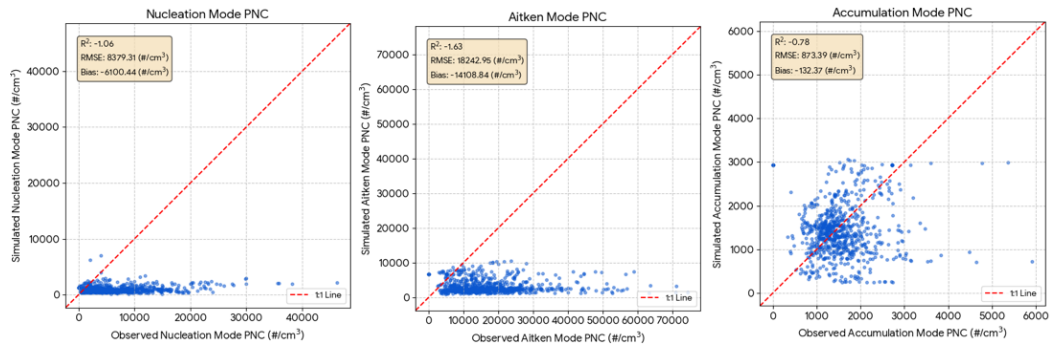

Figure 4 Scatter Plots Comparing Simulated and Observed Particle Number Concentrations in Taichung City over the April 2021 period for a) nucleation mode, b) Aitken mode, and c) accumulation mode PNC.

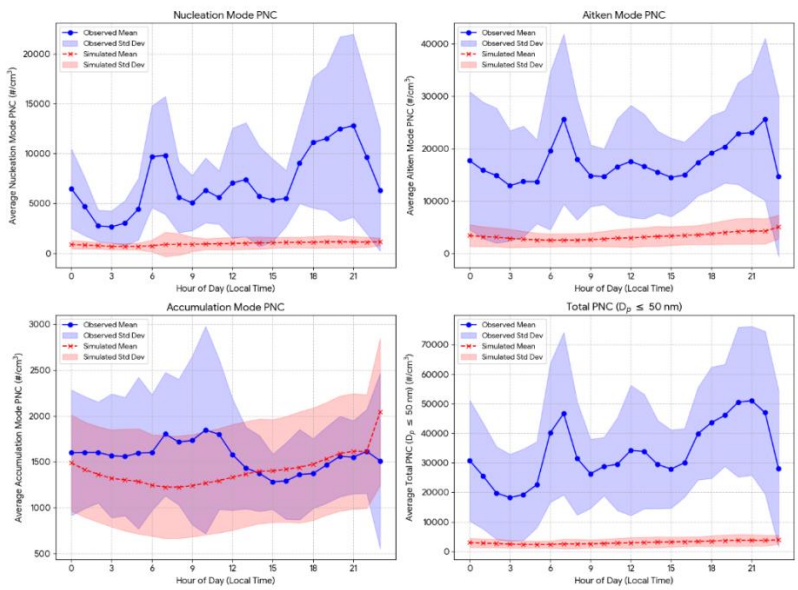

Figure 5 Diurnal Variation of Simulated vs. Observed Mode-Specific Particle Number Concentrations in Taichung City, April 2021

To investigate the sensitivity of particle formation processes, five nucleation schemes were evaluated: Basecase, Binary, Binary ion, Ternary, and Ternary ion. The Basecase, Ternary, and Ternary ion schemes demonstrated comparable behavior, effectively simulating sporadic temporal nucleation burst events, with peak values reaching approximately 1.17 #/cm³/s. However, as confirmed by the simulated PNSD contour plots (Figure 2), these simulated bursts did not consistently lead to sustained growth characteristic of classical NPF events. In contrast, the Binary and Binary ion schemes exhibited negligible activity, suggesting that binary nucleation mechanisms were not thermodynamically favored under the ambient conditions in Taichung. Elevated H_2SO_4 concentrations visually corresponded with the timing of nucleation bursts in the active schemes, highlighting its role as a key precursor. However, quantitative analysis revealed a weak statistical relationship (Pearson R ≈ -0.04), indicating that nucleation is a non-linear, multi-factorial process influenced by other variables beyond just sulfuric acid, including ammonia, amines, and organic vapors.

The consistent underestimation of UFP concentrations and the model's limited ability to capture sustained, classical NPF events highlight several contributing factors. These include Model Resolution Constraints, here the 0.25° × 0.3125° resolution may be insufficient to fully resolve sharp concentration gradients and localized emissions, leading to underestimation and weakened temporal correlations. Uncertainties in Emission Inventories are also a factor, as discrepancies could arise from underestimations in primary particle emissions or precursor gas emissions (e.g., SO_2, VOCs, NH_3); emission inventories often rely on averaged data and may not fully capture temporal or spatial heterogeneity.

Furthermore, limitations in the representation of nucleation and growth mechanisms in the model's schemes to accurately represent complex chemical pathways and environmental conditions can lead to discrepancies in timing and magnitude of NPF events, with the underestimation of particle growth suggesting inadequate capture of condensable vapors or the efficiency of condensational growth and coagulation processes. Meteorological input accuracy also plays a role, as inherent uncertainties or resolution limitations in assimilated meteorological fields can propagate into the chemical transport simulation, leading to misrepresentation of dilution, transport, and removal processes. Finally, measurement uncertainty, where the SMPS instrument begins detection at approximately 11 nm while the model resolves particles down to 3.41 nm, can contribute to the observed underestimation of nucleation-mode particles, as a significant fraction of newly formed particles can exist in the sub-10 nm range.

Conclusions

This study investigated the spatial and temporal characteristics of ultrafine particle (UFP) number concentrations and size distributions over Taichung City, Taiwan, utilizing GEOS-Chem-TOMAS simulations and ground-based SMPS observations. The model successfully captured broad spatial patterns of particle number concentration (PNC), including an inland shift of concentration hotspots influenced by the northeastern monsoon and regional advection.

In terms of temporal behavior, the model reproduced some general trends in total UFP number concentration (≤50 nm). However, it substantially underestimated the overall magnitude compared to observations. The model also exhibited lower temporal variability than the observed SMPS data with sharp and frequent fluctuations, highlighting challenges in capturing UFP dynamics at local scales.

Correlation analysis further underscored these limitations. An R value of 0.06 (R^2 value of 0.0036) and a Normalized Mean Bias (NMB) of -90.88% indicated poor agreement between simulated and observed concentrations. These discrepancies likely stem from uncertainties in nucleation parameterizations, underrepresentation of localized emissions, and limited resolution of meteorological processes.

Contour plots of particle size distributions (PNSDs) showed no distinct clear, classical "banana-shaped" new particle formation (NPF) events in either the simulation or the observations for April 2021. This consistent absence could be attributed to unfavorable atmospheric conditions during the study period or limitations in both model sensitivity and observational resolution. Further analysis by segregating particle size modes reveals that while accumulation mode PNC showed relatively good agreement for magnitudes, other size modes demonstrate underprediction. The model currently cannot capture the peak concentrations appearing at different times of day as shown in the observations.

While the World Health Organization (WHO) provides air quality guidelines for particle mass concentrations (e.g., $PM_{2.5}$), no such standards exist for UFP number concentrations. Given the potential health impacts associated with UFP exposure, model underestimations pose a risk of misinforming exposure assessments and policy decisions if not properly accounted for. Overall, these findings highlight the potential of GEOS-Chem-TOMAS for regional air quality analysis but also reveal key areas needing improvement. Future work should prioritize refining nucleation schemes (such as incorporating organic aerosol effects),

enhancing the resolution of local emissions and meteorology, and expanding validation datasets, particularly for size-resolved comparisons. Addressing the model's persistent underestimation and weak agreement with observations will be critical to improving its utility for both scientific analysis and public health applications.

Acknowledgement

The authors would like to thank the Graduate Institute of Environmental Engineering at National Taiwan University for providing access to the observation data. The author extend heartfelt gratitude for the Chulalongkorn air quality research group for their collaborative spirit throughout this research with support in simulations and analysis. This work is a result of the collaborative partnership between Chulalongkorn University, Thailand, and National Taiwan University, Taiwan under the Double Degree Program.

References

[1] Pope, C.A. and Dockery, D.W. 2006. Health Effects of Fine Particulate Matter: A Critical Review of Recent Epidemiological Studies. J Air Waste Manag Assoc., 56(6): 705-740.

[2] Chen, L-C., and Lippmann, M. 2009. Particulate Matter Neurotoxicity in Culture is Size-Dependent. Neuro Toxicology., 36: 112-117.

[3] Oberdörster, G., Oberdörster, E. and Oberdörster, J. 2005. Nanotoxicology: An Emerging Discipline Evolving from Studies of Ultrafine Particles. Environmental Health Perspectives., 113(7): 823-839.

[4] HEI Panel on Ultrafine Particles. 2013. Understanding the Health Effects of Ambient Ultrafine Particles. HEI Review Panel on UFPs, Health Effects Institute, Boston, MA.

[5] World Health Organization. 2021. WHO Global Air Quality Guidelines: Particulate Matter ($PM_{2.5}$ and PM_{10}), Ozone, Nitrogen Dioxide, Sulfur Dioxide and Carbon Monoxide. Geneva: World Health Organization. ISBN: 9789240034228.

[6] Kulmala, M., et al. 2014. New Particle Formation in the Urban Atmosphere: The Importance of Meteorological Factors. Atmospheric Chemistry and Physics., 14(10): 5323-5338.

[7] Wang, J., et al. 2023. Analysis of New Particle Formation Events and Comparisons to Simulations of Particle Number Concentrations Based on GEOS-Chem–Advanced Particle Microphysics in Beijing, China. Atmos. Chem. Phys., 23(7): 4091-4104.

[8] Trivitayanurak, W., Adams, P.J., Spracklen, D.V. and Carslaw, K.S. 2008. Tropospheric Aerosol Microphysics Simulation With Assimilated Meteorology: Model Description and Intermodel Comparison. Atmospheric Chemistry and Physics., 8: 3149-3168.

[9] Bey, I., Jacob, D.J., Yantosca, R.M., Logan, J.A., Field, B.D., Fiore, A.M., Li, Q., Liu, H.Y., Mickley, L.J. and Schultz, M.G. 2001. Global Modeling of Tropospheric Chemistry With Assimilated Meteorology: Model Description and Evaluation. Journal of Geophysical Research: Atmospheres., 106(D19): 23073-23095.

[10] Dal Maso, M., Kulmala, M., Riipinen, I. and Wagner, R. 2005. Formation and Growth of Fresh Atmospheric Aerosols: Eight Years of Aerosol Size Distribution Data From SMEAR II, Hyytiälä, Finland. Boreal Environment Research., 10: 323-336.

[11] Kürten, A., Jokinen, T., Simon, M., Sipilä, M., Sarnela, N., Junninen, H., Adamov, A., Almeida, J., Amorim, A., Bianchi, F., et al. 2016. Neutral Molecular Cluster Formation of Sulfuric Acid–Dimethylamine Observed in Real Time Under Atmospheric Conditions. Atmospheric Chemistry and Physics., 16(19): 12793-12813.

Thai Environmental Engineering Journal Vol. 39 No. 2 (2025) : 63-71
www.eeat.or.th

Treatment of Fishery Wastewater Using a Floating Treatment Wetland Planted with Umbrella Sedge

Parichat Supasee[1], Supreeda Homklin[2], Satawat Tanarat[3], Anusorn Boonpoke[4] and Somanat Somprasert[5*]

[1-5]Environmental Engineering, School of Energy and Environment, University of Phayao, Phayao 56000, Thailand
[*]E-mail : somanat.so@up.ac.th

Article History; *Received: 6 May 2025, Accepted: 25 August 2025, Published: 28 August 2025*

Abstract

This study evaluates the effectiveness of floating treatment wetlands (FTWs) using umbrella sedge (*Cyperus* spp.) for removing organic and nitrogen from fishery wastewater in Thailand. Aquaculture in Thailand produces significant wastewater with high organic matter and nitrogen, necessitating effective treatment solutions. FTWs are designed to float in fishponds, providing a flexible and space-saving method for wastewater treatment compared to traditional wetlands. The study used four laboratory-scale FTW reactors with varying hydraulic loading rates (5, 10, 15, and 20 cm/d) to assess their impact on pollutant removal. The FTW with the lowest hydraulic loading rate, 5 cm/d (HRT 20 days) achieved the highest removal efficiencies of 45% 63% and 61% for COD TKN and NH_3-N, respectively, demonstrating the system's effectiveness. Umbrella sedge grew best in the 5 cm/d reactors, where improved aerobic conditions boosted biodegradation, nitrification, and pollutant decomposition. The study concludes that FTWs are a sustainable and efficient solution for treating aquaculture wastewater, particularly at lower hydraulic loading rates, thus supporting better aquaculture practices.

Keywords : floating treatment wetland; synthetic fishery wastewater; nitrogen removal; organic removal; umbrella sedge

Introduction

Aquaculture in Thailand is a significant source of wastewater from agricultural activities in the country. Leftover fish food and excrement results in high levels of organic matter and nitrogen in the water discharged from fishponds. Generally, tilapia farming involves transferring water from upstream ponds to downstream ponds without wastewater treatment. This leads to the accumulation of organic matter and nitrogen in the water of the downstream ponds, reducing oxygen levels and making the water unsuitable for fish growth. Additionally, it affects public water sources when wastewater is discharged from the farming area, causing pollution in the receiving water bodies. Aquaculture farmers need a simple and low-cost wastewater treatment system, and constructed wetlands suit this purpose. However, traditionally constructed wetlands require large areas, reducing the space available for aquaculture. Therefore, floating treatment wetlands (FTW) have been designed to float in fishponds, reducing the additional space needed for treatment. They are also flexible to changes in water levels in the ponds. Floating treatment wetlands (FTW) were created using floating rafts for growing wetland plants without soil, which is recognized as an effective mechanism of water treatment and is used in a wide range of applications. The raft will float on the surface of the water. The pollutant removal mechanism occurs in the root zone of plants under the water surface, which helps increase the amount of oxygen in the water to microorganisms living both around the roots and

suspended in the water, causing a reaction to decompose organic matter and other pollutants. Newman [1] found that FTW systems provide design flexibility that can be built in small spaces. The system can be scaled to fit a pond or water source. It is a habitat for living creatures, enhancing their beauty and creating fascinating scenery. Water level fluctuations, as long as they are attached to the bottom or water source, thus the system is not damaged. Therefore, FTW systems are an interesting option used to treat wastewater from fish ponds. Floating treatment wetlands use a variety of plants to help improve water quality by absorbing excess nutrients and breaking down contaminants. Some commonly used plants in FTW such as cattail (*Typha* spp.) umbrella sedge (*Cyperus* spp.) and bulrushes (*Schoenoplectus* spp.). These plants absorb nutrients and contaminants and provide a habitat for beneficial microbes that further enhance the water purification process. The plants in floating constructed wetlands that provide good treatment efficiency include *Cyperus spp*. These plants are tolerant of pollutants in wastewater, grow quickly, and increase biomass, resulting in a high accumulation of organic matter and nitrogen. Additionally, their long roots help distribute oxygen in the water, enhancing the efficiency of pollutant treatment in wastewater. The FTWs planted with umbrella sedges show higher organic and nitrogen removal efficiency than other plants, which were 85% and 77% for organic in the form of COD and TKN, respectively [2]. This study compared the different hydraulic loading rates' organic and nitrogen removal efficiency. However, there is not much information on the use of floating treatment wetland systems to treat wastewater from fishery farming in Thailand. As a result, there is insufficient information on treatment efficacy, plant species, or design requirements to decide on the right treatment system for wastewater. Therefore, this study analyzed the treatment efficiency of a floating treatment wetland system using umbrella sedge (*Cyperus* spp.) to treat wastewater from fish farming by comparing the treatment efficiency with different hydrological load rates. The results of this study can be used to design this system more appropriately in the future.

Materials and Methods

This study used a lab-scale model with four wastewater flow rates to compare the efficiency of organic matter and nitrogen treatment. Four laboratory-scale floating treatment wetland reactors were used in this study, as shown in Figure 1. Each reactor is 0.5 meters wide, 1.0 meters long, and has a water depth of 0.6 meters, with a freeboard of 0.1 meters. The 40x80 cm floating raft was planted with an umbrella sedge (*Cyperus* spp.) 2-3 clumps per raft. The experiment was set in four different hydraulic loading rates (HLR) of 5, 10, 15, and 20 cm/d (C1, C2, C3 and C4, respectively).

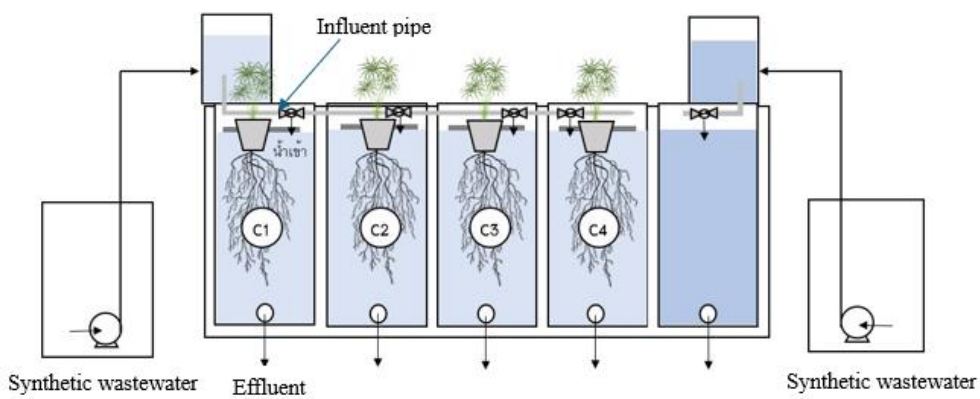

Figure 1 Schematics of the lab-scale reactor

The fishery wastewater was synthesized by mixing molasses and urea as an organic and nitrogen source to match the COD NH_3-N and TKN concentrations of 80-200 mg/L and 20-50 mg/L, respectively shown in Table 1. Synthetic wastewater with an average COD of 168 mg/L, NH_3-N, and TKN at 26 mg/L was pumped into the floating treatment wetland reactor continuously. The peristatic pump was set to feed at HLR 5, 10, 15 and 20 cm/d with the hydraulic retention time at 20, 10, 6.7 and 1.4 days, respectively. The removal efficiencies were determined by collecting the Influent and effluent samples every week and analyzed for COD TKN and ammonia nitrogen. The steady state of the experiment was determined primarily by the ammonia nitrogen concentration in the effluent was almost constant.

This experiment uses umbrella sedge as a plant in the FTW reactor because the previous study reports that the FTWs planted with umbrella sedge provide good efficiency in removing pollutants, specifically, nitrogen removal. This plant can be found in general and is also popular to grow as an ornamental plant. An umbrella sedge grows well in wastewater, can increase the height and number of plants quickly, and has a well-distributed root system. The square raft was made of PVC pipes with a 1-inch diameter a width of 40 cm and a length of 80 cm. In the middle of the raft were cut for planting pots. At the beginning of the experiment, plants were cut to the same initial height as 30 centimeters and an average initial root length of 30 cm and planted 1 clump per pot as shown in Figure 2. About 2 months before the beginning of the experiment, the wastewater was diluted to a concentration of about 25-30% so that the plants could grow easier. The 100% wastewater was fed when the average height of the plants increased from 20 cm to 30 cm, and new plant shoots had grown. Plant height and root length were measured at the beginning and the end of the experiment.

Results and Discussion

The reactors C1, C2, C3 and C4 were fed at 15, 30, 45 and 60 L/d (HRT 20, 10, 6.7 and 1.4 days, respectively). Influent and effluent samples were collected for the 3-month study period. The steady state of the experiment started 14 days of an experiment where nitrogen effluent was nearly constant.

The averages COD TKN and NH_3-N concentration in the influent and effluent is shown in Table 2. There was no significant difference of COD concentration in the effluent for all reactors at the 95% confidence level. The COD removal efficiency was in the range of 32-45%. The COD in the effluent tendency increased as the experimental period lengthened, as shown in Figure 3.

Table 1 Comparison of synthetic and fishery wastewater

Parameters	**Averaged concentration,**	
	Fishery wastewater	**Synthetic wastewater**
COD, mg/L	80-200	168
TKN, mg/L	20-50	26
NH_3-N, mg/L		26
SS, mg/L	2	1.5
pH	6-7.5	7.29

Figure 2 Umbrella sedge at the beginning of the experiment

Table 2 Average concentration of influent effluent plant height and plant root length

Parameter	Influent	Average Concentration			
		5 cm/d (C1)	10 cm/d (C2)	15 cm/d (C3)	20 cm/d (C4)
HRT, d		20	10	6.7	1.4
pH	6.6 (SD 0.16)	6.8 (SD 0.07)	7.2 (SD 0.23)	7.4 (SD 0.20)	7.3 (SD 0.18)
COD, mg/L	171 (SD 4.8)	94 (SD 20)	102 (SD 23)	108 (SD 24)	116 (SD 24)
TKN, mg/L	27 (SD 0.3)	10 (SD 1.1)	15 (SD 1.2)	16 (SD 0.7)	17 (SD 0.5)
NH_3-N, mg/L	26 (SD 0.3)	10 (SD 0.3)	13 (SD 0.4)	16 (SD 0.2)	18 (SD 0.7)
Root Length, cm		70.8	57.8	65.8	54.2
Plant Height, cm		50.3	60.3	50.8	58.9

A large number of algae was found to occur in the system because the vegetation on the raft was not dense enough. Therefore, light could penetrate the water, stimulate the growth of algae and fall off with the effluent. The TKN and ammonia nitrogen in the influent were similar because the synthesis of wastewater used urea fertilizer as a representative of nitrogen in the wastewater, which gave nitrogen in the form of ammonia rather than organic nitrogen. The nitrogen in the effluent both TKN and NH_3-N shows a steady state after 14 days of the experiment as shown in Fig 3. At the HLR 5 cm/d (C1) showed significantly high nitrogen removal efficiency for both TKN 63% and NH_3-N 61%, compare to the reactor C2, C3 and C4 at 95% confidence level. At this hydraulic loading rate the retention time was 20 days. There are not many reports related to the water retention period in the FTW system and wastewater treatment efficiency. However, Nuruzzaman [3] found that the FTW system planted with Carex *fascicularis* was able to remove up to 93.3% of TN in just 3 days, and it was found that nitrogen removal in FTW depends on the initial nutrient concentration and plant performance. Toet [4] used a surface-flow wetland treating sewage and found that increasing the HRT enhanced the removal efficiencies of fecal coliform and nitrogen, with a HRT of 4 days required to meet desired standards.

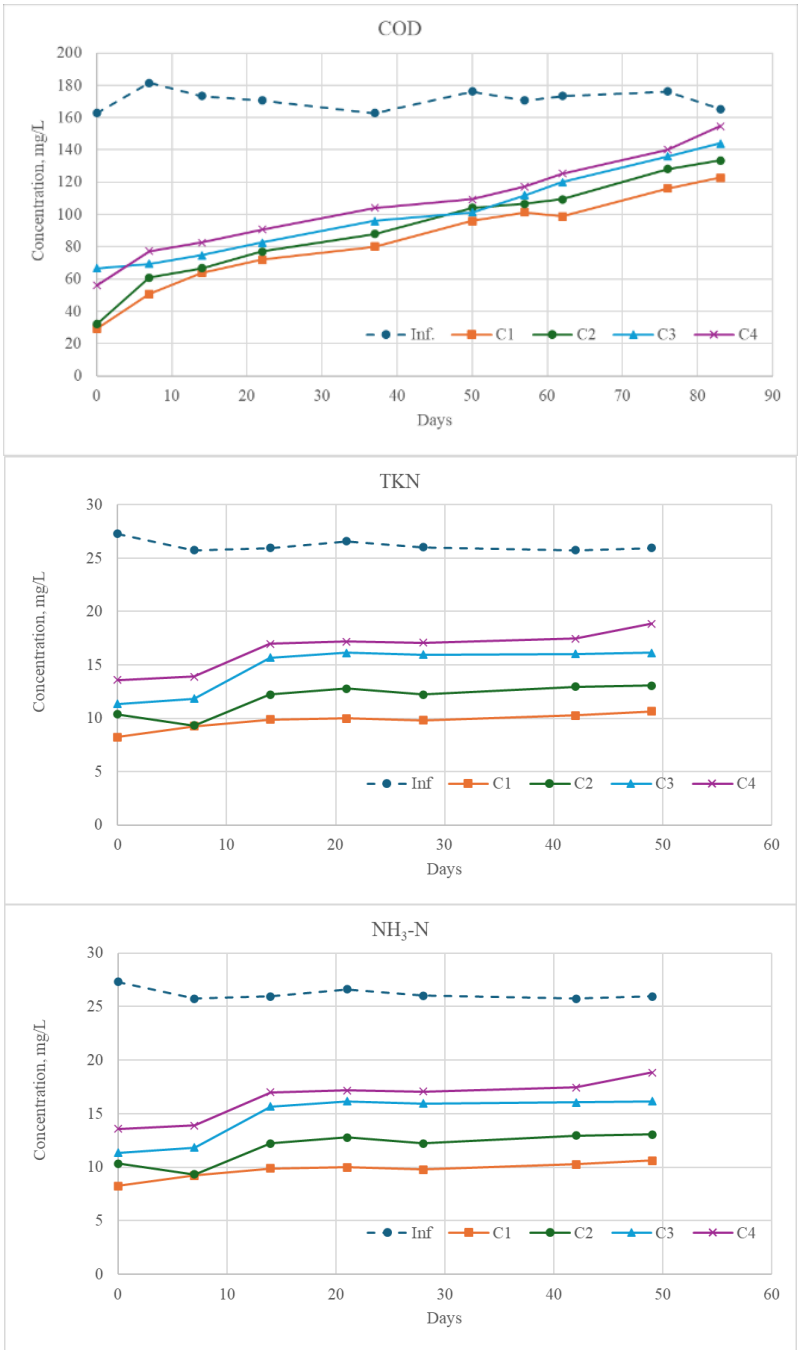

Figure 3 Changes in COD TNK and NH_3-N concentrations

It was found that as the hydraulic loading rate increased, the treatment efficiency decreased, as shown in Figure 4. The TKN removal efficiency was slightly lower than the NH3-N removal efficiency because the algae formed in the system were also mixed into the effluent. It was found that the C1 model provided similar TKN and NH_3-N removal efficiency because the plants in the system grew well above the water, thus blocking the light and reducing the growth of algae more compared to the C2, C3, and C4 models, which had less dense above-water plants (Fig 5). Plant uptake is a process that decreases nitrogen levels in wastewater by converting it into plant tissue. In the C1 reactor, which

achieved the highest nitrogen removal, plant weight increased from about 0.02-0.03 kg initially to 2-3 kg by the end of the experiment, with moisture content at 70-80%.

The control system without plants showed slightly lower removal efficiency. Algae thrived due to increased sunlight exposure, resulting in higher organic matter levels in the effluent compared to systems with plants. In comparison, the nitrogen treatment of the control system is like the planted reactors, since the algae themselves contribute to nitrification and help to accumulate nitrogen. This makes the nitrogen value in the effluent similar to that of the system planted with an umbrella sedge.

Nitrogen balance analysis showed that nitrogen removal in this FTW system primarily occurs through nitrification and denitrification, which converted nitrogen to gas and releases to the atmosphere. Effluent nitrate levels were low (0.3–0.45 mg/l), confirming denitrification in the experiments. Nitrogen accumulation in plants during the experiment ranged from 0.06 to 0.8 gN/m^2, with the C1 model showing the highest accumulation (0.8 gN/m^2), representing 2.8% of input nitrogen. Compared to nitrogen accumulation in plants in Hanneke's experiment [5], nitrogen accumulation in cattail and iris was 1.2 and 18.6 g/m^2, respectively. About 60% of nitrogen accumulated in algae or was lost as gaseous nitrogen through nitrification and denitrification; however, algal nitrogen was not directly measured. In the control reactor (without plant), at HLR 5 cm/d, only 27% of nitrogen was removed by deposition in algae or as nitrogen gas in plant-free systems about half the removal seen in planted models. This indicated that plants significantly increase nitrogen transformation. With plants, 10.4 gN/m^2 (37%) remains in effluent, while without plants this rises to 20.6 gN/m^2 (73%), showing that plants significantly lower nitrogen levels. Plants improve total nitrogen removal through uptake and other biological processes, making them effective for reducing effluent nitrogen in wastewater treatment systems. A well-distributed root system allows for aerobic conditions in which microorganisms can decompose organic matter well. Zhang et al. [6] studied the causes of oxygen environments and the response characteristics of plant oxygen release (POR) in subsurface-flow constructed wetlands and reported that the root zone DO increased significantly to 2.05-4.37 mg/L, and was positively correlated with the TN and TP removal rates. *Cyperus* spp. showed a good tendency to release oxygen in the root zone. Yao et al. [7] showed that oxygen released by *Vetiveria zizanioides* L. roots through the biochemical process contributed to 77% and 74% of total root oxygen release under nutrient solution conditions and artificial wastewater conditions, respectively, and that was 72% and 71% of total root oxygen release for *Cyperus alternifolius* L. At experiment's end, plant height and root length in C2, C3, and C4 reactors matched C1, but shoot and root density was lower leading to reduced organic matter and nitrogen removal efficiency. Well-distributed plant roots cause aerobic conditions, which enhance biodegradation and nitrification, were mainly present where dense roots occurred (Fig 6).

In addition, as the hydraulic load rate rises, the flow becomes even more turbulent. This shortens the duration of the wastewater in the model and provides less treatment efficiency. Asaeda and Rashid [8] studied the effect of water turbulence motion and the growth of three types of aquatic plants. The study found that high turbulence velocity inhibits the normal metabolic activities of all three plants, while low to medium turbulence does not harm the floating-leaved plants. This study found that nitrogen reduction followed a first order plug-flow model (R^2=0.95) more closely than a completely mixed-flow model. This aligns with observed flow characteristics, which showed intermediate dispersion (D/L = 0.02–0.03). Plug flow facilitates continuous reactions, such as nitrogen treatment, by maintaining the movement of substances in one direction with minimal mixing.

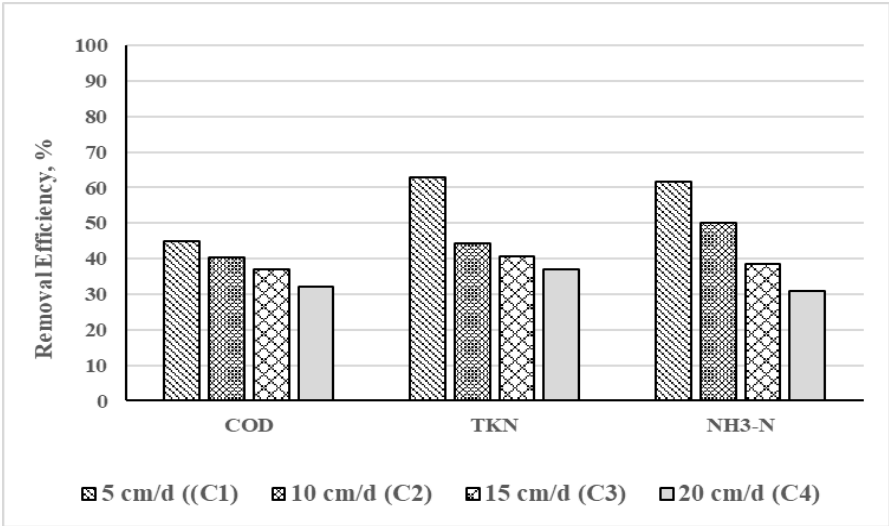

Figure 4 Removal efficiencies compared to HLRs

Figure 5 Plant shoot above the water surface in C1 C2 C3 and C4 at the end of the experiment

Figure 6 Plant root at the end of the experiment at 5 cm/d (C1)

This process makes it possible to establish aerobic zones for nitrification and subsequent anoxic zones for denitrification, which is necessary for effective nitrogen removal. It was found that intermediate dispersion in water flow pattern led to moderate nitrogen removal, influenced by substance dispersion and occasional recirculation.

The removal efficiency in this study was higher compared to the other studies. Barco and Borin [9] report that FTW in Northern Italy has significantly reduced COD and NH_4-N by 16.7% and 25.2%, respectively, whose effectiveness depends on the concentration in the inlet and the wastewater temperature. According to a study by Nichols et al. [10] which used FTW to treat stormwater runoff over 2 months, it was found that 53% of phosphorus and 17% of total nitrogen could be treated. In this study, long, dispersed plant roots throughout the width and length of the reactor provide aerobic conditions. Combined with a long hydraulic retention time (20 days) resulting in the complete degradation reaction for both organic and ammonia nitrogen. A full-scale FTW with Cyperus spp. treating Nile Tilapia aquaculture wastewater reduced COD by 20.3-33.96% and NH_4-N by 25.86-27.87% [11]. However, in real wastewater treatment, floating wetlands may be less efficient due to uncontrollable factors like wind or water flow direction, which influence microbial and plant performance.

Conclusions

This study concluded that FTW planted with an umbrella sedge was effective in removing organic and nitrogen from fishery wastewater, especially at lower hydraulic loading rates. The lowest HLR (5 cm/d) showed the highest removal efficiency for both organic and nitrogen 45% and nitrogen removal at 63% and 61% for TKN and NH_3-N, respectively. Even root distribution boosts organic matter and nitrogen treatment, improving biodegradation and nitrification. This approach offers a sustainable, space-saving way to treat aquaculture wastewater.

Acknowledgment

This research project was financially supported by the Thailand Science Research and Innovation Fund and the University of Phayao (Grant No. FF65- RIM007).

References

[1] Majer Newman, J., Clausen, J. C. and Neafsey, J. A. 1999. Seasonal Performance of a Wetland Constructed to Process Dairy Milkhouse Wastewater in

Connecticut. Ecological Engineering. 14(1): 181-198.

[2] Wiphada Wongruankaew and Somanat Somprasert. 2016. Nitrogen Removal Efficiency of Floating Constructed Wetland System in Treating Catfish Farming Wastewater. Thai Environmental Engineering Journal. 30(3): 75-83.

[3] Nuruzzaman, Md & Anwar, A. H. M. & Sarukkalige, Ranjan. 2022. Nutrient Removal from Stormwater in Floating Treatment Wetland: Prediction of Kinetic Rates, Effect of Initial Concentration and Plant Performance Assessment. Environmental Science: Water Research & Technology. 8: 3113-3126.

[4] Toet, S., Van Logtestijn, R. S. P., Kampf, R., Schreijer, M. and Verhoeven, J. T. A. 2005. The Effect of Hydraulic Retention Time on the Removal of Pollutants from Sewage Treatment Plant Effluent in a Surface-flow Wetland System. Wetlands, 25(2): 375-391.

[5] Hanneke E. Keizer-Vlek, Piet F.M. Verdonschot, Ralf C.M. Verdonschot, Dorine Dekkers. 2014. The Contribution of Plant Uptake to Nutrient Removal by Floating Treatment Wetlands, Ecological Engineering. 73: 684-690.

[6] Jingying Zhang, Qiuhui Yan, Ge Bai, Dun Guo, Yanbin Chi, Bin Li, Lei Yang, Yongxiang Ren. 2023. Inducing Root Redundant Development to Release Oxygen: An Efficient Natural Oxygenation Approach for Subsurface Flow Constructed Wetland. Environmental Research. 239(1): 117377.

[7] Fang Yao, Gen-xiang Shen, Xue-lian Li, Huai-zheng Li, Hong Hu, Wu-zhong Ni. 2011. A Comparative Study on the Potential of Oxygen Release by Roots of Selected Wetland Plants. Physics and Chemistry of the Earth, Parts A/B/C. 36 (9-11): 475-478.

[8] Takashi Asaeda, M.H. Rashid. 2017. Effects of Turbulence Motion on the Growth and Physiology of Aquatic Plants. Limnologica. 62: 181-187.

[9] Alberto Barco, and Maurizio Borin. 2020. Treatment Performances of Floating Wetlands: A Decade of Studies in North Italy. Ecological Engineering. 158, 106016.

[10] Nichols, P., Lucke, T., Drapper, D. and Walker, C. 2016. Performance Evaluation of a Floating Treatment Wetland in an Urban Catchment. Water. 8: 244.

[11] Somprasert, S., Mungkung, S., Kreetachat, N., Imman, S. and Homklin, S. 2021. Implementation of an Integrated Floating Wetland and Biofilter for Water Treatment in Nile Tilapia Aquaculture. Journal of Ecological Engineering, 22(8): 146-152.

Thai Environmental Engineering Journal Vol. 39 No. 2 (2025) : 73-83
www.eeat.or.th

Long-Term Analysis of $PM_{2.5}$ Concentrations and Seasonal Variation in Bangkok and Chiang Mai, Thailand: Impacts of COVID-19 Lockdowns and Fire Control Measures

Vineeth Vijayan[1], Supandee Maneelok[2] and Nantaporn Noosai[3*]

[1]Department of Mechanical and Mechatronics Engineering, Faculty of Engineering, Prince of Songkla University, Hat Yai, Songkhla 90110, Thailand
[2]Department of Occupational Health and Safety, Faculty of Health and Sports Science, Thaksin University, Phatthalung 93210, Thailand
[3*]Department of Civil and Environmental Engineering, Faculty of Engineering, Prince of Songkla University, Hat Yai, Songkhla 90110, Thailand
[*]E-mail : nantaporn.no@psu.ac.th

Article History; *Received: 13 June 2025, Accepted: 27 August 2025, Published: 28 August 2025*

Abstract

An analysis of ten years of daily 24-h $PM_{2.5}$ data (2015–2024) from Thailand's Pollution Control Department at Bangkok (59T) and Chiang Mai (36T) reveals strong but distinct seasonality: Bangkok peaks in December–February with secondary formation and urban sources, whereas Chiang Mai exhibits pronounced February–April haze consistent with biomass burning. Two policy "experiments" were evaluated. During Bangkok's COVID-19 Wave-1 (22 Mar–31 May 2020), the window mean declined from a 2017–2019 baseline of 20.00 to 17.01 μg m^{-3} (Δ = −2.99 μg m^{-3}; −14.9%), a statistically significant reduction of small-to-moderate magnitude (permutation p = 0.0036; Cohen's d = −0.39); two-way ANOVA showed a significant group effect, and daily exceedances of the 24-h standard (37.5 μg m^{-3}) fell from 3.3% to 0%. In Chiang Mai, January–April 2022 (first year of burning control) decreased from 54.2 to 29.5 μg m^{-3} versus 2019 (Δ = −24.7 μg m^{-3}; −45.5%), a large, statistically significant reduction (permutation p = 0.0001; Cohen's d = −0.89), with significant group, month, and interaction terms; exceedances ≥37.5 μg m^{-3} dropped from 63.3% to 31.7%. NASA FIRMS hotspots concurrently decreased sharply in February–April 2022, corroborating reduced fire activity. Annual means show a steady decline in Bangkok (≈16.4 μg m^{-3} in 2024) and policy-sensitive variability in Chiang Mai; under the current Thai annual standard (15 μg m^{-3}), neither city achieves compliance. The combined ground-satellite evidence indicates that sustained, region-specific measures—traffic/precursor controls in Bangkok and consistent burning management in the North—are required to meet tightened standards.

Keywords : $PM_{2.5}$; Bangkok; Chiang Mai; biomass burning; COVID-19 lockdown; FIRMS; air quality standards; policy evaluation

Introduction

$PM_{2.5}$ is recognized as one of the most harmful air pollutants because fine particles penetrate deeply into the respiratory system and are linked to multiple adverse health outcomes [1]. In Thailand, concentrations often exceed national standards during the dry season, reflecting marked seasonality in regional emissions and meteorology [2, 3]. In 2022, Thailand strengthened its standards to 37.5 μg m^{-3} for the 24-hour limit and 15 μg m^{-3} for the annual limit, a policy change relevant for interpreting recent trends [3]. Health assessments continue to indicate substantial public-health burdens where annual means exceed 15 μg m^{-3} [4]. In Bangkok, source apportionment and process studies identify traffic emissions and secondary with intermittent roles for industry and construction; boundary-layer dynamics can sustain elevated $PM_{2.5}$ during stagnant conditions [5-8]. In Chiang Mai and the northern region, multiple lines of evidence attribute first-quarter haze primarily to open biomass burning and transboundary transport; chemical markers and oxidative-potential assays corroborate biomass-burning dominance during smoke episodes [9-12].

Policy interventions offer natural experiments. Several Bangkok studies report $PM_{2.5}$ reductions during COVID-19 restrictions, although magnitudes vary with window and meteorology [13, 14]. In the North, authorities moved toward regulated burning and operational tools such as FireD; peer-reviewed evaluations are emerging, which motivates pairing hotspot data with ground $PM_{2.5}$ for empirical assessment [15-17].

Against this context, Bangkok and Chiang Mai are analyzed as contrasting cases. Daily 24-hour observations from station 59T (Bangkok) and station 36T (Chiang Mai) for 2015–2024 are used because they provide the most complete records in their urban cores; siting and representativeness are detailed in the Methodology. Because burning is episodic and spatially heterogeneous, ground measurements are complemented with NASA EOSDIS LANCE FIRMS (MODIS/VIIRS) active-fire detections for January to April to contextualize the 2022 burning-control enforcement in Chiang Mai [17]. The study characterizes seasonal and interannual variability at both sites, evaluates Bangkok's COVID-19 Wave-1 window (22 March to 31 May 2020) relative to a 2017–2019 baseline, compares Chiang Mai conditions in January to April of 2019 and 2022 using ground $PM_{2.5}$ with FIRMS hotspot distributions, and assesses compliance relative to the revised Thai standards (37.5 μg m^{-3} for 24-hour and 15 μg m^{-3} for annual).

Methodology

Study sites and data:

Two contrasting Thai settings were analyzed: Bangkok (urban, traffic/industry dominated) and Chiang Mai (biomass-burning influenced). Ground $PM_{2.5}$ came from Thailand's Pollution Control Department (PCD) as daily 24-h averages for 2015–2024. The primary monitors were Bangkok 59T and Chiang Mai 36T, selected for record continuity, central siting, and use in official reporting. Station metadata appear in Table 1; locations in Figure 1.

Table 1 Monitoring station metadata

Station ID	City	Station name	Latitude	Longitude	District	Province
59T	Bangkok	The Government Public Relations Department	13.7831	100.5404	Khet Phaya Thai	Bangkok
36T	Chiang Mai	Yupparaj Wittayalai School	18.7909	98.9900	Mueang	Chiang Mai

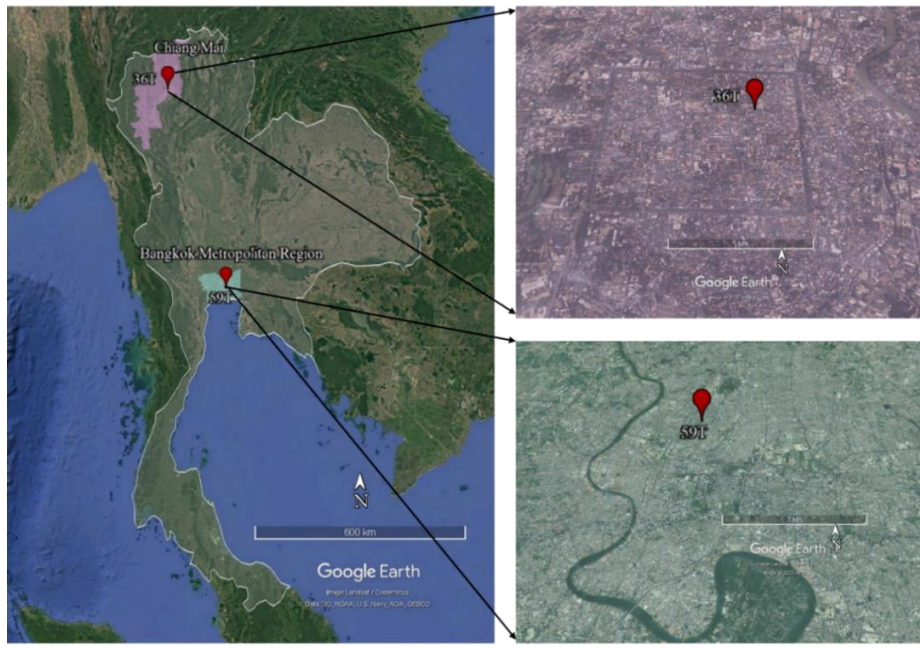

Figure 1 Map of monitoring stations 59T (Bangkok) and 36T (Chiang Mai)

Data and windows

Daily 24-h $PM_{2.5}$ (2015–2024) from Thailand PCD were analyzed at Bangkok 59T and Chiang Mai 36T, selected for long, continuous records and urban-core representativeness (see station table and map). Intervention windows were (i) Bangkok COVID-19 Wave-1: 22 Mar–31 May 2020 vs a 2017–2019 baseline restricted to the same dates; and (ii) Chiang Mai burning control: January–April 2022 vs January–April 2019. NASA EOSDIS LANCE FIRMS (MODIS/VIIRS) daily hotspot counts were aggregated over Chiang Mai for January –April 2019 vs 2022.

Metrics and inference

Seasonality (2015–2024) was summarized by monthly boxplots and monthly tables (mean, median, IQR, n, and daily exceedances ≥37.5 μg m^{-3}—Thai 24-h standard). For policy windows, group differences in daily means were tested with two-sided permutation tests (e.g., 20,000 shuffles; report mean difference, 95% CI, and Cohen's d). Two-way ANOVA (Group × Month) tested overall and month-specific effects for Bangkok (Mar–May) and Chiang Mai (Jan–Apr). Annual compliance used yearly means compared against the Thai annual standard of 15 μg m^{-3} (revised 2022). FIRMS corroboration used grouped monthly boxplots (2019 vs 2022) with dashed red lines for 2022 medians and month-wise permutation tests on daily hotspot counts. Cohen's d quantifies the standardized mean difference (about 0.2 small, 0.5 medium, 0.8 large). The sign indicates the direction of change. The permutation *p* value is the probability, under the null hypothesis of no group effect, of obtaining a difference as large as or larger than the observed difference after random shuffling of group labels. Smaller *p* values indicate stronger evidence for a real difference.

Processing and software

Dates were parsed to daily means; non-numeric/NaT rows were dropped; no imputation or meteorological normalization was applied. Analyses used Python (pandas, numpy, matplotlib, statsmodels).

Limitations

No meteorological normalization was applied; interannual differences may reflect both emission/activity changes and weather. FIRMS detections depend on satellite overpass, clouds, and detection thresholds and are interpreted as activity indicators, not emission fluxes.

Results and Discussions

Seasonal Patterns and Yearly Trends

Figure 2 (Bangkok, 59T) shows monthly boxplots of daily 24-h $PM_{2.5}$ for 2015–2024 with summary statistics in Table 2. The Chiang Mai results appear in Figure 3 (36T) with statistics in Table 3.

Both cities exhibit a strong seasonal cycle (dry-season highs, wet-season lows). Exceedance analyses below reference the Thai 24-hour $PM_{2.5}$ standard of 37.5 µg m^{-3} and are applied to daily values; counts of days ≥ 37.5 µg m^{-3} indicate short-term exposure pressure.

Bangkok (59T). $PM_{2.5}$ peaks in Jan–Feb (means ≈ 30–31 µg/m^3) and Dec (≈ 28 µg m^{-3}), and falls to ≈ 11–12 µg/m^3 in Jun–Aug. Exceedances of the 37.5 µg m^{-3} daily standard are concentrated in the cool-dry months: Jan 28% (78/276), Feb 31% (70/225), Mar 11% (28/249), Apr 10% (29/280), Dec 16% (50/308); they are rare elsewhere (May 0.6%, Jun–Aug 0%, Sep 1.7%, Oct 3.2%, Nov 6.0%).

Chiang Mai (36T). A pronounced haze season dominates Feb–Apr (means ≈ 45, 74, 61 µg m^{-3}). Daily exceedances of 37.5 µg m^{-3} are very persistent in this period: Jan 28% (84/298), Feb 65% (184/282), Mar 88% (268/304), Apr 73% (219/298), then drop sharply (May 15.8%) and are essentially zero in Jun–Oct (≤0.7%), with small upticks in Nov 0.4% (1/265) and Dec 4.3% (13/302).

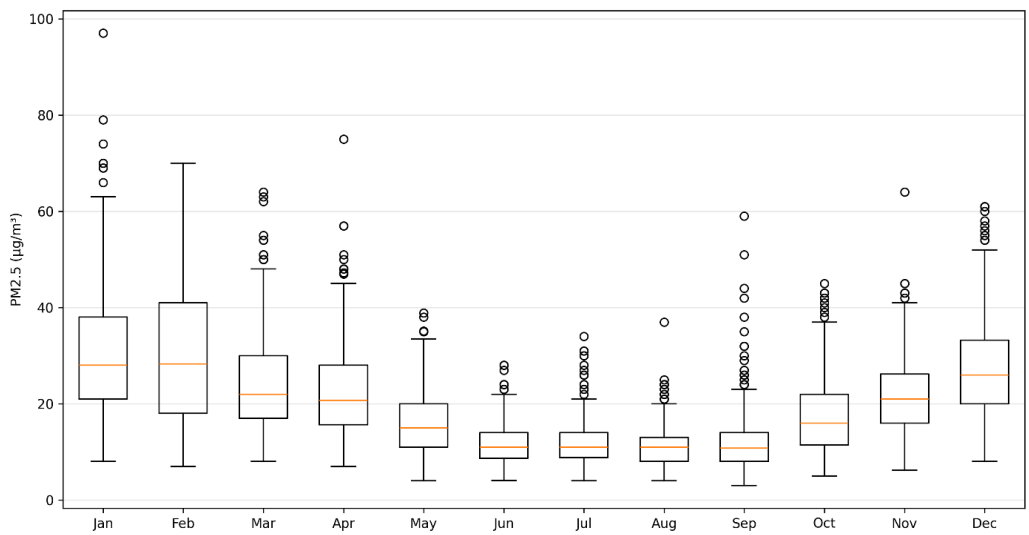

Figure 2 Bangkok (59T) $PM_{2.5}$ monthly boxplots (2015–2024).
Boxes: IQR; line: median; whiskers: 1.5×IQR; points: outliers

Table 2 Bangkok (59T) monthly statistics (2015–2024): mean, median, IQR, exceedance days (≥ 37.5 µg m^{-3}), n

Month	Mean	Median	IQR	Exceed days ≥ 37.5 µg m^{-3}	n	Month	Mean	Median	IQR	Exceed days ≥ 37.5 µg m^{-3}	n
Jan	31.3	28	17	78	276	Jul	12.1	11	5.2	0	294
Feb	30.4	28.3	23	70	225	Aug	11.4	11	5	0	301
Mar	24.5	22	13	28	249	Sep	12.4	10.8	6	5	298
Apr	22.9	20.7	12.3	29	280	Oct	17.6	16	10.5	10	308
May	15.9	15	9	2	309	Nov	22.1	21	10.1	17	283
Jun	11.9	11	5.4	0	298	Dec	27.5	26	13.2	50	308

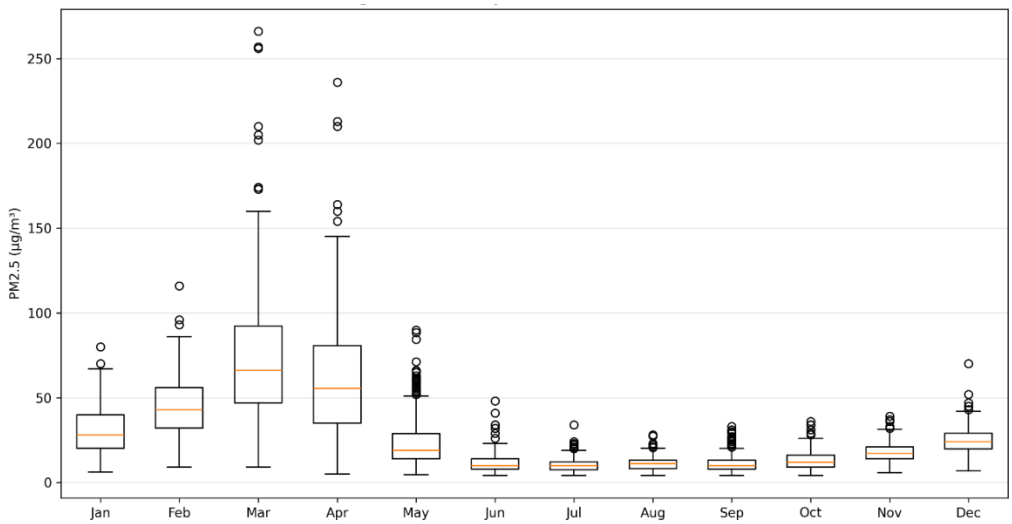

Figure 3 Chiang Mai (36T) $PM_{2.5}$ monthly boxplots (2015–2024). Boxes: IQR; line: median; whiskers: 1.5×IQR; points: outliers

Table 3 Chiang Mai (36T) monthly statistics (2015–2024): mean, median, IQR, exceedance days (≥ 37.5 µg m^{-3}), n

Month	Mean	Median	IQR	Exceed days ≥ 37.5 µg m^{-3}	n	Month	Mean	Median	IQR	Exceed days ≥ 37.5 µg m^{-3}	n
Jan	30.7	28	19.6	84	298	Jul	10.5	10	4.6	0	303
Feb	45.1	43	23.9	184	282	Aug	11.4	11	4.9	0	304
Mar	73.7	66	45.2	268	304	Sep	11	10	5	0	296
Apr	60.9	55.5	45.8	219	298	Oct	13.2	12	7.1	0	275
May	23.8	19	14.9	48	304	Nov	17.8	17	7	1	265
Jun	11.5	10	6	2	294	Dec	24.3	24	9.1	13	302

Both sites exhibit seasonality, but the signal is much more coherent in Chiang Mai. $PM_{2.5}$ rises sharply and persists through February to April, consistent with the burning season, then collapses in the monsoon months. Bangkok, in contrast, shows only a modest cool-season elevation, mainly in December to February, and a wide day to day spread across the broader dry season from November to April without a stable intra-seasonal pattern. This variability reflects overlapping and episodic influences such as weekday traffic intensity, construction and industrial activity, stagnant boundary-layer conditions, and occasional regional smoke intrusions, superimposed on the rain-season cleansing that drives the May to October minima. In summary, the absence of a consistent pattern during the dry season indicates that seasonal averages can mask short episodes of high exposure. This finding supports the need for real-time monitoring and targeted episodic control measures, alongside seasonal policy planning.

COVID-19 Lockdown Effects in Bangkok

To assess the impact of pandemic-related restrictions on $PM_{2.5}$ concentration, Figure 4 compares daily $PM_{2.5}$ concentrations at station 59T during the strictest COVID-19 Wave 1 lockdown period (March 22–May 31, 2020) against a three-year pre-pandemic baseline matched to the same calendar days (2017–2019). Table 4 reports the statistical analysis. During the restriction window 22 March–31 May 2020, daily $PM_{2.5}$ decreased from

a 2017–2019 baseline mean of 20.00 to 17.01 µg m^{-3} (−2.99 µg m^{-3}, −14.9%; permutation p = 0.0036, 95% CI −4.71 to −1.24; Cohen's d = −0.39). Cohen's d = −0.39 indicates a small-to-moderate reduction in 2020 relative to the 2017–2019 baseline; the negative sign indicates lower 2020 values. The permutation p value of 0.0036 means that, if there were truly no group difference, a shift of this size would be very unlikely, supporting a genuine lockdown-period reduction. A two-way ANOVA (group by month) indicated significant effects of group (F = 8.80, p = 0.003) and month (F = 5.44, p = 0.005), with a non-significant interaction (p = 0.207), implying a broadly consistent reduction across March–May.

The proportion of days at or above 37.5 µg m^{-3} declined from 7/213 (3.3%) in the baseline to 0/71 (0%) in 2020, with the clearest visual shift in May, consistent with the onset of early-monsoon cleansing. The results indicate a moderate, statistically robust improvement during Wave-1, while remaining dry-season variability points to continuing influences of background and secondary formation processes in Bangkok.

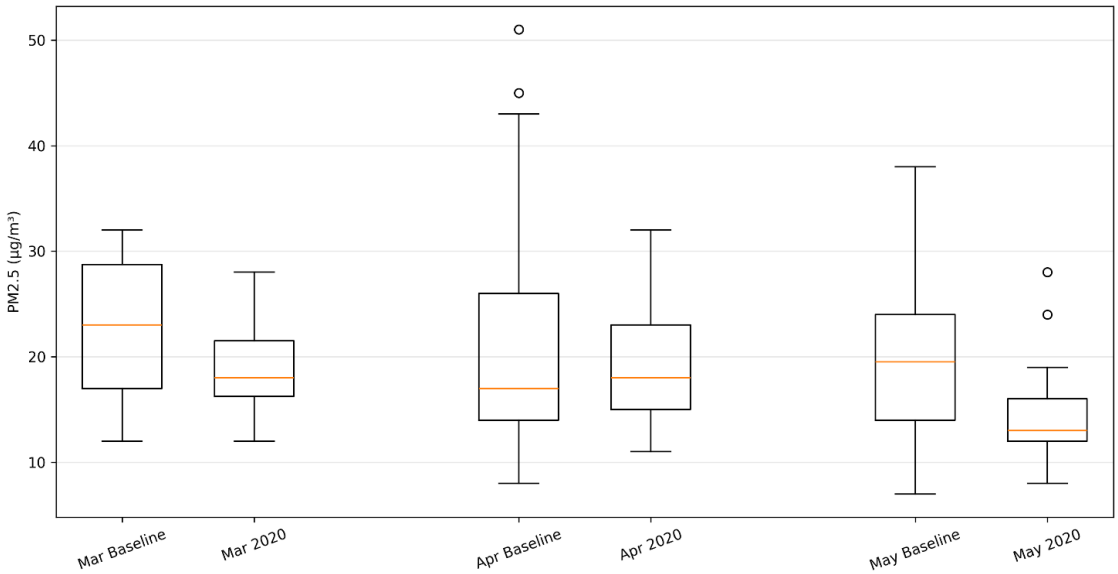

Figure 4 Bangkok (59T): Lockdown window (Mar 22–May 31) boxplots comparing Baseline (2017–2019) vs 2020

Table 4 Bangkok (59T) — COVID-19 Wave-1 restriction window (22 Mar–31 May 2020) vs baseline (2017–2019): summary metrics and two-way ANOVA

Window-level summary	**Baseline (2017–2019)**	**2020**	**Change (2020−Base)**	**Percent change**	**95% CI (µg m^{-3})**	**Cohen's d**	**Exceedance days ≥37.5 µg m^{-3} (base → 2020)**
Mean $PM_{2.5}$ (µg/m³)	20.00	17.01	−2.99	−14.9%	[−4.71, −1.24]	−0.39	**7 → 0 (3.3% → 0.0%;** n=213 → 71)
Two-way ANOVA (Group×Month)				**sum_sq**	**df**	**F**	**p (PR>F)**
Group (baseline vs 2020)				496.091	1.0	8.803	0.003
Month (Mar, Apr, May)				613.408	2.0	5.443	0.005
Group×Month				178.827	2.0	1.587	0.207
Residual				15158.751	269.0	—	—

Fire Control Measures in Chiang Mai

To evaluate the first year of burning control enforcement, Figure 5 compares January to April 2022 with the pre regulation season in 2019, and Table 5 reports the statistical analysis result. For January–April, $PM_{2.5}$ declined from 54.2 in 2019 to 29.5 µg m^{-3} in 2022 (Δ = −24.7 µg m^{-3}, −45.5%; permutation p = 0.0001, 95% CI −32.1 to −17.9; Cohen's d = −0.89). Cohen's d = −0.89 indicates a large reduction in 2022 relative to 2019; the negative sign indicates lower 2022 values. The permutation p value of 0.0001 indicates that such a decrease would be extremely unlikely under the null hypothesis of no difference. A two-way ANOVA showed significant group, month, and group×month effects (all $p < 0.001$), with the largest decreases in March–April, matching the core haze season. Using the 24-hour standard (37.5 µg m^{-3}), exceedance days decreased from 76/120 (63.3%) in 2019 to 38/120 (31.7%) in 2022. Consistent with these averages, the 2022 boxplots are lower and less dispersed in all four months, indicating both reduced central tendency and fewer extreme smoke days.

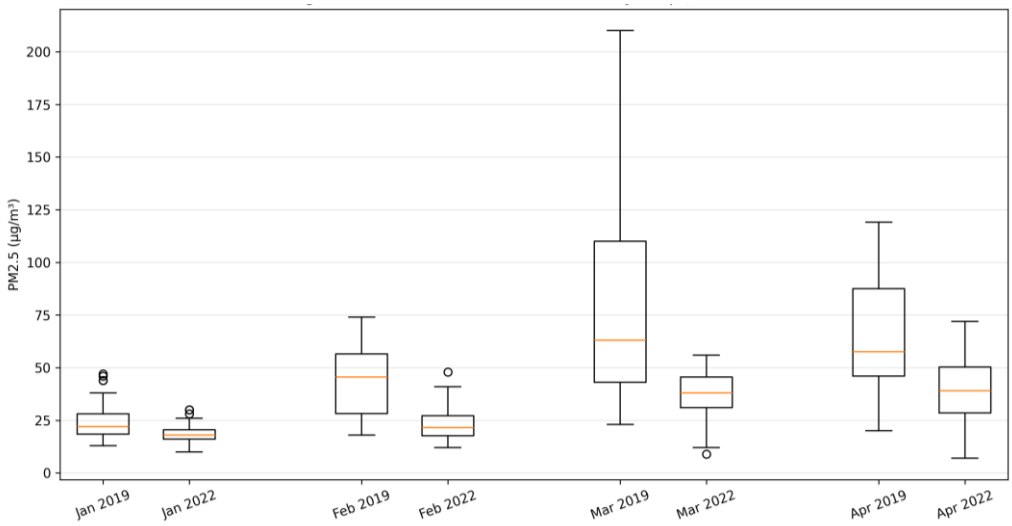

Figure 5 Chiang Mai (36T): Jan–Apr boxplots comparing 2019 vs 2022 during burning-control enforcement

Table 5 Chiang Mai (36T) — Burning-control season (Jan–Apr) 2022 vs 2019: summary metrics and two-way ANOVA

Window-level summary	**Baseline (2017–2019)**	**2020**	**Change (2020−Base)**	**Percent change**	**95% CI (µg/m³)**	**Cohen's d**	**Exceedance days ≥37.5 µg/m³ (base → 2020)**
Mean $PM_{2.5}$ (µg/m³)	20.00	17.01	−2.99	−14.9%	[−4.71, −1.24]	−0.39	**76 → 38** (63.3% → 31.7%)
Two-way ANOVA (Group×Month)				**sum_sq**	**df**	**F**	**p (PR>F)**
Group (baseline vs 2020)				496.091	1.0	8.803	0.003
Month (Mar, Apr, May)				613.408	2.0	5.443	0.005
Group×Month				178.827	2.0	1.587	0.207
Residual				15158.751	269.0	—	—

To verify that the 2019→2022 reduction in Chiang Mai $PM_{2.5}$ coincided with less open burning rather than only meteorological variability, a parallel analysis used NASA EOSDIS LANCE FIRMS active-fire detections. Daily hotspot counts were aggregated for January–April and compared between 2019 (pre-regulation) and 2022 (first enforcement year). The systematically lower and tighter 2022 distributions in February–April can be observed in Figure 6. Table 6 summarizes the month-wise differences in daily means with permutation p-values (20,000 shuffles). Month-wise permutation tests on daily hotspot counts yielded $p < 0.001$ in February–April, indicating the 2019-2022 reductions are highly unlikely under the null of no change in fire activity, aligning with the ground-level $PM_{2.5}$ decreases during the main haze months. The large and statistically significant decreases in February–April align with the ground-level $PM_{2.5}$ declines and indicate materially fewer or smaller fires during the core haze months in 2022. The January increase in hotspots alongside lower $PM_{2.5}$ suggests timing or dispersion differences (for example, changes in wind, mixing depth, fuel moisture, or burn size) that can decouple hotspot counts from surface concentrations early in the season. Taken together, the FIRMS evidence corroborates the interpretation that burning-control enforcement in 2022 reduced smoke load during the main haze period.

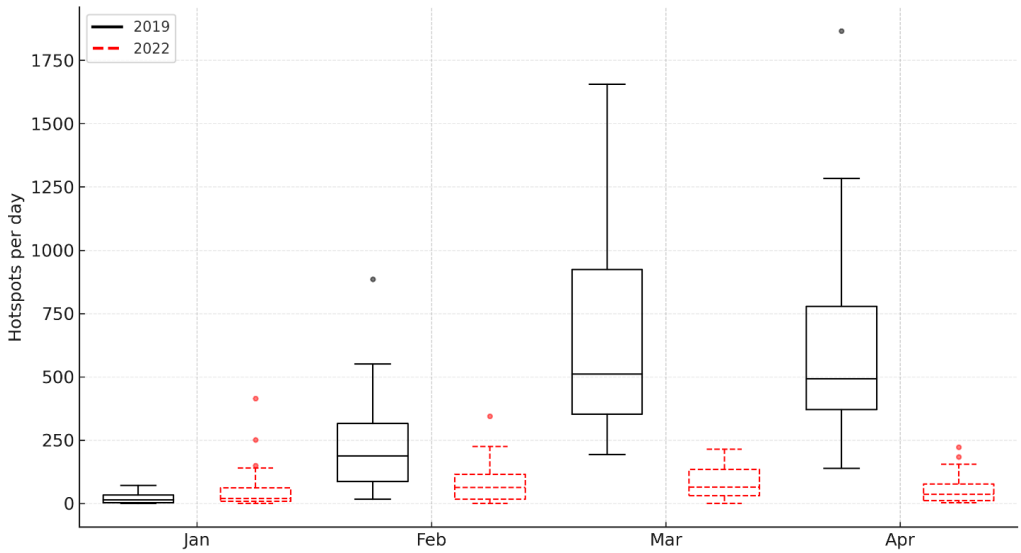

Figure 6 NASA FIRMS daily hotspot counts for Chiang Mai (Jan–Apr), grouped boxplots comparing 2019 and 2022 on a single axis. The dashed red line marks each month's 2022 median. Distributions in Feb–Apr 2022 are markedly lower and less dispersed than in 2019

Table 6 Month-wise FIRMS daily hotspot means for 2019 and 2022, differences (2022−2019), and permutation test p-values. Significant reductions in Feb–Apr support attribution of the $PM_{2.5}$ decrease to reduced burning activity

Month	Mean2019	Mean2022	Diff(2022-2019)	p_perm
Jan	22.552	59.759	37.207	$p = 0.014$
Feb	229.464	84.593	-144.872	$p < 0.001$
Mar	688.387	86.69	-601.697	$p < 0.001$
Apr	618.633	57.6	-561.033	$p < 0.001$

Yearly Average Analysis

Figure 7 summarizes decade-long annual means for Bangkok (59T) and Chiang Mai (36T) against Thailand's annual $PM_{2.5}$ standards (25 µg m^{-3} prior to June 2022; 15 µg m^{-3} since). The purpose of this analysis is to distill the many daily and seasonal fluctuations into a policy-relevant trajectory that can be compared directly with the national benchmarks and contrasted across the two cities. Bangkok shows a gradual decline from a local peak around 2017 (~24.9 µg m^{-3}) to ~16.4 µg m^{-3} in 2024 (≈−34%), with a small rebound in 2023. Chiang Mai exhibits much larger interannual variability governed by the burning season: a drop from ~30.3 µg m^{-3} (2019) to ~19.3 µg m^{-3} (2022) (≈−36%) coincident with burning-control enforcement, followed by a sharp rebound to ~32.8 µg m^{-3} (2023) and a partial easing in 2024 (~27.6 µg m^{-3}). Relative to the former 25 µg m^{-3} annual standard, Bangkok is below the limit in all years shown, whereas Chiang Mai exceeds it in most years except 2017 and 2022.

Under the current 15 µg m^{-3} annual standard, neither city meets the annual benchmark in any year, underscoring that, despite improvements, additional structural controls are required—especially for Chiang Mai, where year-to-year swings track the intensity of biomass-burning seasons. As annual means can mask short, severe episodes, these trends should be interpreted alongside the monthly distributions presented earlier, which show that Bangkok's exceedances cluster in Dec–Feb, while Chiang Mai's concentrations surge during Feb–Apr.

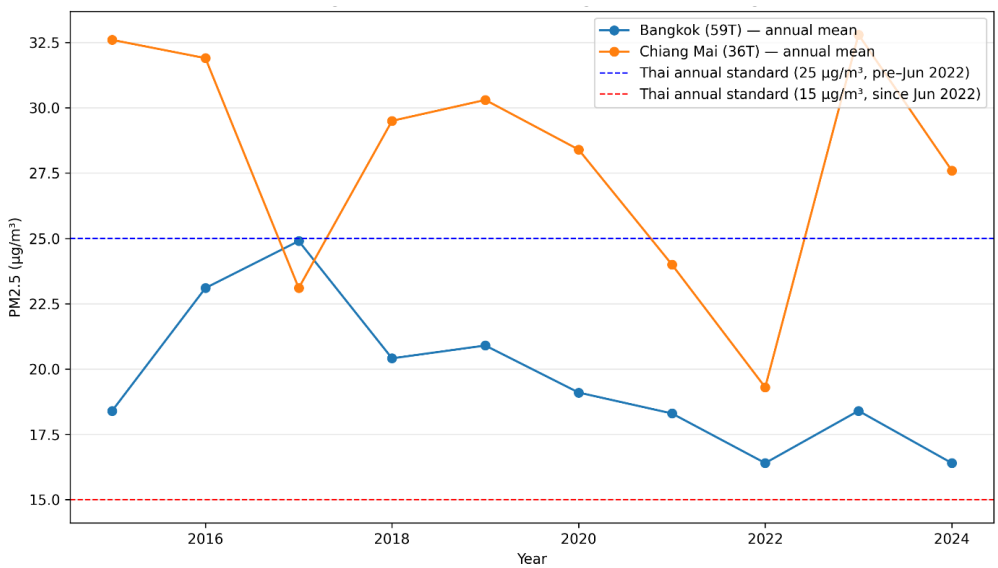

Figure 7 Annual average $PM_{2.5}$ at Bangkok (59T) and Chiang Mai (36T), 2015–2024. Dashed lines show Thai annual standards (25 µg m^{-3} pre-June 2022; 15 µg m^{-3} since)

Conclusions

From 2015–2024, both Bangkok (59T) and Chiang Mai (36T) show clear seasonality; Bangkok peaks in Dec–Feb and eases in Jun–Aug, while Chiang Mai has a stronger Feb–Apr haze pulse driven by burning. Interventions yielded different magnitudes: Bangkok's Wave-1 restrictions (22 Mar–31 May 2020) produced a moderate decline (−14.9% in the window) and eliminated daily exceedances ≥37.5 µg/m³ in that period; Chiang Mai's 2022 burning control delivered a large reduction (−45.5% Jan–Apr) and halved exceedance frequency. Annual means confirm a steady decline in Bangkok and policy-sensitive variability in Chiang Mai; under the current 15 µg/m³ annual standard, neither city achieves compliance. Policy priorities therefore differ: sustained control of traffic/precursor

emissions for Bangkok, and consistent burning management with regional coordination for Chiang Mai.

References

[1] World Health Organization (WHO). 2021. Global Air Quality Guidelines: Particulate matter ($PM_{2.5}$ and PM_{10}), ozone, nitrogen dioxide, sulfur dioxide and carbon monoxide. Geneva: WHO.

[2] Pollution Control Department (PCD), Thailand. 2023. Thailand's Air Quality Management Framework (slides announcing the 2022 $PM_{2.5}$ standards: 24-h 37.5 μg m^{-3}; annual 15 μg m^{-3}), 30 May 2023, EANET Workshop.

[3] Bran, S. H., Macatangay, R., Chotamonsak, C., Chantara, S. and Surapipith, V. 2024. Understanding the seasonal dynamics of surface $PM_{2.5}$ mass distribution and source contributions over Thailand. Atmospheric Environment. 331: 120613.

[4] Air Quality Life Index (AQLI). 2024. Thailand Fact Sheet 2024. Chicago: Energy Policy Institute at the University of Chicago (EPIC).

[5] Rattanapotanan, T., Thongyen, T., Bualert, S., Choomanee, P., Suwattiga, P., Rungrattanaubon, T., Utavong, T., Phupijit, J. and Changplaiy, N. 2023. Secondary sources of $PM_{2.5}$ based on the vertical distribution of organic carbon, elemental carbon and water-soluble ions in Bangkok. Environmental Advances. 11: 100337.

[6] Ratanavalachai, T. and Trivitayanurak, W. 2023. Application of a $PM_{2.5}$ dispersion model in the Bangkok central business district for air quality management. Frontiers in Environmental Science. 11: 1237366.

[7] Ahmad, M., Manjantrarat, T., Rattanawongsa, W., Muensri, P., Saenmuangchin, R., Klamchuen, A., Aueviriyavit, S., Sukrak, K., Kangwansupamonkon, W. and Panyametheekul, S. 2022. Chemical composition, sources, and health risk assessment of $PM_{2.5}$ and PM_{10} in urban sites of Bangkok, Thailand. International Journal of Environmental Research and Public Health. 19(21): 14281.

[8] Archer, D., Bhatpuria, D. Nikam, J. and Taneepanichskul, N. 2024. Particulate matter pollution in central Bangkok: assessing outdoor workers' perceptions and exposure. Cities & Health. 1-19.

[9] Chansuebsri, S., Kolar, P., Kraisitnitikul, P., Kantarawilawan, N., Yabueng, N., Wiriya, W., Thepnuan, D. and Chantara, S. 2024. Chemical composition and origins of $PM_{2.5}$ in Chiang Mai (Thailand) by integrated source apportionment and potential source areas. Atmospheric Environment. 318: 120192.

[10] Ponsawansong, P., Prapamontol, T., Rerkasem, K., Chantara, S., Tantrakarnapa, K., Kawichai, S., Li, G., Fang, C., Pan, X., and Zhang, Y. 2023. Sources of $PM_{2.5}$ oxidative potential during haze and non-haze seasons in Chiang Mai, Thailand. Aerosol and Air Quality Research. 23(10): 230030.

[11] Suriyawong, P., Chuetor, S., Samae, H., Piriyakarnsakul, S., Amin, M., Furuuchi, M., Hata, M., Inerb, M. and Phairuang, W. 2023. Airborne particulate matter from biomass burning in Thailand: Recent issues, challenges, and options. Heliyon. 9(3): e14261.

[12] Inlaung, K., Chotamonsak, C., Macatangay, R. and Surapipith, V. 2024. Assessment of transboundary $PM_{2.5}$ from biomass burning in Northern Thailand using the WRF-Chem model. Toxics. 12(7): 462.

[13] Dejchanchaiwong, R. and Tekasakul, P. 2021. Effects of coronavirus induced city lockdown on $PM_{2.5}$ and gaseous pollutant concentrations in Bangkok. Aerosol and Air Quality Research. 21: 200418.

[14] Sanghatawatana, P., Thaithatkul, P., Anuchitchanchai, O., Liang, J. and Chalermpong, S. 2023. The effect of COVID-19 lockdown on particulate matters concentration: Case of land use regression difference modeling in Bangkok, Thailand. City and Environment Interactions. 20: 100125.

[15] AP News. 2024. As Thailand gasps through another haze season, researchers hope a fire-charting app can help. June 18, 2024.
[16] ABC News (Australia). Thailand seeks pollution solutions as fires exacerbate haze; FireD described. June 23, 2024.
[17] NASA Earthdata (EOSDIS LANCE). 2025. Fire Information for Resource Management System (FIRMS): Overview and Data Access. Greenbelt, MD: NASA.

Thai Environmental Engineering Journal

Aims and Scope

Thai Environmental Engineering Journal is published 3 times a year by Environmental Engineering Association of Thailand in aims of provide an interdisciplinary platform for the disseminating recent research work in Environmental field. The journal's scope includes:

- Treatment Processes for Water and Wastewater
- Air Pollution and Control
- Solids and Hazardous Wastes Management
- Site Remediation Technology
- Water Resource Management; Surface water and Groundwater
- Environmental Management Protection and Conservation
- Impact Assessment of Pollution and Pollutants
- All areas of Environmental Engineering and Sciences

Frequency; 3 issues per year, every four months at April, August and December

Information for Authors

Manuscript submitted for publication should be of high academic merit and have never before, in whole or in part, been published elsewhere and will not be published elsewhere, except in abstract form. Manuscripts, parts of which have been previously published in conference proceeding, may be accepted if they contain additional material not previously published and not currently under consideration for publication elsewhere.

Submission of Manuscripts

All manuscripts should be submitted in https://www.tci-thaijo.org/index.php/teej/index

Manuscript Format and Style

Text format

Manuscript should be prepared using a text processing software such as Microsoft Word for windows. A4 size paper is conventionally accepted. Margins set up (in Page set up Menu) are outlined as follow.

Top Margin 3.0 cm., Bottom Margin 3.0 cm.
Left margin 2.5 cm., Right Margin 2.5 cm.

Title, author co-authors, address of correspondence and abstract are included in the first section while the remainder of paper is to appear in the second section. The total pages including figures, tables and references should not exceed 10 pages.

Font, font size & typeface

Times New Roman font type is required for Thai text and English text. Font size [Pica] for various text function are tabulated as follow.

Text functions	Font = Times New Roman	
	Pica Size**	Typeface
Title [English]	16 [CT]	Bold
Author & Co-authors	11 [CT]	Bold
Address of correspondence	11 [CT]	Normal
Abstract heading	12 [LRJ]	Bold
Abstract & Main Texts	11 [LJ]	Normal
Section Heading & Number*	12 [LJ]	Bold
Subsection Heading & Number	11 [LJ]	Bold

* Including "Abstract" "Acknowledgement" and "References"

** CT = Centre Text, LJ = Left Justified, LRJ = Left & Right Justified

Title

All titles of manuscript should be short and precise; long title should be condensed whenever possible (not more than 42 characters). Title should be printed with every first letter of every word capitalized, excluding prepositions and articles. Directly below the title, author should print their full names (first name then family name), address and institution. E-mail of corresponding author and between 3-5 key words should also be provided.

Abstract

Abstract should be provided on separate sheets and be not more than 300 words. International contributor who are unable to provide an abstract in Thai may submit an English abstract alone.

Style Guidelines

Units of measurement should be indicated in SI units throughout.

Tables

Tables and figures should be numbered with Arabic numerals, in order in which they are cited in the text. The table's titular heading should concisely detail the content of the table and include units of measure for all numerical data.

Format of Research Paper

The format of research paper is listed as follows:

1) Title
2) Author
3) Abstract
4) Introduction
5) Materials and Methods
6) Results and Discussion
7) Conclusions
8) References

References

The references section at the end of the manuscript should list all and only the references cited in the text in numberical order, with references given in Thai first and those in English following. In this section, the names of all authors should be provided if more than six, or the first three followed by *et. al.*

Reference to a journal article:

List all authors when six or fewer; when seven or more list only the first three (3) and add *et. al.* Titles of articles from academic journals should be listed in full and begin with a capital letter.

[1] Inthorn, D., Sidtitoon, N., Silapanuntakul, S. and Incharoensakdi, A. 2002. Sorption of mercury, cadmium and lead in aqueous solution by the use of microalgae. Science Asia. 28(3): 253-261.

Reference to article or abstract in a conference proceedings:

[1] Inthorn, D., Singhakarn, C. and Khan, E. Decolorization of reactive dyes by pre-treated Flute reed (phargmites karka (Retz)). At 34th Mid-Atlantic Industrial & Hazardous Conference, Annual Mid Atlantic Industrial and Hazardous Waste Conference at Rugers University, New Jersey, USA on September 20-21, 2002.

Reference to a book:

[1] Polprasert, C. 1996. Organic Waste Recycles. John Wiley & Sons Inc., New York.

Reference to article in a conference proceedings:

[1] Inthorn, D. Heavy metal removal. In: Kojima, H. and Lee, Y.K. Photosynthetic Microorganisms in Environmental Biotechnology, Springer-Verlag, 2001; 111-135.

Reference to an electronic data source:

Use the above format and supply the complete URL as well as the access date.

Subscription Form
Thai Environmental Engineering Journal

Date_____

Name_____

Address_____

_____

_____

_____

_____

Tel:_____ Fax:_____E-mail:_____

A subscription to the Thai Environmental Engineering Journal is request for_____year
(1,000 Baht/year for 3 Volume)

Signature_____

(_____)

Payment by "Environmental Engineering Association of Thailand"

- ❍ Bank Transfer: Savings Account No. 053-1-24040-3, Bank of Ayudhya Plc., Klong Prapa Branch
- ❍ Bank Transfer: Savings Account No. 056-2-32298-0, Siam Commercial Bank Plc., Aree Sampan Branch

Environmental Engineering Association of Thailand
122/4 Soi Rawadee, Rama VI Rd., Phayathai,
Phayathai, Bangkok 10400
Tel: +66 (0) 2617-1530-1 Fax: +66 (0) 2279-9720
E-mail: teej@eeat.or.th Website: http://www.eeat.or.th

THAI
ENVIRONMENTAL ENGINEERING JOURNAL
Environmental Engineering Association of Thailand (EEAT)

ISSN (PRINT) : 1686 - 2961
ISSN (ONLINE) : 2673 - 0359

Vol. 39 No. 2 May – August 2025

The Effect of Carbon Capture and Storage (CCS) on Quartz Rock and Groundwater: The case study of Thailand
Chanita Sirisaksathaporn, Supreeda Homklin, Sukhuma Chitapornpan, Chatkaew Chailuecha, Pimluck Kijjanapanich, Sulak Sumitsawan, Prattakorn Sittisom, Pharkphum Rakruam, Napat Jakrawatana, Patiroop Pholchan, Sarunnoud Phuphisith, Ekbordin Winijkul and Wanawan Pragot 1-8

Knowledge, Behavior, and Household Hazardous Waste Composition: Implications for Environmental Health in Nakhon Nayok Province, Thailand
Jitjira Chaiyarit, Kanittha Saengpae, Koranitch Jomkathok, Piyawan Roshom, Thananya Seehatab and Prat Intarasaksit 9-17

The Variability in Soil Community and Its Enzymatic Function to Plant Promotion after Biochar Addition
Mujalin Pholchan, Jearanai Thassana and Khajitmanee Muangprom 19-30

Mass Flow Analysis of Carbon Capture, Utilization, and Storage (CCUS) Potential in Thailand
Danupon Srinongsaeng, Napat Jakrawatana and Wanawan Pragot 31-41

Carbon Footprint Assessment and GHG Mitigation Potential of Canned Tuna Spread Products in Thailand
Jirawat Jirajitmeechai, Cheema Soralump, Vorapot Kanokkantapong and Sirakarn Leungsakul 43-52

A Study of Characteristics, Origins, and Fates of Ultrafine Particles Over Taichung City, Taiwan
Kijpat Thavorn, Win Trivitayanurak and Ta-Chih Hsiao 53-61

Treatment of Fishery Wastewater Using a Floating Treatment Wetland Planted with Umbrella Sedge
Parichat Supasee, Supreeda Homklin, Satawat Tanarat, Anusorn Boonpoke and Somanat Somprasert 63-71

Long-Term Analysis of $PM_{2.5}$ Concentrations and Seasonal Variation in Bangkok and Chiang Mai, Thailand: Impacts of COVID-19 Lockdowns and Fire Control Measures
Vineeth Vijayan, Supandee Maneelok and Nantaporn Noosai 73-83